EXPLORING THE FACTORS THAT DETERMINE THE ADSORPTION OF PER- AND POLYFLUOROALKYL SUBSTANCES ON CONVENTIONAL ADSORBENTS AND NOVEL CYCLODEXTRIN POLYMERS WITH DIFFERENT SURFACE PROPERTIES

A Thesis

Presented to the Faculty of the Graduate School

of Cornell University

in Partial Fulfillment of the Requirements for the Degree of

Master of Science

by

Ri Wang

May 2021

ABSTRACT

As the concerns over the ubiquity and toxicity of per- and polyfluoroalkyl substances (PFASs) grow, research has focused on finding both technically and financially efficient PFAS remediation technologies. When evaluating certain technologies, research has focused on the removal of perfluoroalkyl acids from water, but contaminated groundwater often contains complex mixtures of diverse groups of PFASs. Utilizing a more comprehensive method to evaluate the performance of different PFAS treatment technologies involving the consideration of environmental matrix complexity can bring more useful insights into practical application. Adsorption-based processes are among the most promising technologies available for PFAS removal from water. The conventional adsorbents including activated carbon (AC) and anion exchange (AE) resins have been implemented in pilot or full-scale processes targeting PFAS removal from water. Emerging adsorbents, including novel β-cyclodextrin polymers (CDPs), have also exhibited potential for PFAS removal from water. The efficacy of CDPs on PFAS removal and the importance of varying surface properties of different CDPs on determining the affinity and selectivity to contaminants have been demonstrated. However, the mechanisms by which adsorbates bind to CDPs remains poorly understood. More research is needed to elucidate the mechanisms about the relative contributions of hydrophobic and electrostatic interactions for the adsorption of PFASs on CDPs.

Two studies were designed to systematically explore the potential of conventional adsorbents and novel CDPs to remove mixtures of PFASs from contaminated groundwater and probe the adsorption binding mechanisms for anionic PFAS removal on CDPs. The first study aimed to evaluate the performance of five adsorbents including one AC, one AE resin and three different CDPs with varying surface charges to remove 68 PFASs in contaminated groundwater

integrating a suspect screening approach. The PFAS removal performance of the adsorbents was evaluated with respect to adsorption affinity, kinetics, and selectivity. This evaluation provided insights on the factors that determine PFASs adsorption, which can be associated with the increasing length of the perfluorinated tail or could be more strongly related to properties of the head group. The second study aimed to evaluate the relative contributions of hydrophobic and electrostatic interactions on the adsorption of anionic PFASs by CDPs under controlled experimental conditions in nanopure water and different salt-amended nanopure water matrices. This study provided new insights into the adsorption binding mechanisms between anionic PFASs and CDPs as a function of chain length, and revealed the effects of different types and concentrations of inorganic constituents on the adsorption mechanisms. Together, the research described in this thesis furthers the understanding of different PFAS removal patterns by different adsorbents, and the understanding of anionic PFAS adsorption mechanisms on CDPs. These findings can serve as guidance and knowledge support on the future development and practical application of CDPs for different PFAS species under a range of environmental conditions.

BIOGRAPHICAL SKETCH

Ri Wang was born in Weihai, China in 1998. She graduated with a Bachelor of Science degree in Environmental Science and Engineering and a Bachelor of Management in Accountancy from Shanghai Jiao Tong University (SJTU) in 2019. While studying at SJTU, her experiences in the environmental engineering field include a six-month lab research on advanced oxidation processes for wastewater treatment in Dr. Yixin Zhao's research group, an eight-month research on self-cleaning ultrafiltration membranes utilizing photocatalysts in Dr. Lina Chi's research group and a one-month internship as an analyst assistant at the Shanghai Environmental Monitoring Center. She also completed a nine-month internship as a project assistant and a research assistant in China Alliance of Social Value Investment (Shenzhen) focusing on evaluating the sustainable development value of listed companies in China and conducting research on sustainability measuring frameworks and sustainable investing. During the summer of 2018, she attended a six-week summer session at University of California, Berkeley studying environmental earth sciences.

In August 2019, she joined the Environmental Processes focus area in the School of Civil and Environmental Engineering at Cornell University to pursue her M.S. degree. In November 2019, she joined Dr. Damian Helbling's research group and focused on the study of emerging contaminants in groundwater and adsorption technologies. During the summer of 2020, she did a three-month internship as an associate environmental engineer at Cyclopure Inc. One peer-reviewed article (**Chapter 2**) was published during Ri's study at Cornell University and another one (**Chapter 3**) is in preparation for publication:

> Wang, R.; Ching, C.; Dichtel, W. R.; Helbling, D. E. Evaluating the Removal of Per- and Polyfluoroalkyl Substances from Contaminated Groundwater with Different Adsorbents Using a Suspect Screening Approach. Environ. Sci. Technol. Lett. 2020, acs.estlett.0c00736. https://doi.org/10.1021/acs.estlett.0c00736. (**Chapter 2**)

ACKNOWLEDGMENTS

First and foremost, I would like to express my sincere gratitude to my major advisor, Dr. Damian Helbling, for his continued help, support and encouragement throughout my time at Cornell University. I could not have asked for a better M.S. advisor. Dr. Helbling's expertise was invaluable in formulating the research questions and methodology and the insightful feedback pushed me to sharpen my thinking and brought my work to a higher level. I would also like to thank Dr. Matthew Reid for serving as a minor advisor on my committee, for the support on the use of ion chromatography and for the valuable feedback.

I am thankful to the rest of the Helbling Research Group (HRG) members past and present for their kindness and support. I want to thank Casey for patiently tutoring me in the procedures of batch experiments and the use of instruments. I would like to thank Dr. Yuhan Ling for his suggestions on academic life and career.

I want to acknowledge our collaborators from Northwestern University, Dr. William Dichtel and his research group members, especially Dr. Max Klemes, Brittany Trang and Zhi-Wei Lin, for providing the adsorbents and their characterization data including Zeta-potential and BET measurements.

Last but not least, I want to extend my gratitude to all my friends and family. They have provided tremendous support to me, especially during the tough time in this global pandemic. I would like to give my special thanks to my parents, for their unconditional love and support throughout my lifetime.

致谢

首先，我要向我的导师达米安·赫伯林博士（Dr. Damian Helbling）致以最诚挚的谢意，感谢他对于我在康奈尔大学求学期间的悉心指导、帮助和鼓励。我再也找不到一个可能比赫伯林博士更好的硕士生导师了。赫伯林博士的专业知识对我的研究问题和方法的探索提供了宝贵的帮助，而他颇有见地的反馈时常激发我更深层次的思考，使我的研究工作更上一层楼。此外，我还要感谢马修·里德博士（Dr. Matthew Reid）担任我的另一位导师，感谢他对于我使用离子色谱仪器的支持以及他宝贵的反馈意见。

我还要感谢许多赫伯林课题组的成员，感谢他们的关爱与支持。我要特别感谢凯西（Casey）耐心细致地教我如何进行批处理实验以及如何使用仪器。我要感谢凌雨涵博士对我提供的学术以及职业发展方面的宝贵建议。

与此同时，我要感谢西北大学的合作方迪希特尔博士（Dr. William Dichtel）及其课题组的其他成员，感谢麦克斯博士（Dr. Max Klemes）提供的吸附剂和 BET 表征数据，感谢布列塔尼（Brittany）和林志伟提供的电动电势测量值。

最后，我想要感谢所有的朋友和家人。尤其是在全球抗击新冠疫情的艰难时期，感谢他们对我的支持和关心。我还想特别感谢我的父母，感谢他们对我的教导和无私的关爱。

TABLE OF CONTENTS

LIST OF FIGURES

LIST OF TABLES

CHAPTER 1 – Background

1.1 Introduction to PFASs

Per- and polyfluoroalkyl substances (PFASs) are a family of anthropogenic chemicals that are used in a wide variety of applications. Since the middle of the 20th century, many products commonly used by consumers and industry have been manufactured with or from PFASs.[1] Nowadays, more than 3,000 PFASs are available on the global market for intentional uses.[2,3] As shown in **Figure 1-1**, the fully or partially fluorinated carbon chain and the hydrophilic head groups of PFASs impart unique physicochemical properties, including chemical and thermal stability, water- and oil-repellency, and surfactant properties.[3] Therefore, they become major constituents in industrial processes (e.g., medical devices, oil production, pesticide formulations, metal plating and etching, and semiconductors) and commercial products (e.g., cosmetics, fire-fighting foams, food contact materials, household products, textiles and leathers).[3–6]

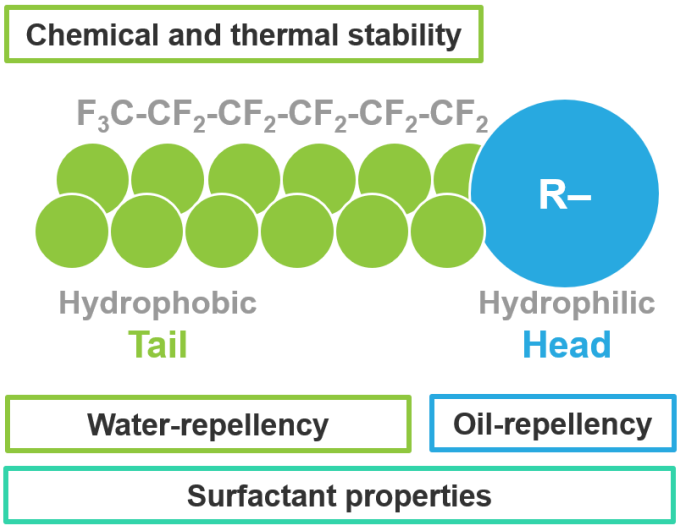

Figure 1-1. The head and tail structure of PFAS and the correspondingly imparted properties.

The widespread use of PFASs in industrial processes and commercial products has resulted in the ubiquitous occurrence of PFASs in the environment.[3,4] The family of perfluoroalkyl acids

PFCA homologues

Structure	Molecular Formula	Individual Acronym	Number of Perfluorinated Carbons
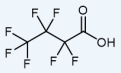	C4HO2F7	PFBA	3
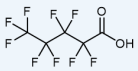	C5HO2F9	PFPeA	4
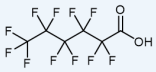	C6HO2F11	PFHxA	5
	C7HO2F13	PFHpA	6
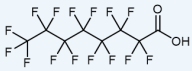	**C8HO2F15**	**PFOA**	**7**
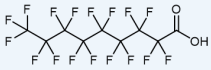	C9HO2F17	PFNA	8
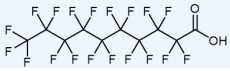	C10HO2F19	PFDA	9

PFSA homologues

Structure	Molecular Formula	Individual Acronym	Number of Perfluorinated Carbons
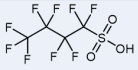	C4HO3SF9	PFBS	4
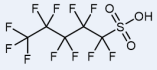	C5HO3SF11	PFPeS	5
	C6HO3SF13	PFHxS	6
	C7HO3SF15	PFHpS	7
	**C8HO3SF17**	**PFOS**	**8**
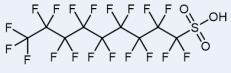	C9HO3SF19	PFNS	9
	C10HO3SF21	PFDS	10

Figure 1-2. Homologous series of perfluorocarboxylic acids (PFCAs) and perfluorosulfonic acids (PFSAs).

(PFAAs), including the perfluorocarboxylic acids (PFCAs) and perfluorosulfonic acids (PFSAs), is the most widely detected family of PFASs in varying environmental media.[3,4,7–9] More specifically, the eight carbon homologues of the PFCAs and PFSAs (**Figure 1-2**), perfluorooctanoic acid (PFOA) and perfluorooctanesulfonic acid (PFOS), respectively, have become emerging contaminants of global concern.[3,10] Major PFAS contamination sources are runoff plumes from aqueous film-forming foams (AFFFs) used for firefighting activities,[11–13] and industrial discharges from facilities manufacturing or utilizing PFASs.[4,14–16] As reported in many studies, the PFAAs (especially PFOA and PFOS) at elevated levels are most often found downstream of nearby airports and manufacturing facilities.[4,13] However, the existence of PFAA contamination has also been found where there is not a clear link to an identifiable source.[7,17,18] The occurrences of PFAAs in air, water, and soil, would ultimately lead to human exposure through subsequent contamination of drinking water, food, livestock, and wildlife.[4,7–9,19] Human

PFAA exposure has been linked to many adverse health effects even at trace concentrations, such as cancer, elevated cholesterol, obesity, immune suppression, and endocrine disruption.[19–24]

As concern over the ubiquity and toxic effects of PFASs grow, a cascade of new regulations has been formulated regarding PFASs control. In May 2016, the U.S. EPA established health advisories for PFOA and PFOS at 70 ng L^{-1} (individual or total) limit for lifetime exposure in drinking water.[25,26] In addition to values that specify health-based concentration limits, agencies have used various strategies to limit the use and release of PFASs. The Organization for Economic Co-operation and Development (OECD) has described various international policies, voluntary initiatives, biomonitoring, and environmental monitoring programs to control PFASs.[27,28] In 2017, the European Union (EU) banned the sale, use, and import of PFOA, its salts and PFOA-related substances with phase-outs occurring through 2032 and certain allowed uses.[29] There are several states in the U.S. making state-level regulations for PFAS to protect drinking water mainly focusing on PFCAs and PFSAs.[30,31] Meanwhile, more emerging regulations are being made. Through the Unregulated Contaminant Monitoring Rule (UCMR) program of the Safe Drinking Water Act (SDWA), U.S. EPA and some states use the occurrence data which is produced not only for PFOA and PFOS, but also for other PFASs (mainly PFCAs and PFSAs) to help determine which substances to consider for future regulatory action.[28,32]

Although federal and local regulations in the U.S. have focused on a few dozen PFASs of concern, many other PFASs that are used in industrial processes or commercial products and their chemical structures remain unknown and held as proprietary. There are estimates suggesting that more than 4,000 PFASs exist in the environment.[33] Recent studies indicate that not all PFASs are anions, they are also consisting of a variety of other classes, including cationic, zwitterionic, and nonionic PFASs.[4,34–38] PFASs produced for intentional use can be transformed to other known or

unknown PFASs during their production, application or transportation processes, which amplifies the challenges of PFAS monitoring and remediation.[38–41]

1.2 Measuring PFAS in the Environment

The main analytical tool that has been used to measure PFASs in environmental matrices is liquid chromatography (LC) coupled with mass spectrometry (MS).[34] LC is a separation technique that allows for separation of chemicals in a complex sample. MS is a detection technique that allows for detection by the molecular masses of ionized precursors. Fragmentation masses can be measured from tandem mass spectrometry (MS/MS) which could provide more information on PFAS structural features. Compared with MS, high-resolution mass spectrometry (HR-MS) has higher mass accuracy and higher mass resolution which affords greater potential to measure PFASs in environmental samples. The growth, evolution, and accessibility of HR-MS offer the possibility to further explore the complexity of the PFAS family of chemicals, allowing for the development of different techniques for PFAS analysis.[42]

Target analysis is the conventional approach for measuring PFASs in environmental matrices.[43] Target analysis can be done using triple quadrupole mass spectrometry or HR-MS where the mass analyzer could be time-of-flight (ToF) or orbitrap. The goal of target analysis is sensitive quantitation of target compounds. Target analysis requires the use of reference standard chemicals where the target list usually includes no more than 40 PFASs.[43] For PFAS target analysis, U.S. EPA has published and validated two methods (Method 537.1 and Method 533) in drinking water,[44,45] and one method (Method 8327) for non-drinking water aqueous (groundwater, surface water, and wastewater) samples.[46] The methods for other environmental matrices (e.g., landfill leachate, biosolids, soils, sediments, and air) are still under development.[47]

In contrast to target analysis, suspect screening is an emerging technique that requires the use of HR-MS but does not rely on the availability of reference standards.[42,43,48] Suspect screening can confirm the presence or absence of compounds in a suspect list and achieve semi-quantitative detection. The suspect list is the list of known PFASs which may be present in the sample and it contains the PFAS information such as molecular formula and chemical structure. The use of HR-MS enables the linkage of detected features from the mass spectral acquisition to theoretical features of the suspect compounds. The number of PFASs in the suspect list usually can be from hundreds to thousands. There are no standard methods for conducting suspect screening, but some techniques and workflows on suspect screening are described in the literature.[16,48–51]

Non-target screening is a technique on the frontier of this field that allows one to identify the structures of previously unknown or unexpected PFASs in an environmental sample using HR-MS.[3,42,43] The goal of non-target screening tends to be the discovery of new PFASs that may be of concern. Many non-target screening methods rely on the homologous series approach[15] and/or the characteristic fragment approach.[52] No standard methods are available for non-target screening, but innovative techniques are in development and some techniques are published in the literature.[35,52–54]

1.3 Current PFAS Treatment Technologies

Due to their high persistence, bioaccumulation potential and toxicity, recent studies focused on finding effective methods in both technical and financial aspects to remove PFASs from environmental matrices.[2,3,55,56] Many studies over the past several years have demonstrated that conventional water and wastewater treatment technologies are ineffective for removing PFASs from water due to the low concentration of PFASs in water, the high hydrophilicity of PFASs and the strong C-F covalent bond of PFASs.[2,57,58] Both aerobic and anaerobic biological treatment are

shown to be ineffective to degrade PFASs, though they can lead to the formation of short-chain PFASs by breaking the C-C bond.[2,59] It is found that in conventional drinking water treatment processes (e.g., peroxidation, sand filtration, and ozonation), PFOA and PFOS were not removed at all.[60] It is also reported that the concentrations of most of the detected perfluoroalkyl compounds remained relatively unchanged with successive conventional wastewater treatment steps (i.e., de-nitrification, coagulation/flocculation, ozonation, sand filtration and biologically activated carbon filtration).[61] Further, there is a study showing that some polyfluoroalkyl substances such as zwitterionic/cationic polyfluoroalkyl amide (FA) and sulfonamide (FS) may ultimately transform into highly stable end products such as PFOA and PFOS after the water disinfection processes.[39] These transformations might make the PFAS remediation more challenging, although some individual precursors of PFAAs may also be problematic on their own.[3,21,62,63]

Because of the ineffectiveness of conventional treatment technologies on removing PFASs from water, significant studies have been focused on the development of advanced treatment technologies. There are generally two categories of advanced treatment technologies that are considered: destruction technologies and separation technologies.[2,56,64] Destruction technologies aim to defluorinate and mineralize PFASs, and involve a wide variety of methods such as advanced reduction processes (ARPs), advanced oxidation processes (AOPs), mechanochemical treatment, hydrothermal treatment, sonolysis, plasma and others.[64–67] Even though some studies on PFAS destruction have been proven to be effective, there are some limitations, including production of toxic by-products, greenhouse gases, and expensive operating cost.[56,64] Besides, more research is needed on the further development of destruction technologies to different PFASs, and the evaluation of the influences produced by other co-contaminants or environmental matrix constituents.[56,64]

Separation technologies aim to completely remove PFASs from water without the destruction of the C-F bonds. The two main classes of separation technologies include membrane filtration and adsorption process.[2,55] Nanofiltration (NF) and reverse osmosis (RO) are the two applicable membrane technologies for PFAS removal due to the desirable pore sizes and have been proven to be effective.[14,60,64,68,69] Though membrane technology has the potential to provide an effective solution for PFAS removal, the high cost, extensive energy requirement and membrane fouling issues limit the wide application of this technology on PFAS treatment.[2,64]

Adsorption is an established and economical technology that utilizes less energy and is less expensive than membrane processes, becoming one of the most feasible technologies for PFAS removal.[70] One of the most widely used adsorbents is activated carbon (AC).[2,71] AC is relatively inexpensive, widely available, and has shown effectiveness to several (but not all) PFASs.[2,55] AC is a nonselective adsorbent that mainly relies on hydrophobic interactions to remove PFASs from water. AC can exhibit moderate affinity for long-chain PFAAs but perform poorly for short-chain PFAAs.[2,72] Additionally, AC exhibits slow, diffusion-limited adsorption kinetics, poor ability to be regenerated and is readily fouled by matrix constituents including inorganic ions and natural organic matter (NOM).[73–75] These deficiencies have motivated studies focused on anion-exchange (AE) resins as an alternative adsorbent for PFAS remediation.[57,76,77] The predominant mechanisms of AE resins are ion exchange and electrostatic interactions. In contrast to AC, AE resins are of higher affinity for short-chain PFAAs, exhibit higher adsorption capacity, and exhibit feasibility of regeneration and faster adsorption kinetics.[2,72,78] However, the performance of AE resins can likewise be inhibited by the presence of NOM or inorganic ions.[69,79,80] Due to the deficiencies of

AC and AE resins, there has been a lot of research on next-generation adsorbents such as magnetite nanoparticles,[81,82] metal organic frameworks,[83] and cyclodextrin-based polymers.[84,85]

1.4 Cyclodextrin Polymers

Cyclodextrins are macrocycles of glucose that are sustainably produced from glucose by means of enzymatic conversion.[86] The three major commercially available cyclodextrins are known as α, β, and γ cyclodextrin and they are distinguished from each other by the number of glucose molecules contained in their structure.[86] β-cyclodextrin is a macrocycle of seven glucose molecules, which results in a cup-like shaped structure with a hollow interior cavity that has a diameter of 0.78 nm.[75] Whereas the hydroxyl groups along the perimeter of cyclodextrins make them hydrophilic and soluble in water, the interior cavity is hydrophobic and is known to form host-guest complexes with thousands of organic molecules.[86–88]

Cyclodextrin polymers (CDPs) are synthesized by crosslinking beta-cyclodextrin with one or more co-monomers.[85,89] The water-insoluble epichlorohydrin-cyclodextrin polymers (EPI-CDPs) were first proposed in the mid-1960s and are of continued interest to the scientific community. Since the early 1990s, EPI-CDPs have been studied particularly for their environmental applications in the removal of pollutants present in industrial wastewater.[87,90] EPI-CDPs have been used as adsorbents for micropollutants (MPs) removal.[87] However, it is found that for most analytes, the removal by EPI-CDPs did not outperform the removal by activated carbon, especially for PFASs.[85,91]

In 2016, our research team synthesized a new class of CDP (known as P-CDP) that relies on a rigid aromatic crosslinker (i.e., tetrafluoroterephthalonitrile) to generate a permanently porous CDP with high surface area, as presented in **Figure 1-3**.[85] These properties have been shown to impart relative fast adsorption kinetics and high adsorption capacity.[85] Due to the cavity structure

of CDPs, the adsorption inhibition by large-molecular-weight NOM and other matrix constituents can be limited, because these molecules either cannot access or do not bind to the interior cavity of the cyclodextrins.[75,92,93] The resulting selectivity for target adsorbates, and potential reusability demonstrated by recent studies, make our porous CDPs promising adsorbents for environmental remediation.[85,92–94] Over the last 5 years, our research team has synthesized and evaluated a number of novel CDPs as presented in **Table 1-1**.

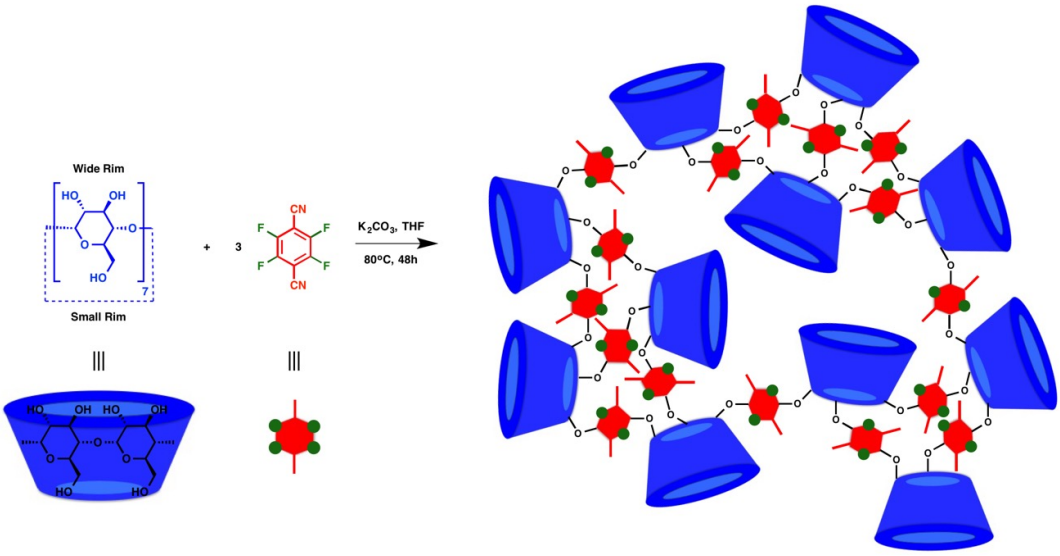

Figure 1-3. Synthesis of the high-surface-area porous P-CDP from β-cyclodextrin and a rigid aromatic crosslinker tetrafluoroterephthalonitrile (TFN).

Besides the promising host-guest complexation brought by the cyclodextrin cavity structure, we have also recognized the importance of crosslinker chemistry in the potential of CDPs to remove ionic contaminants from water. Our first-generation CDPs (i.e., P-CDP which is commercially marketed as DEXSORB) exhibited rapid removal for many types of organic micropollutants (MPs), especially for positively charged MPs and zwitterionic PFASs, implying that negative surface charge of P-CDP plays a considerable role on the adsorbate uptake behavior.[75,84,94] Our next-generation CDPs with a positive surface charge (i.e., amine-CDP, CDP+ which is commercially marketed as DEXSORB+, and M+) exhibited rapid adsorption kinetics and

high adsorption capacity for anionic PFASs and outperformed both activated carbon and ion exchange resin.[93–95] These findings again emphasize the importance of the positive surface charge of the next-generation CDPs on anionic pollutant removal.

Although crosslinker chemistry is clearly important for determining the selectivity of CDPs for contaminants with different ionization, the mechanisms by which adsorbates bind to CDPs remains elusive. One of the expected mechanisms is host-guest complex formation in the interior cavity of the cyclodextrins driven by hydrophobic interactions. Additionally, electrostatic interactions are clearly also important, particularly for ionic adsorbates. But the exact role the electrostatic interactions play in the adsorption mechanism remains unknown.

Table 1-1. Summary of cyclodextrin polymers (CDPs) synthesized and studied by our research team from 2016-2021.

CDP Acronym [a]	Crosslinker Acronym [b]	First Published Year	References	Current Stage	Surface charge [c]	Surface area (m^2 g^{-1}) [c]	Summary on Tested Pollutants
DEXSORB	TFN	2016	75,84,85,88,92,94,95,101,102,156	Commercial application	Negative	218~263	More than 250 MPs, including more than 70 PFASs
NP-CDP	TFN	2016	85	Research: batch experiment	/	6	Lead ions and around 200 MPs, including PFBA and PFOA
EPI-CDP	EPI	2016	85,91	Research: batch experiment	Negative	23	18 MPs including 10 PFASs
DFB-CDP	DFB	2017	91,101	Research: batch experiment	/	140~<10	10 PFASs
TFN-CDP	TFN	2018	110	Research: SPE	/	~40	189 MPs, including PFOA
CD-TFN	TFN	2019	157	Research: CDP on granular media	/	/	15 MPs
CD-TFN@CMC	TFN	2019	157	Research: CDP on granular media	/	/	15 MPs
IEM-CDP	IEM	2019	91,93	Research: mechanism	Negative	/	10 PFASs
amine-CDP	TFN	2019	84,94,102	Research: mechanism, batch experiment	Positive	135	More than 100 MPs, including 20 PFASs
DEXSORB+	TFN	2020	93–95	Commercial application	Positive	20	More than 70 PFASs
CDP1 (amine)	TREN	2020	118	Research: mechanism	Positive	169	10 PFASs
CDP2 (amide)	TREN	2020	118	Research: mechanism	/	78	10 PFASs
M+	MDI	2020	95	Commercial application	Positive	80	68 PFASs
Stydex/+	Styrene	expected 2021	this thesis	Research: mechanism	Positive	237	11PFASs, including 7 PFCAs and 4 PFSAs
Stydex/MA	Styrene	expected 2021	this thesis	Research: mechanism	Negative	402	11PFASs, including 7 PFCAs and 4 PFSAs
Stydex/Styrene	Styrene	expected 2021	this thesis	Research: mechanism	Negative	392	11PFASs, including 7 PFCAs and 4 PFSAs

[a] Other acronyms for some CDPs: for DEXSORB, it is also known as P-CDP and TFN-CDP; for amine-CDP, it is also called as aCDP; for DEXSORB+, it is also known as CDP+;

[b] Names for crosslinker acronyms: TFN is "Tetrafluoroterephthalonitrile", EPI is "Epichlorohydrin", DFB is "Decafluorobiphenyl", IEM is "Isocyanatoethyl methacrylate", TREN is "Tris(2-aminoethyl)amine", MDI is "Methylene diphenyl diisocyanate".

[c] The symbol "/" means the corresponding characterization information was not reported in the published article(s).

1.5 Research Objectives

The research conducted for this Master's thesis aimed to fill some of the major knowledge gaps with respect to the removal of PFASs from water. The focus of the research is on PFAS adsorption using a variety of novel CDPs, though experiments were also performed with AC and AE resins. The overarching research objectives addressed in this thesis include:

Objective 1: Evaluate the potential of three different CDPs, one AC, and one AE resin to remove a complex mixture of PFASs from contaminated groundwater;

Objective 2: Examine the relative contributions of hydrophobic interactions and electrostatic interactions on PFAS adsorption via analyzing the effects of PFAS properties (i.e., chain length and headgroups) on PFAS removal by different adsorbents;

Objective 3: Determine the relative contributions of hydrophobic interactions and electrostatic interactions on PFAS removal by CDPs;

Objective 4: Explore the influence of different salt concentrations and salt types on adsorption mechanisms.

The aim of research described in **Chapter 2** entitled *Evaluating the Removal of Per- and Polyfluoroalkyl Substances from Contaminated Groundwater with Different Adsorbents Using a Suspect Screening Approach*[a] was to address **Objective 1** and **Objective 2** by conducting experiments directly in AFFF-contaminated groundwater. A suspect screening approach was used to identify 68 unique PFASs in a groundwater sample. Batch experiments were conducted to evaluate the removal of the 68 PFASs from the groundwater using three CDPs, one AC, and one AE resin. Then the comprehensive dataset resulting from the batch experiments was used to explore the influence of PFAS properties on their removal by each adsorbent. This is the first study

[a] **Chapter 2** was published in *Environmental Science & Technology Letters* and reformatted for this thesis as **Chapter 2**. DOI: 10.1021/acs.estlett.0c00736

that has evaluated the comprehensive removal of PFASs from AFFF-contaminated groundwater using a suspect screening approach. The results significantly improve our understanding of the ways in which different adsorbents perform with respect to comprehensive PFAS removal.

The aim of research described in **Chapter 3** entitled *Identifying the Relative Contributions of Hydrophobic and Electrostatic Interactions on Adsorption of Perfluoroalkyl Acids on Cyclodextrin Polymer*[b] was to address **Objective 3** and **Objective 4** by conducting experiments with a newly developed CDP platform called styrene-linked cyclodextrin polymers (Stydex). The Stydex platform enables the direct evaluation of the adsorption binding mechanisms across polymers more accurately. Three Stydex adsorbents with different surface charge and/or crosslinker hydrophobicity were synthesized. The equilibrium adsorption experiments were conducted with different mixtures of anionic PFASs in nanopure water and salt-amended nanopure water. The performance of three Stydex adsorbents for the removal of seven PFCAs and four PFSAs was evaluated. The resulting data was used to explain the relative contributions of hydrophobic and electrostatic interactions on the adsorption of the anionic PFASs as a function of chain-length. This study provides new insights into the anionic PFAS adsorption mechanisms on CDPs and reveals the impact of different types and concentrations of inorganic constituents on adsorption process.

[b] **Chapter 3** will be submitted for peer-reviewed publication.

CHAPTER 2 – Evaluating the Removal of Per- and Polyfluoroalkyl Substances from Contaminated Groundwater with Different Adsorbents Using a Suspect Screening Approach

Abstract

Per- and polyfluoroalkyl substances (PFASs) are ubiquitous environmental contaminants. Research has focused on technologies for the removal of perfluoroalkyl acids from water, but contaminated groundwater often contains complex mixtures of diverse groups of PFASs. We explored the potential of five adsorbents to remove mixtures of PFASs from contaminated groundwater. We used high-resolution mass spectrometry to identify 68 unique PFASs in a groundwater sample. We then performed batch experiments with activated carbon (AC), an anion exchange resin, and three different cyclodextrin polymers (CDPs) with varying surface charge to evaluate their potential to remove the 68 PFASs from the groundwater. We found that each adsorbent exhibits a different removal pattern among the 68 PFASs. AC is the most non-selective adsorbent, but has relatively slow adsorption kinetics. The CDPs exhibit rapid adsorption kinetics and are more selective than AC, performing better in removing PFAS classes that are complementary to their surface charge. Analysis of the complete dataset revealed that adsorption of some PFAS classes can be associated with increasing length of the perfluorinated tail, while adsorption of other classes is more strongly related to properties of the head group. Our study offers new insights into PFAS adsorption and a novel approach to evaluate remediation technologies for PFAS removal from groundwater.

2.1 Introduction

Per- and polyfluoroalkyl substances (PFASs) are persistent organic contaminants that are ubiquitously measured in drinking water resources.[4,96,97] For example, studies have reported the presence of PFASs in groundwater adjacent to military facilities that have hosted firefighting training activities relying on aqueous film-forming foams (AFFFs).[11,35,38,41,98,99] Human exposure to PFASs in drinking water has been linked to adverse health effects,[3,19–21] and recent research has focused on technologies to remove PFASs from groundwater.[56,64,100] Adsorption-based processes are among the most promising technologies available for PFAS removal from water;[70] activated carbon (AC) and anion exchange (AE) resins have been implemented in pilot or full-scale processes targeting PFAS removal from groundwater.[57,71,76,77] Emerging adsorbents, including novel β-cyclodextrin polymers (CDPs), have also exhibited potential for PFAS removal from groundwater.[85,101,102]

Most studies evaluating PFAS removal and remediation focus on perfluoroalkyl acids (PFAAs) such as perfluorooctanoic acid (PFOA) and perfluorooctanesulfonic acid (PFOS).[41,103,104] However, over 1,000 unique PFASs have been discovered in AFFF-contaminated groundwater including cationic, nonionic, and zwitterionic PFASs.[3,34,35,37,98,105] Further, most experiments aimed at assessing PFAS removal from water are conducted in simulated conditions using a mixture of a few PFAAs at a fixed concentration,[2,57] whereas relatively few experiments sufficiently replicate the complexities of real systems with respect to matrix chemistry or the concentration and distribution of individual PFAS species[106,107]. Finally, although some data has emerged describing the role that PFAS properties play in their removal[55,69,77,108,109], these insights

have been mostly derived using homologues of PFAAs and the behavior of other types of PFASs remains unknown[2].

We aimed to address these knowledge gaps by conducting experiments directly in AFFF-contaminated groundwater. We used a suspect screening approach to identify 68 unique PFASs in an AFFF-contaminated groundwater sample. We conducted batch experiments to evaluate the removal of the 68 PFASs from the groundwater using five different adsorbents. To the best of our knowledge, this is the first study that has evaluated the removal of PFASs from AFFF-contaminated groundwater with a dedicated suspect screening approach.

2.2 Material and Methods

2.2.1 Adsorbents

We selected five adsorbents for this study including two commercially available β-cyclodextrin polymers (DEXSORB and DEXSORB+, Cyclopure, Inc., Encinitas, CA), one novel β-cyclodextrin polymer (M+), one activated carbon (AC), and one anion exchange (AE) resin. DEXSORB has a negative surface charge and has been previously shown to have poor affinity for anionic PFASs but moderate to high affinity for zwitterionic PFASs[75,88,94,110]. DEXSORB+ and M+ have a positive surface charge and the former has exhibited high affinity for anionic PFASs[93,94]; M+ is a novel material developed by Cyclopure, Inc. that incorporates a proprietary monomer, and its performance is reported here for the first time. The activated carbon was Filtrasorb® 400-M (Calgon Carbon, Pittsburgh, PA) and was pulverized to obtain a particle size range of 75 - 125 μm. The AE resin was PFA694E (Purolite, Philadelphia, PA) and consisted of polystyrene crosslinked with divinylbenzene and functionalized with amino acids. Additional details on each of the adsorbents are provided in **Table A-1** of **Appendix A**.

2.2.2 Water samples

AFFF-contaminated groundwater samples were collected in 1 L HDPE bottles from a single source in Pennsylvania and transported to our laboratory on the same day packed in ice. Groundwater samples were stored at 4 °C and in the dark until experimentation. Background water quality parameters and the concentrations of eleven PFASs are provided in **Table A-2**.

2.2.3 HRMS analysis and suspect screening

Groundwater samples were filtered through 0.45 μm cellulose acetate syringe filters (Restek) into six 10 mL glass LC-MS vials (Fisher) and were measured by means of high-resolution mass spectrometry (HRMS, quadrupole-orbitrap, ThermoFisher Scientific) using

previously established methods detailed in the **Appendix A**.[93,94] We measured the groundwater sample in triplicate in positive polarity mode and in negative polarity mode. Triplicate blank samples consisting of LC-MS grade water were also measured in positive and negative polarity mode. The HRMS acquisitions were converted to *mzXML* format using MSConvert and imported into the R Statistical Software (v 3.3.3) to screen for the presence of 1,432 PFASs that have been previously reported in the literature.[34,35,37,98,105,111] We used the *enviMass* package for peak picking and the *blind* and *replicate* filter functions to remove peaks that were present in at least one of the triplicate groundwater samples with a peak area less than 100 times the maximum peak area among the blank samples or that were not present in each of the triplicate groups within a mass (*m/z*) tolerance of 12 ppm and a retention time window of 30 seconds, respectively. We then screened for peaks that were measured at the exact mass (± 10 ppm) of the predicted $[M\text{-}H]^-$, $[M+H]^+$ and $[M]^+$ adducts for each of the 1,432 PFASs on the suspect list. We examined all of the suspect hits and removed false positives using a conservative procedure that is described in the **Appendix A**. We used the XCalibur software (ThermoFisher Scientific) to extract the peak areas of the final set of suspect hits for evaluation of PFAS removal.

2.2.4 Rotator batch experiments

Adsorption experiments were conducted in 15 mL polypropylene centrifuge tubes (Corning) with 10 mL of groundwater and an adsorbent concentration of 10 mg L^{-1} in triplicate as previously described.[93,94] Prepared centrifuge tubes were placed on a tube revolver and rotated at 40 rpm at 23 °C for 0.5 hr, 9 hr, or 48 hr. After rotating, samples were filtered through 0.45 µm cellulose acetate filters (Restek) and transferred into 10 mL glass LC-MS vials (ThermoFisher Scientific). Control experiments were conducted in triplicate using the same procedure but in the absence of adsorbents. Samples were measured by means of HRMS using the same method

described for suspect screening. Removal was calculated based on the average peak areas of each PFAS in the experimental group and the control group. An additional control experiment was performed to evaluate the changes in peak areas of nine isotope-labelled internal standards (ILISs; $^{18}O_2$-PFHxS, $^{13}C_4$-PFOS, $^{13}C_4$-PFBA, $^{13}C_2$-PFHxA, $^{13}C_4$-PFOA, $^{13}C_5$-PFNA, $^{13}C_2$-PFDA, $^{13}C_2$-PFUnA, and $^{13}C_2$-PFDoA) after they were spiked in untreated groundwater and treated samples from each adsorption experiment. Data from this control experiment were used to evaluate changes in matrix effects that may have emerged during experimental treatment.

2.3 Results and Discussion

2.3.1 Removal of PFASs in groundwater

Our suspect screening identified 68 PFASs in the AFFF-contaminated groundwater sample. Based on an inspection of functional groups, we expect that 43 PFASs were anionic, 12 PFASs were nonionic, and 13 PFASs were zwitterionic at the pH of the groundwater sample (pH = 6.7, **Table A-2**). The component name, component acronym, class acronym, and SMILES notation for each of the 68 PFASs are provided in **Table A-3,** definitions of class acronyms are provided in **Table A-4**, and analytical details are provided in **Table A-5**. The removal efficiencies calculated for the 68 PFASs by each of the five adsorbents after 0.5 hr, 9 hr, and 48 hr of contact time are provided in **Tables A-6** through **A-10** and in the box plots in **Figure 2-1**. Results from our ILIS control experiment demonstrate that matrix effects do not significantly influence our estimates of PFAS removal, with uncertainty resulting from changes in matrix effects in the range of the standard deviation reported for removal among our triplicate experiments (**Tables A-6** through **A-10**). Although the 68 PFAS species were present at widely varying abundances in the groundwater sample, we note that there is no abundance-dependency in the removal of the 68 PFASs from groundwater by any of the adsorbents (**Figure A-1**). Several additional insights can be derived from these data.

First, each adsorbent exhibits a unique removal profile for the 68 PFASs present in the groundwater. Considering the data from 0.5 hr of contact time, DEXSORB+ exhibits the highest removal across all PFASs, whereas M+ and AC exhibit moderate removal, and DEXSORB and the AE resin exhibit relatively low removal. We have previously shown that DEXSORB+ has high affinity for anionic PFASs[93] and some nonionic PFASs[94], though the high removal of zwitterionic PFASs by DEXSORB+ is observed here for the first time. We have also previously shown that

DEXSORB has relatively weak affinity for anionic PFASs but moderate to high affinity for some zwitterionic PFASs.[75,88,94,110] Interestingly, the only zwitterionic PFAS that exhibits moderate to high removal by DEXSORB in this study (i.e., > 60% removal at 9 hr and 48 hr) is 6:2 FTSA-PrB, which also exhibited moderate to high affinity for DEXSORB in previous experiments.[94]

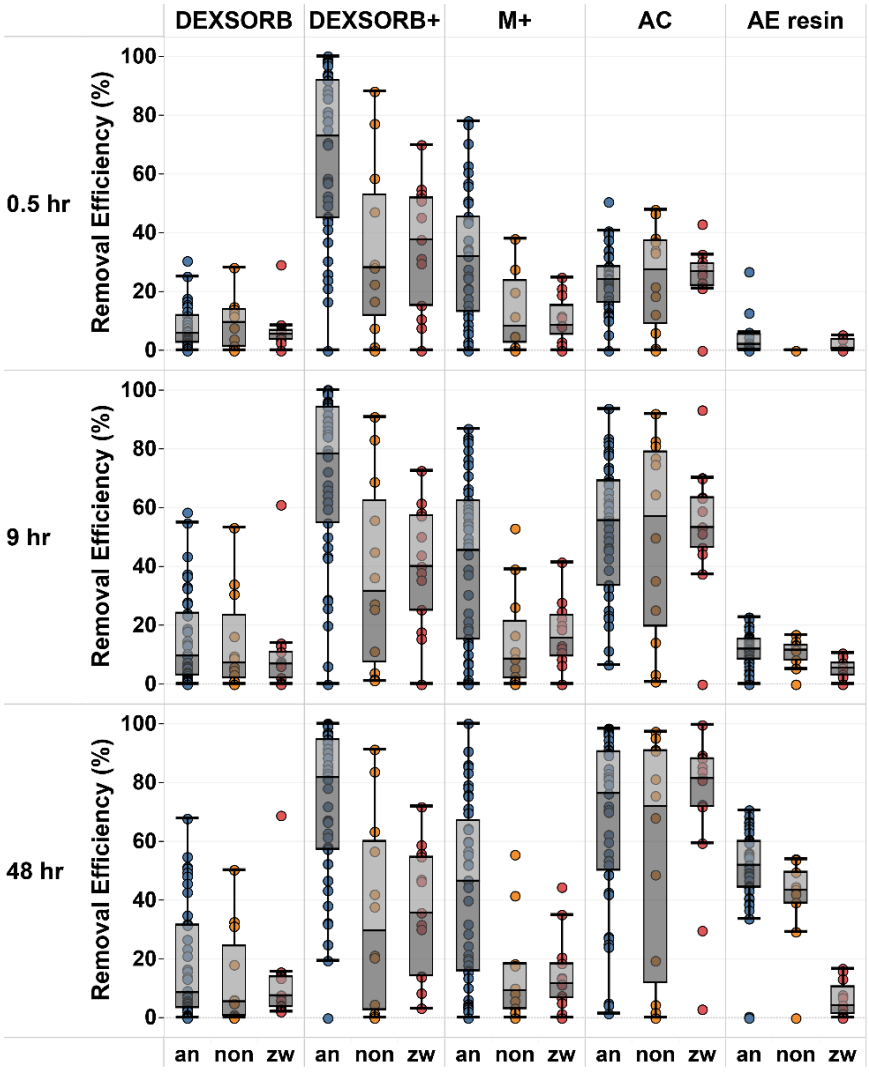

Figure 2-1. Blue data represent anionic (an) PFASs, orange data represent nonionic (non) PFASs, and red data represent zwitterionic (zw) PFASs. Each data point represents the average removal efficiency of triplicate measurements. Error is generally smaller than the data points and is therefore not plotted, but the values are available in **Tables A-6** through **A-10**.

Compared to the other twelve zwitterionic PFASs in the groundwater sample, 6:2 FTSA-PrB has the longest chromatographic retention time, has a relatively long CF_2 chain length, and was

measured in positive polarity mode. These features suggest that 6:2 FTSA-PrB is relatively hydrophobic and that the cationic functional group dominates its adsorption behavior compared to its weakly acidic carboxylic acid group, making it a better adsorbate for DEXSORB than the other zwitterionic PFASs.

Second, the adsorption kinetics are relatively rapid for DEXSORB+ and M+, and relatively slow for AC and the AE resin. This observation is consistent with our previous studies reporting nearly instantaneous uptake of organic chemicals on CDPs[75,85] and the known diffusion-limited kinetics associated with AC.[106,112] We attribute the relatively slow adsorption kinetics observed for the AE resin to the relatively large particle size of the AE resin (**Table A-1**) and the relatively low concentration of adsorbents used in this study; research conducted with pulverized AE resin particles or at higher resin concentrations has resulted in more rapid adsorption of PFASs.[113,114]

Finally, considering the data from 48 hr of contact time, AC exhibits the most non-selective removal of the 68 PFASs from groundwater with >80% removal noted for at least one anionic, nonionic, and zwitterionic PFAS. This observation demonstrates that AC has the potential to remove PFASs of all ionized states from AFFF-contaminated groundwater, albeit with relatively slow adsorption kinetics. The removal of 16 PFASs (including PFSAs, PFCAs, FASAs, SPr-FASAs, and two PFOS-like components) on AC aligns well with previous studies that have evaluated PFAS removal on AC in contaminated groundwater.[106,107] DEXSORB+ is best suited to rapidly remove anionic PFAS from AFFF-contaminated groundwater, with additional rapid removal noted for some nonionic and zwitterionic PFASs. DEXSORB, M+, and the AE resin

exhibit some potential to remove some specific PFASs from AFFF-contaminated groundwater, but do not exhibit consistent removal among the different classes of PFASs.

2.3.2 Effects of PFAS properties on removal from groundwater

To the best of our knowledge, this is the first study that has systematically examined the removal of PFASs from AFFF-contaminated groundwater using five different adsorbents and a dedicated suspect screening approach. As a result, we generated a dataset that offers the best opportunity to examine the effects of chain length and head group on PFAS removal efficiency with both conventional and emerging adsorbents.

Our suspect screening revealed the presence of at least one PFAS constituent among 29 unique classes of PFASs (**Table A-4**). Eleven of those classes contain at least three unique homologues with varying CF_2 chain length (**Table A-11**). To evaluate the effect of chain length on PFAS removal efficiency among the five adsorbents, we performed a Pearson correlation analysis between the CF_2 chain length and the removal efficiency observed at 48 hr across the eleven PFAS classes. The slope and coefficient of determination (R^2) of the regression for each of the eleven classes and for each of the five adsorbents are provided in **Table 2-1**. Increasing CF_2 chain length primarily results in increasing hydrophobicity of PFAS species, but may also alter other physicochemical properties of PFAS that influence adsorption including electronic[114,115] and steric[116,117] properties. We observed a positive and significant association (p-value < 0.05) for the PFSAs (perfluorosulfonic acids) and the FASAs (perfluoroalkane sulfonamide) across all of the CDPs and AC, regardless of the extent of removal observed for any individual member of these classes on any adsorbent. This finding suggests that chain length plays a considerable role in the removal of these two classes of anionic PFASs. Interestingly, a positive and significant association (p-value < 0.01) was also observed for FASA removal on the AE resin, which suggests a role for

hydrophobic interactions on the removal of this putatively nonionic class of PFAS on the AE resin or increasing deprotonation of the sulfonamide functional group with increasing chain length.[114,115] A positive and significant association (p-value < 0.10) was also observed for the PFCAs (perfluorocarboxylic acids) and the MeFASAAs (N-methyl perfluoroalkane sulfonamido acetic acids) on M+ and DEXSORB+, again highlighting the role of chain length on the removal of these anionic PFASs by CDPs with a positive surface charge. No significant association was observed for the PFCAs or the MeFASAAs on DEXSORB or the AE resin, reflecting the limited removal of these two classes of PFASs on DEXSORB and the relative importance of electrostatic interactions on their removal on the AE resin. None of the remaining classes exhibited a consistent set of significant associations among the adsorbents, though the strongest positive associations were consistently found for M+ (SPr-FASA), DEXSORB+ (MeFASA, SPrAmPr-FASAA), and AC (H-PFCA, FASAA, SPrAmPr-FASAA), with weaker positive associations found for

Table 2-1. Pearson correlation analysis between removal efficiency (%) in groundwater sample and CF_2 chain length for different PFAS classes.

Class		M+		DEXSORB+		DEXSORB		AC		AE resin	
Acronym	n	Slope	R^2	Slope	R^2	Slope	R^2	Slope	R^2	Slope	R^2
PFCA	6	9.3*	0.63	14.2***	0.96	2.8	0.38	16.8***	0.96	2.5	0.40
PFSA	7	12.8***	0.96	9.4***	0.86	8.1***	0.93	15.7***	0.92	-2.4*	0.57
H-PFCA	3	1.0	0.96	17.3	0.93	1.0	0.03	23.9*	0.99	2.0	0.26
H-PFSA	4	-0.2	0.00	0.3	0.04	4.8	0.38	2.8	0.25	-5.0*	0.82
FASA	6	11.7***	0.91	18.2***	0.99	6.2**	0.77	20.0***	0.97	4.7***	0.89
FASAA	3	23.0	0.97	17.0	0.95	1.4	0.31	18.6**	1.00	-4.1**	1.00
MeFASA	3	6.3	0.89	21.0*	0.98	22.1**	0.99	10.9	0.95	2.9	0.87
MeFASAA	3	20.5*	0.98	16.4**	1	3.4	0.63	19.3	0.87	-6.3	0.6
SPr-FASA	3	13.3**	1.00	5.8	0.96	-0.2	0.75	13.0	0.68	-5.6	0.33
SPrAmPr-FASAA	3	13.8	0.91	20.9**	1.00	1.8	0.51	11.0*	0.99	-0.6	0.08
SPrAmPr-FASAPrS	3	16.6	0.94	20.8	0.95	6.7*	0.99	6.7	0.97	5.9**	1.00

***, ** and * represent $p < 0.01$, $p < 0.05$ and $p < 0.10$, respectively; **n** refers to the number of observations.

DEXSORB (MeFASA, SPrAmPr-FASAPrS) and both positive (SPrAmPr-FASAPrS) and negative (H-PFSA, FASAA) associations found for AE resin.

The same 11 homologous series were examined to evaluate the effect of the head group on PFAS removal efficiency among the five adsorbents. We noted that 10 of these 11 classes contain at least two homologues with either 4, 6, or 8 CF_2 units. Therefore, we compared the removal efficiencies measured at 48 hr for all PFASs in the 10 homologous series with 4, 6, or 8 CF_2 units; we also include H-PFHpS as a representative H-PFSA with 6 CF_2 units. The results are presented in **Figure 2-2** for M+, DEXSORB+, and AC and in **Figure A-2** for DEXSORB and the AE resin. First, we found that the removal of PFASs with a sulfonic acid head group is always greater than the removal of PFASs with a carboxylic acid head group when the rest of the structure is the same across all five adsorbents. This finding corroborates other studies that have noted this trend among PFAAs,[77,91,108,118,119] but our data can be used to generalize this finding to include the H-PFSAs and H-PFCAs. Interestingly, we also note that H-PFSAs that only differ from PFSAs by one H/F atom are also removed to greater extents by all adsorbents, and the difference is magnified at lower CF_2 chain lengths (**Tables A-6** through **A-10**). Second, we found that the FASAAs (perfluoroalkane sulfonamide acetic acid) were consistently removed to greater extents among all of the adsorbents than the FASAs when the rest of the structure is the same. We attribute this observation to the increased hydrophobicity of FASAAs relative to FASAs (resulting from their larger size) which enhances affinity for all three adsorbents, and the anionic carboxylic acid head group of the FASAAs which enhances affinity for DEXSORB+ and M+. Third, we found that MeFASAA (N-methyl perfluoroalkane sulfonamide acetic acid) was consistently removed to greater extents among M+ and DEXSORB+ than MeFASA (N-methyl perfluoroalkane sulfonamide) when the rest of the structure is the same, but the opposite trend emerged for these

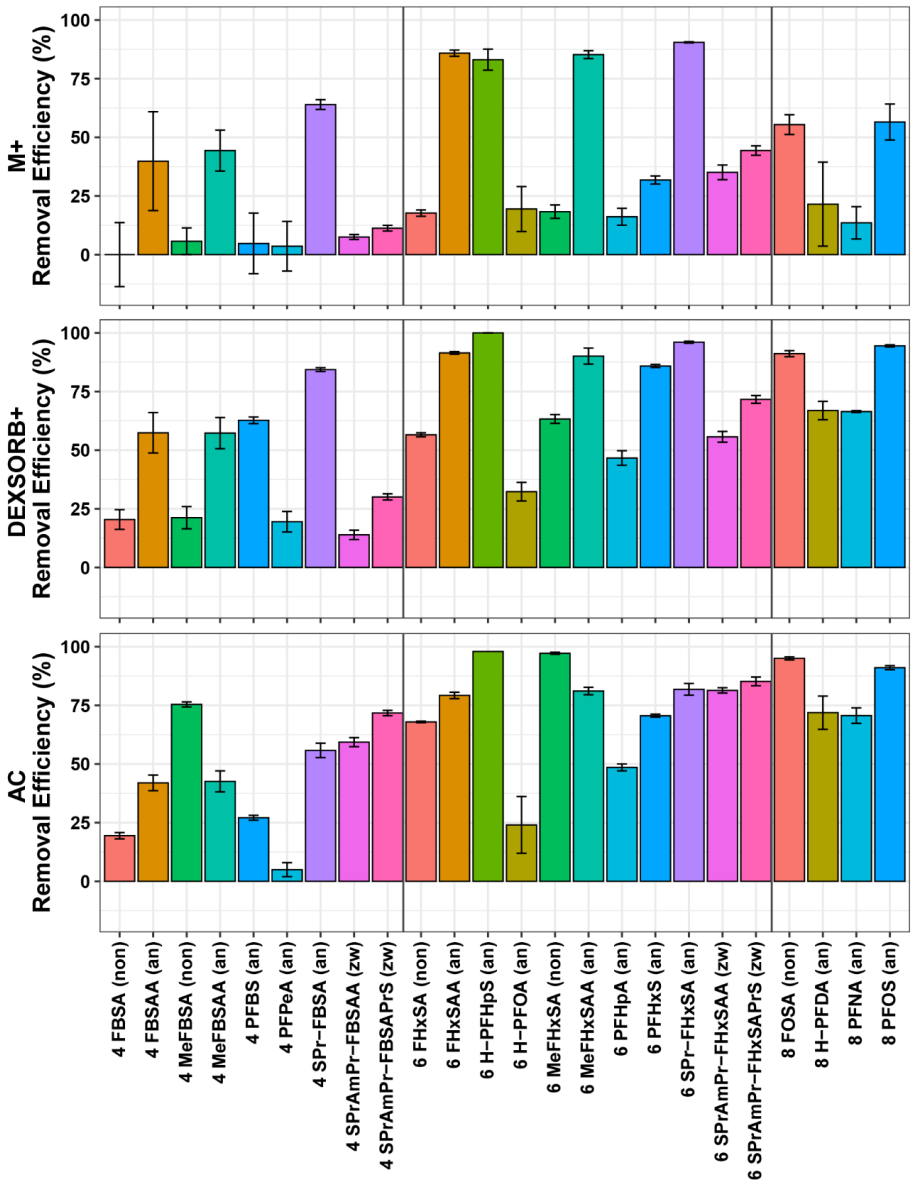

Figure 2-2. Bar plots showing the removal efficiencies for PFASs in 11 different homologous series grouped by 4, 6 and 8 CF_2 chain length on M+, DEXSORB+ and AC after 48 hr contact time. On the horizontal axis, the number in front of PFAS acronym represents the CF_2 chain length counted as the total number of perfluorinated carbon atoms. The notations in the parentheses represent anionic (an) PFASs, nonionic (non) PFASs, and zwitterionic (zw) PFASs.

PFAS classes on AC. The disparate behavior of the MeFASAAs and MeFASAs on AC (relative to the FASAAs and FASAs) may be evidence that the increased hydrophobicity of the MeFASAAs (resulting from their larger size) is insufficient to counteract the effects of the anionic carboxylic acid head group of the MeFASAAs which creates a repulsive electrostatic interaction with the AC

with a negative surface charge (**Table A-1**). Finally, among the three classes of PFASs containing both sulfonamide and sulfonic acid functional groups, we again found similar trends among M+ and DEXSORB+, and a different trend for AC. M+ and DEXSORB+ exhibit the greatest removal of the smallest class, SPr-FASA (perfluoroalkane sulfonamide propanesulfonic acid), and limited removal of the larger, branched classes SPrAmPr-FASAA (N-sulfopropyl dimethyl ammonio propyl-perfluoroalkane sulfonamide acetic acid) and SPrAmPr-FASAPrS (N-sulfopropyl dimethyl ammonio propyl-perfluoroalkane sulfonamido propylsulfonate). We attribute this finding to limited access to the binding sites in the interior cavity of the β-cyclodextrins for the larger, branched classes of PFASs.[75,88] AC exhibits consistent removal among all three classes, demonstrating that neither the head group nor the branching influences adsorption on AC.

2.3.3 Environmental implications

Remediation of PFAS-contaminated groundwater is challenging and solutions must be evaluated with respect to complex mixtures of PFAS species, variable concentrations among PFAS species, and in the presence of groundwater matrix constituents. Our data reveal that conventional and emerging adsorbents exhibit variable adsorption kinetics and affinity for different types of PFASs in AFFF-contaminated groundwater. These findings suggest that different adsorbents may be better suited for applications that rely on limited contact time or required the removal of specific PFASs. Our analysis of chain length and head groups suggests that removal of some short-chain perfluoroalkyl substances (including PFCAs and FASAs) from groundwater will be challenging for all of the adsorbents studied, but removal of PFBS and short-chain polyfluoroalkyl substances (including FASAAs and substituted sulfonamides or sulfonamide acetic acids) can be achieved with one or more adsorbent.

CHAPTER 3 – Identifying the Relative Contributions of Hydrophobic and Electrostatic Interactions on Adsorption of Perfluoroalkyl Acids on Cyclodextrin Polymers

Abstract

Despite the efficacy of CDPs for removing anionic PFASs from water, there remain questions about the relative contributions of hydrophobic and electrostatic interactions on the adsorption mechanisms. We utilized a newly developed CDP platform called styrene-linked cyclodextrin polymers (Stydex) to probe the adsorption binding mechanisms across polymers more accurately. We synthesized three Stydex adsorbents with different surface charge and/or crosslinker hydrophobicity. We then conducted equilibrium adsorption experiments with mixtures of anionic PFASs in nanopure water and different salt-amended nanopure water matrices. We used the resulting data to explain the relative contributions of hydrophobic and electrostatic interactions on the adsorption of the anionic PFASs as a function of perfluoroalkyl chain length. We found that short-chain PFASs mostly rely on electrostatic interactions while long-chain PFASs rely on both electrostatic and hydrophobic interactions. In salt solutions, the performance of positively charged CDPs is inhibited while the performance of negatively charged CDPs is enhanced. The difference of crosslinker hydrophobicity is not an important factor for the adsorption. Higher salt concentration can bring more inhibition or more enhancement on the removal performance, but the effects can get saturated as the salt concentration keeps increasing. The adsorption inhibition on positively charged CDPs is likely linked to direct-site competition and/or a screening effect that decreases the electrostatic attraction. The adsorption enhancement on negatively charged CDPs is likely attributed to the bridging effect for polyvalent cations and/or a screening effect which

decreases the electrostatic repulsion thus facilitates the formation of host-guest complexation. Different valences of inorganic anions (or cations) have different extent of impacts on positively (or negatively) charged adsorbents, where divalent ions have a more significant impact than monovalent ions. Our study provides new insights into the anionic PFAS adsorption mechanisms on CDPs and reveals the impact of different types and concentrations of inorganic constituents on the adsorption mechanism.

3.1 Introduction

The adsorption of anionic PFASs on a variety of adsorbent types has demonstrated the efficacy of adsorption processes for PFAS remediation.[2,55] Conventional adsorbents such as activated carbon,[120,121] ion exchange resins,[77,79,114,120] and mineral materials (e.g., activated alumina,[122] silica,[123] zeolite,[124] kaolinite,[109] and montmorillonite[125]), have been widely investigated for removing PFASs from water. Moreover, biomaterials such as crosslinked chitosan beads,[126] novel materials such as cyclodextrin polymers (CDPs),[91,101,127] and other emerging adsorbents such as magnetite nanoparticles[81,82] and metal organic frameworks[83] have also exhibited their potential as suitable adsorbents for PFAS removal from water.

Among all types of adsorbents, CDPs are one of the most promising emerging adsorbents for PFAS removal, because of their rapid adsorption kinetics, high adsorption affinity, selectivity for target adsorbates, and potential for facile regeneration and reuse.[85,93–95] CDPs are designed to remove organic pollutants rapidly and efficiently from water matrices based on size-exclusive, host-guest complexation. Several promising CDPs for water remediation have been reported. For example, P-CDP (marketed commercially as DESORB) is a CDP with a negative surface charge that exhibits rapid removal of many types of organic micropollutants (MPs), especially neutral and cationic MPs and zwitterionic PFASs, and exhibits the capability of maintaining good performance in the presence of natural organic matter (NOM) and inorganic matrix constituents.[75,94,95] Previous studies have also demonstrated the superiority of CDPs with a positive surface charge (e.g., CDP+ which is marketed commercially as DEXSORB+, amine-CDP, and M+) for the removal of anionic PFASs when compared to activated carbon and ion exchange resin.[93–95]

Despite the efficacy of CDPs for removing anionic PFASs from water, there remain questions about the relative contributions of hydrophobic and electrostatic interactions to the

adsorption mechanism. As presented in **Figure 3-1**, we expect the interior cavity of the cyclodextrin monomer to be the primary binding site for adsorption, where target PFASs form host-guest complexes that are driven by hydrophobic interactions.[86] However, previous data suggest the surface charge on the crosslinker may play at least a complementary role,[95,102,118] though the mechanism of the apparent electrostatic interaction is poorly understood. We expect that the surface charge could: (i) be a separate binding site for anionic PFASs; (ii) facilitate the transport of anionic PFASs to the binding site by means of attractive electrostatic interactions (for an adsorbent with a positively charged surface); or (iii) limit or prohibit access to the binding site by means of repulsive electrostatic interactions (for an adsorbent with a negatively charged surface). Further, we expect the relative importance of the electrostatic interactions versus

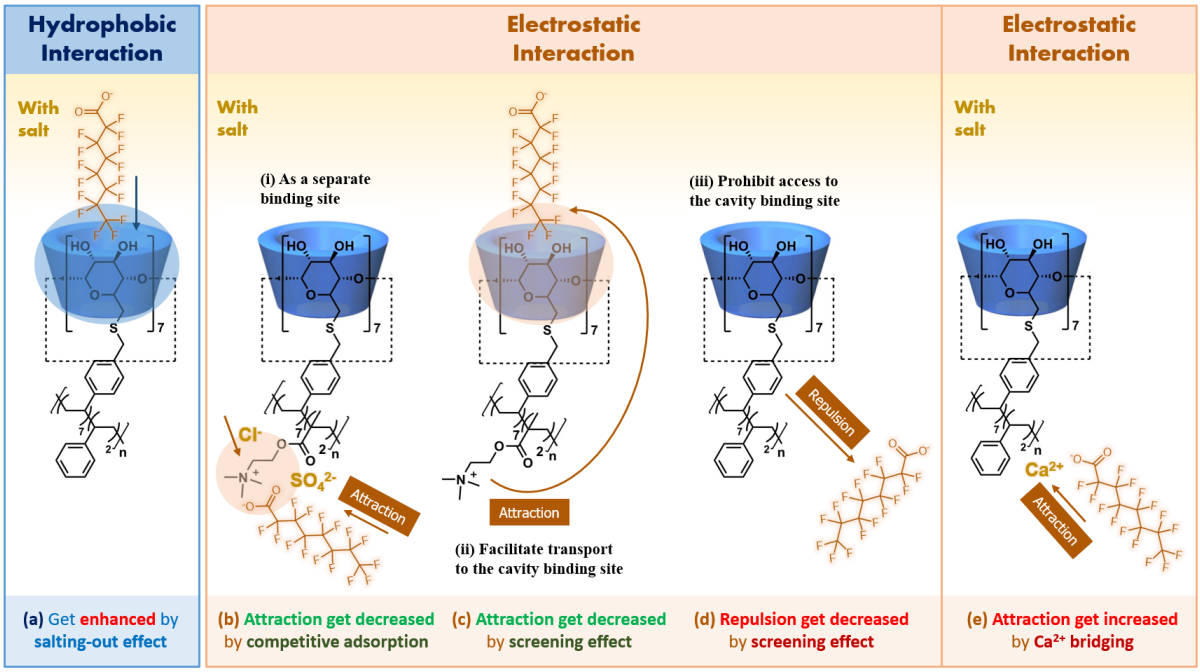

Figure 3-1. Schematic diagram for hydrophobic (left) and electrostatic interactions (right, examples **(i)-(iii)**) for anionic PFAS adsorption on CDPs along with potential effects of inorganic ions on adsorption mechanisms (examples **(a)-(e)**).

hydrophobic interactions to be dependent on the chain-length (or hydrophobicity) of the target PFASs.

One way to evaluate the role of electrostatic interactions on an adsorption process is to evaluate the adsorption behavior in the presence and absence of different types of salts. Any changes in ionic strength (or the concentration of co-occurring inorganic ions) could influence adsorption by inhibiting or enhancing electrostatic interactions.[2,55] Adsorption experiments investigating different types and concentrations of salts have been conducted by many researchers. For adsorbents that rely on a positive surface charge to remove anionic PFASs by means of attractive electrostatic interactions, the adsorption is typically inhibited by the presence of inorganic ions. Mechanisms of adsorption inhibition include direct-site competition (effect **b** in **Figure 3-1**) with inorganic anions (e.g., Cl^-, $SO_4^{2-}$and $Cr_2O_7^{2-}$) [2,55,79,128] competing with anionic PFASs for adsorption sites and a screening effect (effect **c** in **Figure 3-1**) that limits attractive electrostatic interactions due to a compression of the electrical double layer (EDL)[129] where both mechanisms **(i)** and **(ii)** can be inhibited. For adsorbents with a negative surface charge that exhibit limited removal of anionic PFASs due to repulsive electrostatic interactions, the adsorption is typically enhanced by the presence of inorganic ions. Mechanisms of adsorption enhancement include cation bridging (effect **e** in **Figure 3-1**) facilitated by polyvalent cations (e.g., Ca^{2+}, Mg^{2+}, Cu^{2+}, Al^{3+}, and Fe^{3+})[108,130–132] and a screening effect (effect **d** in **Figure 3-1**) that limits repulsive electrostatic interactions due to the compression of the EDL.[109,122,128,133,134] Both of these enhancement mechanisms affect adsorption mechanism **(iii)**. Finally, adsorption driven by hydrophobic interactions can also be enhanced at relatively high salt concentrations due to a so-called salting-out effect (effect **a** in **Figure 3-1**); the solubility of organic molecules decreases as

salt concentrations increase which can lead to a forced partitioning to an adsorbent driven by hydrophobic interactions.[2,55,129,135]

The goal of this study was to evaluate the relative contributions of hydrophobic and electrostatic interactions on the removal of anionic PFASs from water by cyclodextrin polymers. To achieve this, we synthesized styrene-linked cyclodextrin polymers (Stydex) with a positive surface charge and a putatively neutral (actually slightly negative) surface charge, which are based on a new CDP platform enabling us to probe the adsorption binding mechanisms across polymers more accurately. We then conducted equilibrium adsorption experiments with different mixtures of perfluoroalkyl acids (PFAAs) in: (i) nanopure water; (ii) nanopure water amended with different concentrations of Na_2SO_4; and (iii) nanopure water amended with different salts at equimolar concentrations of specific anions and cations. We evaluated the performance of three Stydex adsorbents for the removal of seven perfluorocarboxylic acids (PFCAs) and four perfluorosulfonic acids (PFSAs). We used the resulting data to explain the relative contributions of hydrophobic and electrostatic interactions on the adsorption of the anionic PFASs as a function of chain-length (or PFAS hydrophobicity).

3.2 Materials and Methods

3.2.1 Adsorbents

In collaboration with Prof. William Dichtel and Dr. Max Klemes from Northwestern University, we synthesized three novel cyclodextrin-based polymers for this study. Whereas previously described cyclodextrin-based polymers exhibit random crosslinking and may undergo uncharacterized side reactions during polymerization that make it difficult to characterize the final structure of the material, the new cyclodextrin-based polymer system developed for this study employs a discrete styrene-linked cyclodextrin monomer that enables controlled polymerization reactions that are nearly quantitative with no side reactions. This system enables the synthesis of cyclodextrin-based polymers that are nearly identical from a physical perspective (e.g., high surface area > 200 m^2 g^{-1} and high yield > 90%) but can be functionalized to impart desirable physicochemical properties (e.g., crosslinker hydrophobicity, surface charge) to the polymer. The three novel cyclodextrin-based polymers synthesized for this study are shown schematically in

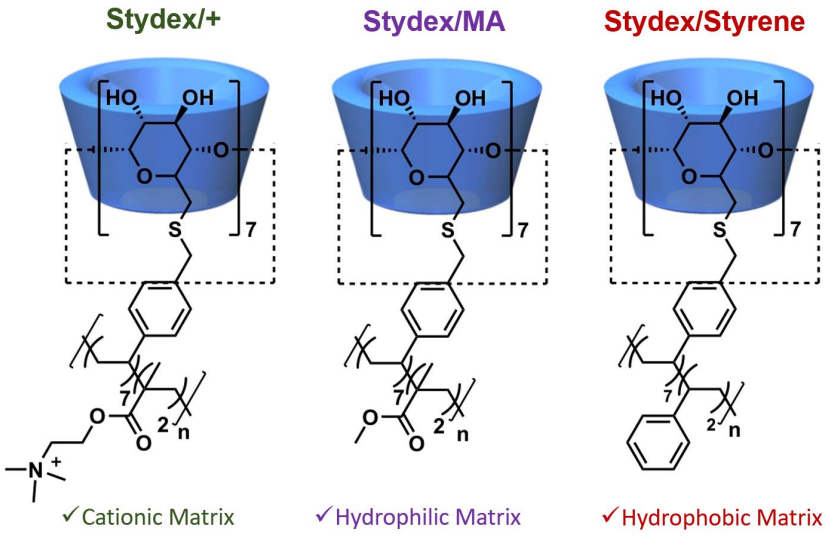

Figure 3-2. Schematic chemical structures of three Stydex adsorbents. Stydex/+ carries a permanently positive surface charge due to the trimethylammonium functional group. Stydex/MA and Stydex/Styrene carry a slightly negative surface charge as indicated by a zeta potential measurement reported in **Table B-1**; the specific functional groups that lead to the negative surface charge are unknown.

Figure 3-2 and are characterized by a cationic crosslinker (Stydex/+), a neutral hydrophilic crosslinker (Stydex/MA), and a neutral hydrophobic crosslinker (Stydex/Styrene). Detailed material characterization information is provided in **Table B-1** of **Appendix B**.

3.2.2 Chemicals and reagents

Two PFAS mixtures of anionic PFASs (PFC-MXA and PFS-MXA) and one mixture of PFAS isotope-labelled internal standards (ILISs) (MPFAC-MXA) were purchased from Wellington Laboratories, Inc. The PFC-MXA mixture contains eleven PFCAs (C4 through C14) dissolved in methanol each at a concentration of 2 mg L^{-1}. The PFS-MXA mixture contains five PFSAs (C4, C6-C8, and C10) dissolved in methanol each at a concentration of 2 mg L^{-1}. The MPFAC-MXA mixture contains seven isotope-labelled PFCAs (C4, C6, C8-C12) and two isotope-labelled PFSAs (C6 and C8) dissolved in methanol each at a concentration of 2 mg L^{-1}. The PFAS standard spike mixtures were diluted from the stock mixtures (PFC-MXA and PFS-MXA) using nanopure water to yield a concentration of 1 mg/L. The ILIS spike mixture was diluted from MPFAC-MXA using nanopure water to yield a concentration of 250 μg L^{-1}. The stock mixtures and the spike mixtures were stored at -20°C and 4°C, respectively. A summary of all PFAS standards and their respective ILISs used for quantification is provided in **Table B-2** of **Appendix B**. Sodium sulfate (Sigma-Aldrich), calcium chloride (Sigma-Aldrich), and sodium chloride (Fisher Scientific) were purchased as solid salts and were stored at room temperature until use.

3.2.3 Rotator batch experiments

Adsorption experiments were conducted in 15 mL polypropylene centrifuge tubes (Corning) with either 10 mL of nanopure water or salt-amended nanopure water as follows: 0.1 mM, 0.5 mM, 1 mM, and 2 mM Na_2SO_4; 2 mM NaCl; or 1 mM $CaCl_2$ as previously described.[93–95] Briefly, all adsorption experiments were conducted with either the PFCA or the PFSA mixture

at a starting concentration of 1 μg/L at pH of 5.5 ~ 6 and an adsorbent concentration of 1 mg L^{-1}, 10 mg L^{-1}, or 100 mg L^{-1} in triplicate. Prepared centrifuge tubes were placed on a tube revolver and rotated at 40 rpm at 23 °C for 48 hr. After rotating, samples were filtered through 0.45 μm cellulose acetate filters (Restek) and transferred into 10 mL glass LC-MS vials (ThermoFisher Scientific). Then all triplicate samples were spiked with the ILISs and stored at 4 °C until analysis. Control experiments were conducted in triplicate using the same procedure but in the absence of adsorbents. Samples were measured to quantify the PFASs included in the experiment. The average and the standard deviation of removal efficiency were calculated based on the triplicate concentrations of each PFAS in the experimental group and the control group.

3.2.4 Analytical methods

Quantification of target PFCAs or PFSAs in all prepared samples (spiked with ILISs) was conducted using high-performance liquid chromatography (HPLC) coupled with high-resolution mass spectrometry (HRMS, quadrupole-orbitrap, ThermoFisher Scientific) using a parallel reaction monitoring (PRM) method optimized for PFAS quantification.[136] For the liquid chromatography parameters, we used previously established methods described in **Appendix B**.[93–95] The HPLC-MS was operated with electrospray ionization in negative polarity mode for all PFAS measurements. The PRM acquisition method relies on a list of targeted precursor ions, a retention time window, and optimized collision energies for each PFAS. When detecting a targeted ion, the system isolates that precursor ion in the quadrupole and triggers the MS/MS experiment, generating MS/MS spectra that can be used for both quantitation and qualitative identification. Both the quantitation and identification are performed taking into account product ions generated after the isolation of a specific precursor ion. PRM monitors all product ions of a mass-selected targeted compound in parallel with one ion injection and full mass range Orbitrap mass analysis.

Analytical information of all PFASs and their ILISs is provided in **Table B-3** of **Appendix B**. Matrix-matched calibration standards (n = 9) were prepared with concentrations ranging between 0 ng L^{-1} to 1000 ng L^{-1}. Analytes were quantified from the calibration standards (spiked with the same amount of ILISs) based on the PFAS target-to-ILIS peak area ratio responses of the designated quantitation product ion by linear least-squares regression. Calibration curves were run at the beginning of the analytical sequence. Instrument blanks (with no target PFASs nor ILISs) were run before and after the calibration curve and each batch of triplicate samples. Two quality control (QC) samples (with target PFASs and ILISs) were placed at the start and end of every analytical sequence, to ensure minimal contamination and adequate MS performance (QC tolerance set at ± 30%). PFAS spike controls were used to determine the PFAS recovery rate during analysis; recovery rate threshold was set at ± 50% for each PFAS to be considered as reliable data.

3.3 Results and Discussion

3.3.1 Removal of PFCAs by Stydex adsorbents

We first aimed to evaluate the performance of the novel Stydex polymers for the removal of PFCAs in nanopure water. For Stydex/+, Stydex/MA, and Stydex/Styrene at 10 mg L^{-1} and with an initial concentration of 1 μg L^{-1} of each PFCA, the results of this experiment are presented as white bars in **Figure 3-3**. We only show data for the C4-C10 PFCAs because the C11-C14 PFCAs failed our recovery rate threshold in the spike control experiments. By comparing PFCA removal in the nanopure water matrix among the different adsorbents, Stydex/+ exhibits superior removal performance among all three Stydex adsorbents under the same adsorbent dose (10 mg L^{-1}). Short-chain and long-chain PFCAs (from PFBA to PFDA) are removed to more than 95% in nanopure water by Stydex/+. Stydex/Styrene and Stydex/MA exhibit poor removal for all tested PFCAs of which their removals are all below 10%. Additionally, Stydex/Styrene and Stydex/MA perform very similarly, suggesting that the difference of the crosslinker hydrophobicity does not affect their adsorption performance significantly. Comparing with Stydex/Styrene and Stydex/MA, the exceptionally high affinity of Stydex/+ indicates the expected importance of electrostatic interactions, as the only difference between Stydex/+ and Stydex/MA is the trimethylammonium

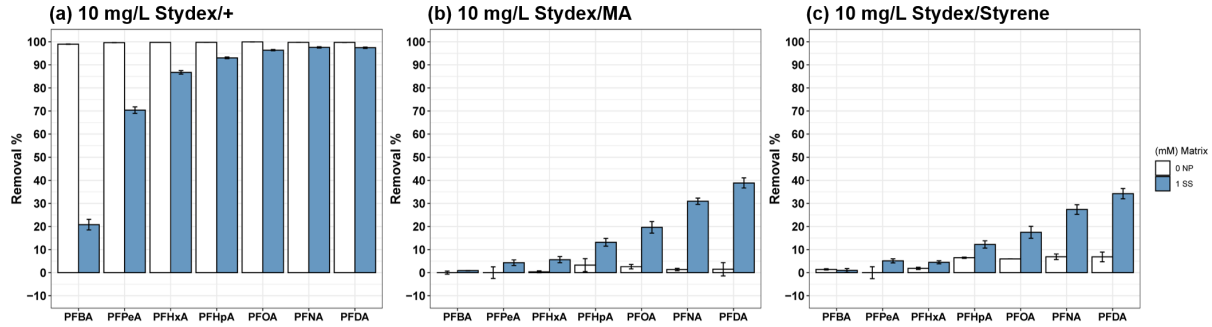

Figure 3-3. PFCAs removal by (a) 10 mg L^{-1} Stydex/+, (b) 10 mg L^{-1} Stydex/MA, and (c) 10 mg L^{-1} Stydex/Styrene in nanopure water (0 NP, white bar) and in 1 mM Na_2SO_4 solution (1 SS, blue bar) after 48 hr contact time.

cationic functional group. Additionally, the removal performance of Stydex/+ for PFCAs is also better than by any other previously studied CDPs including DEXSORB+ and M+.[93–95]

To further evaluate the role of electrostatic interactions on PFCA adsorption to the Stydex polymers, we performed the same experiment (with 10 mg L^{-1} of each adsorbent and an initial concentration of 1 μg L^{-1} of each PFCA) in a 1 mM Na_2SO_4 matrix. The results of this experiment are presented as blue bars in **Figure 3-3**. We found that the removal performance of Stydex/+ for all PFCAs is inhibited in the salt solution, while the removal performances of Stydex/MA and Stydex/Styrene are enhanced in the salt solution. Besides, we note that either the inhibition or the enhancement effects are not equal for PFCAs with different chain lengths. On the one hand, the short-chain PFCAs are inhibited more than long-chain PFCAs on Stydex/+, which implies that with the existing inorganic ions interfering with the electrostatic attractions between PFCAs and Stydex/+, the electrostatic interaction might be a relatively more important mechanism for short-chain PFAS removal. On the other hand, the magnitude of enhanced uptake of long-chain PFASs are larger than that of short-chain PFASs on Stydex/MA and Stydex/Styrene, which implies that the inorganic ions interfere with the repulsive electrostatic interactions between Stydex/MA and Stydex/Styrene, facilitating adsorption by hydrophobic interactions which are more important for the more hydrophobic long-chain PFCAs.

To better observe the magnitude of the adsorption inhibition or enhancement for PFCAs of different chain length on different Stydex adsorbents, we repeated the experiments in nanopure water and in 1 mM Na_2SO_4 solution at different adsorbent doses. Because Stydex/+ performed so well showing no removal difference among short- and long-chain PFCAs at 10 mg L^{-1} in the nanopure water matrix, the adjusted dose is set to 1 mg L^{-1}. Stydex/MA and Stydex/Styrene performed rather poorly for all PFCAs at 10 mg L^{-1} doses, so we increased their doses to 100 mg

L^{-1}. The data in **Figure 3-4** shows the performance of Stydex/+ at 1 mg L^{-1} and of Stydex/MA and Stydex/Styrene at 100 mg/L^{-1}. From these experiments, we see the removals of PFCAs on Stydex/+ start to be different among short-chain and long-chain PFCAs ranging from 57% to 97% in nanopure water, suggesting that the hydrophobic interactions play a role in PFAS adsorption on Stydex/+. With an increased dose (100 mg L^{-1}) of the Stydex/MA and Stydex/Styrene, the same trends are also observed in nanopure water, though the PFCA removals are still all less than 20% in nanopure water. In the 1 mM Na_2SO_4 matrix, the patterns of inhibition using Stydex/+ and enhancement using Stydex/MA and Stydex/Styrene are more obvious with adjusted doses of adsorbents. In summary, the results from these experiments reinforce the conclusions we observed from **Figure 3-3**, and the new polymer doses are useful for demonstrating the hydrophobic interactions as a function of CF_2 chain length.

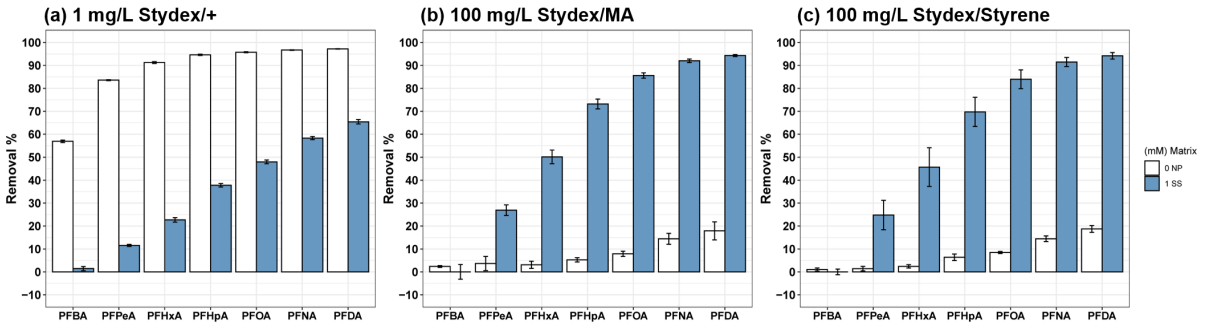

Figure 3-4. PFCAs removal by (a) 1 mg L^{-1} Stydex/+, (b) 100 mg L^{-1} Stydex/MA, and (c) 100 mg L^{-1} Stydex/Styrene in nanopure water (0 NP, white bar) and in 1 mM Na_2SO_4 solution (1 SS, blue bar) after 48 hr contact time.

3.3.2 Removal of PFSAs by Stydex adsorbents

To verify whether the adsorption trends observed between the three Stydex adsorbents and the PFCAs are also true for the PFSAs, we repeated the experiments with the modified adsorbent doses in nanopure and in 1 mM Na_2SO_4 with the PFSA mixture. The results of these experiments are presented in **Figure 3-5** for nanopure (white) and the Na_2SO_4 matrix (blue). We only show data for the C4 and C6-C8 PFSAs because PFDS failed our recovery rate threshold in the spike

controls. Our findings show that Stydex/+ again exhibits moderate to high removal for PFSAs in nanopure, that Stydex/MA and Stydex/Styrene again perform poorly for PFSAs in nanopure, that salt inhibits adsorption for Stydex/+ and enhances adsorption on Stydex/MA and Stydex/Styrene, and that the inhibition or enhancement is again related to the CF_2 chain length, likely due to the same mechanisms described for PFCAs.

The experiments with the mixture of PFSAs also allowed us to test whether competitive adsorption could explain the relative performance of PFASs of varying chain length. Competitive adsorption of PFASs is usually explained by longer-chain PFASs replacing shorter-chain PFASs on the adsorbent surface over time due to the greater hydrophobic interactions.[109,137] We reasoned that if competitive adsorption was a factor for the PFCAs where eleven species were examined at 1 μg L^{-1}, then we should see less of an effect of chain-length on the adsorption of the five PFSAs which were also at 1 μg L^{-1} because there would be fewer long-chain PFSAs to compete with the short-chain PFSAs. Because we observed the no weaker extent of adsorption inhibition or enhancement as a function of chain-length for the PFSAs as we observed with the PFCAs (i.e., the absolute values of slopes between removal difference and CF_2 chain length of PFSAs are all 10%-20% larger than those of PFCAs for all three adsorbents), we rule out competitive adsorption as a possible confounding factor in our study. Finally, considering Stydex/+ in both matrices and Stydex/MA and Stydex/Styrene in 1 mM Na_2SO_4, the PFSAs are better removed than the PFCAs

with the same CF_2 chain length, which corroborates other studies that have noted the greater adsorption of PFSAs on CDPs and other adsorbents.[77,91,108,118,119]

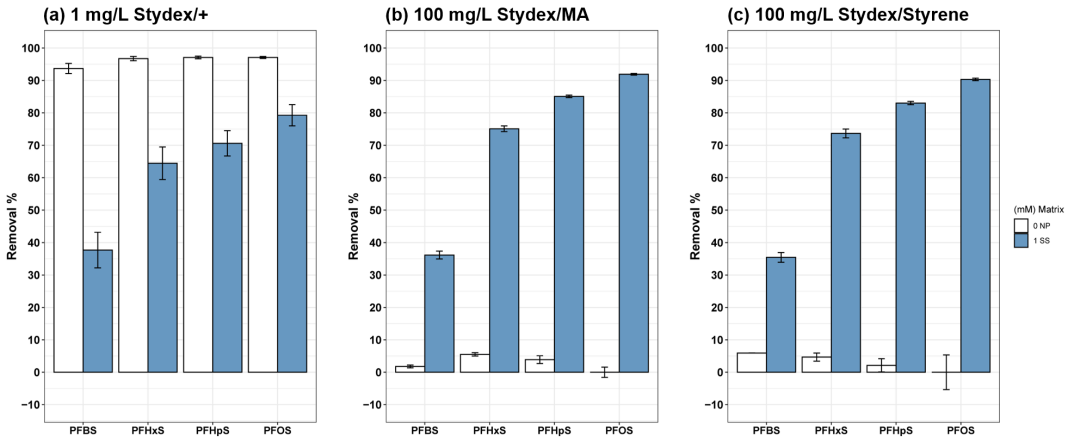

Figure 3-5 PFSAs removal by (a) 1 mg L^{-1} Stydex/+, (b) 100 mg L^{-1} Stydex/MA, and (c) 100 mg L^{-1} Stydex/Styrene in nanopure water (0 NP, white bar) and in 1 mM Na_2SO_4 solution (1 SS, blue bar) after 48 hr contact time.

3.3.3 Effects of different concentrations of inorganic ions

To evaluate the influences of varying salt concentrations on the adsorption of PFCAs on the three adsorbents, we conducted experiments with adjusted adsorbent doses in nanopure water amended with different Na_2SO_4 concentrations. The results of these experiments are presented in **Figure 3-6**. As the concentration of Na_2SO_4 increases, the removal efficiencies of Stydex/+ (1 mg L^{-1}) decrease, but the removal efficiencies of Stydex/MA (100 mg L^{-1}) and Stydex/Styrene (100 mg L^{-1}) increase. The adsorption performance of Stydex/MA and Stydex/Styrene resembles each other closely under all experimental conditions, affirming again that the hydrophobicity of the crosslinker does not play a significant role in the adsorption.

The increasing Na_2SO_4 concentration causes increasing adsorption inhibition on Stydex/+, which is most likely linked to direct-site competition (effect **b** in **Figure 3-1**) and a screening effect due to the compression of the EDL which eliminates the attractive electrostatic interactions (effect **c** in **Figure 3-1**). Increasing salt concentration could lead to a stronger salting-out effect resulting in the increase of hydrophobic interactions.[138] However, the removal of PFCAs on Stydex/+ is

decreased as salt concentration increases highlighting that the effects on electrostatic interactions are more important than the effects on hydrophobic interactions. Interestingly, we observe an apparent saturation of the adsorption inhibition effect at higher Na_2SO_4 concentrations. A small amount of Na_2SO_4 (0.1 mM) already has a dramatic effect on adsorption inhibition, but increases of Na_2SO_4 concentration up to 2 mM have a much weaker inhibition effect. Based on pairwise t-test results, there is no significant difference (**$p > 0.05$**) among the removal from 0.1 mM Na_2SO_4 to 2 mM Na_2SO_4. Therefore, the adsorption performance at 2 mM of Na_2SO_4 likely shows the performance of a CDP with a weakly positive (or near neutral) surface charge, where the adsorption we observe is likely entirely attributed to hydrophobic interactions. Based on this conclusion, we note that PFBA relies entirely on electrostatic interactions, while the hydrophobic and electrostatic interaction contribution ratio to the removal of PFDA in nanopure water on 1 mg

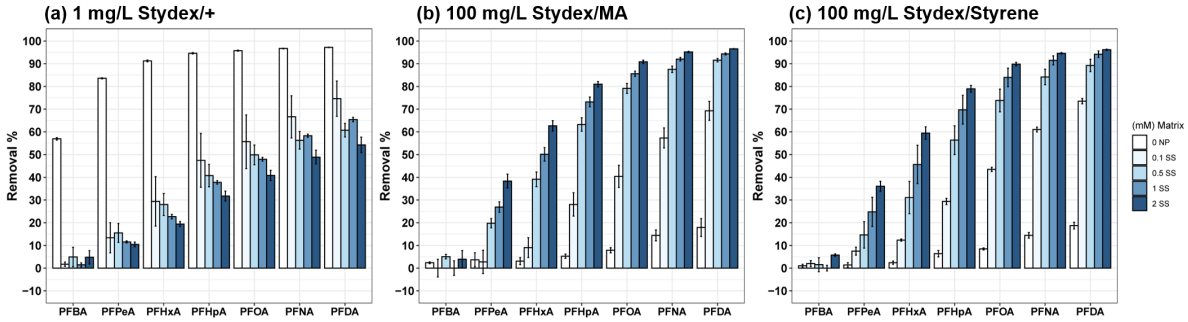

Figure 3-6. PFCAs removal by (a) 1 mg L^{-1} Stydex/+, (b) 100 mg L^{-1} Stydex/MA, and (c) 100 mg L^{-1} Stydex/Styrene in nanopure water (0 NP, white bar) and in various concentrations (0.1 mM, 0.5 mM, 1 mM, 2 mM) of Na_2SO_4 solution (from 0.1 SS to 2 SS, from light blue to dark blue bars) after 48 hr contact time.

L^{-1} Stydex/+ is about 50:50. These findings again highlight the relative importance of electrostatic interactions on PFAS removal from water, especially for short-chain PFASs; long-chain PFASs with greater hydrophobicity can still be removed at a decent rate in the absence of favorable electrostatic interactions.

The increasing Na_2SO_4 concentrations cause increasing adsorption enhancement on Stydex/MA and Stydex/Styrene, which is most likely linked to a screening effect that limits the

repulsive electrostatic interactions (effect **d** in **Figure 3-1**) and a salting-out effect which can increase the hydrophobic interaction between the adsorbent and PFCAs. Interestingly, we also observe an apparent saturation of the adsorption enhancement effect at higher Na_2SO_4 concentrations. A small amount of Na_2SO_4 (0.1 mM) already has a dramatic effect on adsorption enhancement and increasing the concentration to 0.5 mM Na_2SO_4 still has a considerable effect, but the further increases of Na_2SO_4 concentration up to 2 mM lead to a much smaller incremental enhancement of removal. The adsorption performance at 2 mM of Na_2SO_4 likely shows the performance of a CDP with a weakly negative (or near neutral) surface charge; the adsorption that we observe is again likely entirely attributed to hydrophobic interactions. It is worth noting that in **Figure 3-6** the removal on Stydex/MA and Stydex/Styrene at 2 mM of Na_2SO_4 is not directly comparable with the removal on Stydex/+, because the concentration of Stydex/MA and Stydex/Styrene is 100 times the concentration of Stydex/+. We again observe that as we incrementally diminish the effects of electrostatic interactions, hydrophobic interactions are important for long-chain PFASs, but the removal of PFBA completely relies on electrostatic interactions.

3.3.4 Effects of different types of inorganic ions

To further explore the importance of type of inorganic ion (e.g., monovalent or divalent) on the observed adsorption inhibition or enhancement, we performed experiments with nanopure amended with 1 mM Na_2SO_4, 2 mM NaCl, and 1 mM $CaCl_2$. We selected these salts and these concentrations to generate comparable data with 2 mM of monovalent sodium or chloride ions and

1 mM of divalent sulfate or calcium ions. The results of these experiments are presented in **Figure 3-7**.

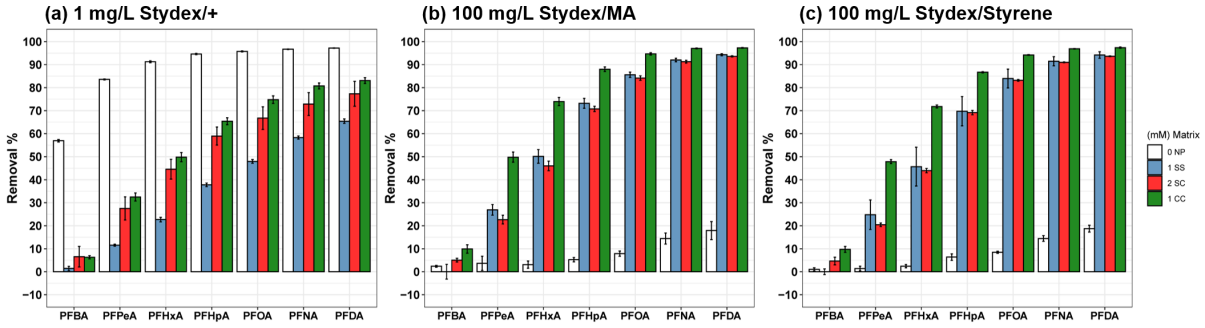

Figure 3-7. PFCAs removal by (a) 1 mg L^{-1} Stydex/+, (b) 100 mg L^{-1} Stydex/MA, and (c) 100 mg L^{-1} Stydex/Styrene in nanopure water (0 NP, white bar), in 1 mM Na_2SO_4 solution (1 SS, blue bar), in 2 mM NaCl solution (2 SC, red bar) and in 1 mM $CaCl_2$ solution (1CC, green bar) after 48 hr contact time.

For Stydex/+, when comparing the removal in NaCl and in $CaCl_2$, there is no significant difference (**$p > 0.05$**) in the extent of adsorption inhibition. This finding suggests that the valence of the cation makes no significant difference on the inhibition. When comparing the removal in Na_2SO_4 and in NaCl, the removal in Na_2SO_4 exhibits significantly more inhibition for C5-C8 PFCAs (**$p < 0.05$**) and with a weaker significance for C9-C10 PFCAs (**$p < 0.1$**). This observation suggests that sulfate is more important for inhibition than chloride and the different types of anions would affect the inhibition to a varying extent. Based on our mechanistic interpretation, we expect either direct-site competition and/or a screening effect to be the key explanation for these observations. One possibility is that chloride competes with PFCAs in NaCl and $CaCl_2$ while sulfate competes with PFCAs more strongly in Na_2SO_4 (effect **b** in **Figure 3-1**). It is also possible that the one unit of divalent anion has a greater screening effect due to the compression of the EDL than two units of monovalent anion (effect **c** in **Figure 3-1**), where the compression should be directly related to ionic strength which is proportional to the square of the ion valence. Both direct-site competition and screening effects tend to neutralize the surface charge of the solid adsorbent resulting in the decrease of the existing electrostatic attraction then causing the inhibition on

removal. Regardless, it is demonstrated that that for positively charged CDPs, (1) anions play a more important role on anionic PFAS adsorption inhibition than cations, and (2) divalent anions are more important than monovalent ones.

For Stydex/MA and Stydex/Styrene, there are no significant differences between the removal in Na_2SO_4 and in NaCl for C5-C10 PFCAs (**$p > 0.05$**). This finding suggests that the valence types of the anion make no significant difference on the enhancement. The exception is PFBA, which has a significant but small removal difference (less than 5% difference at **$p < 0.05$**) between in Na_2SO_4 and in NaCl on using either Stydex/MA or Stysex/Styrene. However, a very significant difference (**$p < 0.05$**) between the removal in $CaCl_2$ and in NaCl is observed for C4-C10 PFCAs. The removal in $CaCl_2$ yields a significantly greater enhancement than in NaCl again indicating the importance of divalent ions for the charged CDPs. Based on our mechanistic interpretation, we expect no direct-site competition here, but the polyvalent cation bridging effect could be another explanation in addition to the screening effect. One possibility could be that Ca^{2+} as a polyvalent cation forms a bridge between anionic PFCA molecule and negatively charged sorbent, thus increasing the sorption performance (effect **e** in **Figure 3-1**), while it is a non-existent effect for Na^+. It is also possible that one unit of calcium ion has a greater screening effect on the compression of the EDL than two units of sodium ion (effect **d** in **Figure 3-1**). Besides, the salting-out effect might also contribute to the uneven enhancement among different types of salt ions (effect **a** in **Figure 3-1**). In summary, both a cation bridging effect and a screening effect neutralize the surface charge of the solid adsorbent resulting in the decrease of existing electrostatic repulsion resulting in the enhancement on removal. The salting-out effect could promote the hydrophobic interactions between PFCAs and adsorbents. Regardless, it is demonstrated that for negatively

charged CDPs, (1) cations play a more important role in adsorption enhancement than anions, and (2) divalent cations are more important than monovalent ones.

3.3.5 Environmental implications

To better identify the relative contributions of hydrophobic and electrostatic interactions on the adsorption of PFAAs on cyclodextrin-based adsorbents, we synthesized a novel series of CDPs with nearly identical physical properties but different crosslinker hydrophobicity and surface charge. We performed adsorption experiments in the presence and absence of different salts to evaluate the role of electrostatic interactions. This research advances our understanding of PFAA adsorption mechanisms on CDPs and reveals the impact of different types and concentrations of inorganic constituents on the adsorption mechanism.

Extrapolating our research findings to practical considerations, it is clear that short-chain PFASs require some favorable electrostatic interactions to facilitate their adsorption onto CDPs; we found that the adsorption of PFBA on the Stydex polymers relied entirely on favorable electrostatic interactions. Therefore, it will be essential to incorporate some positive charge into adsorbents aimed at removing anionic short-chain PFASs from water. We also note that the enhanced removal of PFAAs in the presence of salts for Stydex/MA and Stydex/Styrene offers an important lesson; novel adsorbents are usually evaluated first in nanopure water and are discarded if their performance in nanopure water is poor. Here, we demonstrate that an adsorbent that performs poorly in nanopure water actually performs rather well in the presence of high concentrations of salt. This observation could have a paradigm-shifting effect on the evaluation of new adsorbents for water purification. Finally, we note that the presence of inorganic ions in the water matrix could be either inhibitory or beneficial for the removal of PFASs, a phenomenon which depends on the physicochemical properties of both the adsorbent and the PFAS. Therefore,

implementing a combination of adsorbents with different physicochemical properties simultaneously might lead to the most effective treatment result.

CHAPTER 4 – Summary and Future Work

The research presented in this thesis describes a systematic evaluation of both novel cyclodextrin polymers (CDPs) and conventional adsorbents for the removal of PFASs from water. This evaluation provides insights into the adsorption patterns for adsorbents with different physicochemical properties (e.g., surface charge, porosity and chemical composition) and the effects of PFAS properties (i.e., chain length and headgroups) on PFAS removal by different adsorbents. The suspect screening approach could serve as a new roadmap for treatment technology evaluation in the future. This thesis also carried out further research on the adsorption mechanism with aspects to the determination on the relative contributions of hydrophobic interactions and electrostatic interactions on PFAS removal by CDPs. Meanwhile, the impacts of different salt concentrations and salt types on adsorption mechanisms were fully demonstrated.

In **Chapter 2**, the removal performance of five different adsorbents was evaluated by integrating a suspect screening approach with batch adsorption experiments directly in the groundwater contaminated by aqueous film-forming foams (AFFF). The data **revealed** that conventional and emerging adsorbents exhibit variable adsorption kinetics and affinity for different types of PFASs in AFFF-contaminated groundwater. Activated carbon (AC) is the most non-selective adsorbent but has relatively slow adsorption kinetics. The CDPs exhibit rapid adsorption kinetics and are more selective than AC, performing better in removing PFAS classes that are complementary to their surface charge. These findings suggest that different adsorbents may be better suited for applications that rely on limited contact time or require the removal of specific PFASs. Analysis of the complete dataset **revealed** that adsorption of some PFAS classes can be associated with increasing length of the perfluorinated tail, while adsorption of other classes is more strongly related to properties of the head group. The removal of some short-chain

perfluoroalkyl substances including PFCAs (perfluorocarboxylic acids) and FASAs (perfluoroalkane sulfonamide) from groundwater will be challenging for all of the adsorbents studied, but the removal of perfluorobutanesulfonic acid (PFBS) and short-chain polyfluoroalkyl substances including FASAAs (perfluoroalkane sulfonamide acetic acid) and substituted sulfonamides or sulfonamide acetic acids can be achieved with one or more adsorbent.

One novel aspect of the study reported in **Chapter 2** was the integration of suspect screening into the evaluation of a PFAS remediation technology. Although this approach enabled a more comprehensive evaluation of adsorbent performance, there are still some areas that can be improved. First, different suspect screening software (or workflows) together with a different PFAS exact mass database or fragmentation library may provide different peak picking and annotation capabilities. Suspect screening involves matching data from an HR-MS acquisition of an environmental sample with chemical information contained in a suspect list or database or library. Peak picking generally means the identification and extraction of statistically manageable sets of peaks from raw MS spectral acquisitions from environmental samples.[139] Different software usually has different algorithms for peak picking resulting in different picked features. Annotation refers to tentative matches of picked features with the database based on the same molecular formula and other molecular properties. Different databases containing different PFAS information are very likely to provide different annotation results.[140] Other different steps in the suspect screening workflow can also result in different results for the same environmental sample.[48,49,141] In **Chapter 2**, *enviMass* was used as the tool and an optimized workflow for *enviMass* was adopted to perform a suspect screening but its performance was not compared with other open-source software (e.g., FluoroMatch) or commercially available software (e.g., Compound Discoverer).[51,142] Second, doing non-target screening could provide us more

comprehensive and unbiased results on identifying pollutants in a real contaminated water matrix than doing suspect screening. Non-target screening is not like suspect screening which is restricted to lists of known chemicals of interest ("suspect lists") to identify contaminants. Non-target screening in a strict sense starts without any *a priori* information on the PFASs to be detected.[42,43] But non-target screening could be more challenging on the steps of data processing, analysis and interpretation. Non-target screening requires sophisticated data processing strategies due to the magnitude of data quantity and complexity. The enormous effort for identifying a true unknown can easily last for months, and it requires rigorous prioritization approaches to focus on the most relevant sample components.[52,143] Some innovative techniques and workflows on non-target screening have been published in the literature over the last few years.[15,143–147] Third, the suspect screening evaluation workflow in **Chapter 2** might only work for separation technologies (e.g., membrane filtration and adsorption) where no PFAS transformation and degradation occurred during treatment processes. To evaluate destruction technologies involving the defluorination or mineralization processes that might create new PFASs and other new products, using other methods such as non-target screening, total oxidizable precursor (TOP) assay, extractable organofluorine (EOF) and particle-induced γ-ray emission (PIGE) spectroscopy are required.[143,148–151]

The research in **Chapter 3** aimed to elucidate the relative contributions of hydrophobic and electrostatic interactions on the adsorption of anionic PFASs on CDPs. A series of novel CDPs that had nearly identical physical properties and variable crosslinker hydrophobicity and surface charge were selected to explore PFAS adsorption in the presence and absence of salts to evaluate the role of electrostatic interactions. First, the data **revealed** the impact of different crosslinker chemistry on PFAS removal and the mechanistic explanation on the varying performance. The

positively charged CDP (Stydex/+) exhibited significant inhibition on the removal of anionic PFASs in salt solutions, while the performance of the two negatively charged CDPs (Stydex/MA and Stydex/Styrene) is enhanced under the same conditions. The adsorption inhibition on positively charged CDPs was attributed to the screening effect and direct-site competition which decreased the electrostatic attraction. The adsorption enhancement on negatively charged CDPs likely results from the screening effect, and bridging effect for polyvalent cations, both of which decreased the electrostatic repulsion and thus facilitated the formation of the host-guest complex. Additionally, the identical adsorption behavior of Stydex/MA and Stydex/Styrene indicates the unimportance of crosslinker hydrophobicity on PFAS removal, where the only difference between them is the carboxy group moiety in Stydex/MA and the phenyl group moiety in Stydex/Styrene. Second, analysis of the complete dataset on different PFASs **revealed** that short-chain PFASs require some favorable electrostatic interactions to facilitate their adsorption onto CDPs; it was found that the adsorption of PFBA on the Stydex polymers relied entirely on favorable electrostatic interactions. Therefore, it will be essential to incorporate some positive charge into adsorbents aimed at removing anionic short-chain PFASs from water. Third, our data also **revealed** the effects of salt concentrations and salt types on PFAS adsorption. Higher salt concentration can bring more inhibition or more enhancement on the removal performance, but the effects can get saturated as the salt concentration keeps increasing. Different valences of inorganic anions (or cations) have different extent of impacts on positively (or negatively) charged adsorbents, where divalent ions have a more significant impact than monovalent ions.

Whereas in **Chapter 3** the relative contributions of hydrophobic and electrostatic interactions for short-chain PFASs and long-chain PFASs were determined to some extent, molecular level support about the actual adsorption binding mechanism remains to be explored.

There remain questions about whether ionic surface function groups provide direct binding sites, facilitate adsorbate transport to the interior cavity of the cyclodextrin cup, or some combination of both depending on the physicochemical properties of the adsorbate. There are several characterization techniques that have been used to elucidate the adsorption mechanism on the binding site of cyclodextrin-based adsorbents.[87,152–154] For example, Raman, Fourier Transform-IR spectroscopy (FTIR), differential scanning calorimetry (DSC) and nuclear overhauser effect spectroscopy (NOESY) could provide insights into the nature of the surface interactions that occur in such adsorbent/adsorbate systems; isothermal titration calorimetry (ITC) can provide molecular-level insights on the adsorption process.[87,153,154] These characterization techniques can serve as great complements to enable further understanding of CDP adsorption mechanisms.

REFERENCES

(1) ITRC. *History and Use of Per-and Polyfluoroalkyl Substances (PFAS)*; 2020.

(2) Gagliano, E.; Sgroi, M.; Falciglia, P. P.; Vagliasindi, F. G. A.; Roccaro, P. Removal of Poly- and Perfluoroalkyl Substances (PFAS) from Water by Adsorption: Role of PFAS Chain Length, Effect of Organic Matter and Challenges in Adsorbent Regeneration. *Water Research*. Elsevier Ltd March 15, 2020, p 115381. https://doi.org/10.1016/j.watres.2019.115381.

(3) Wang, Z.; Dewitt, J. C.; Higgins, C. P.; Cousins, I. T. A Never-Ending Story of Per- and Polyfluoroalkyl Substances (PFASs)? *Environ. Sci. Technol.* **2017**, *51* (5), 2508–2518. https://doi.org/10.1021/acs.est.6b04806.

(4) Hu, X. C.; Andrews, D. Q.; Lindstrom, A. B.; Bruton, T. A.; Schaider, L. A.; Grandjean, P.; Lohmann, R.; Carignan, C. C.; Blum, A.; Balan, S. A.; Higgins, C. P.; Sunderland, E. M. Detection of Poly- and Perfluoroalkyl Substances (PFASs) in U.S. Drinking Water Linked to Industrial Sites, Military Fire Training Areas, and Wastewater Treatment Plants. *Environ. Sci. Technol. Lett.* **2016**, *3* (10), 344–350. https://doi.org/10.1021/acs.estlett.6b00260.

(5) Kissa, E. *Fluorinated Surfactants and Repellents*, 2nd ed.; CRC Press: Boca Raton, FL, 2001.

(6) Cui, J.; Gao, P.; Deng, Y. Destruction of Per- A Nd Polyfluoroalkyl Substances (PFAS) with Advanced Reduction Processes (ARPs): A Critical Review. *Environmental Science and Technology*. American Chemical Society April 7, 2020, pp 3752–3766. https://doi.org/10.1021/acs.est.9b05565.

(7) Kim, S. K.; Kannan, K. Perfluorinated Acids in Air, Rain, Snow, Surface Runoff, and Lakes: Relative Importance of Pathways to Contamination of Urban Lakes. *Environ. Sci. Technol.* **2007**, *41* (24), 8328–8334. https://doi.org/10.1021/es072107t.

(8) Scher, D. P.; Kelly, J. E.; Huset, C. A.; Barry, K. M.; Hoffbeck, R. W.; Yingling, V. L.; Messing, R. B. Occurrence of Perfluoroalkyl Substances (PFAS) in Garden Produce at Homes with a History of PFAS-Contaminated Drinking Water. *Chemosphere* **2018**, *196*, 548–555. https://doi.org/10.1016/j.chemosphere.2017.12.179.

(9) Sharma, B. M.; Bharat, G. K.; Tayal, S.; Larssen, T.; Bečanová, J.; Karásková, P.; Whitehead, P. G.; Futter, M. N.; Butterfield, D.; Nizzetto, L. Perfluoroalkyl Substances

(PFAS) in River and Ground/Drinking Water of the Ganges River Basin: Emissions and Implications for Human Exposure. *Environ. Pollut.* **2016**, *208*, 704–713. https://doi.org/10.1016/j.envpol.2015.10.050.

(10) Yamashita, N.; Kannan, K.; Taniyasu, S.; Horii, Y.; Petrick, G.; Gamo, T. A Global Survey of Perfluorinated Acids in Oceans. In *Marine Pollution Bulletin*; Pergamon, 2005; Vol. 51, pp 658–668. https://doi.org/10.1016/j.marpolbul.2005.04.026.

(11) Anderson, R. H.; Long, G. C.; Porter, R. C.; Anderson, J. K. Occurrence of Select Perfluoroalkyl Substances at U.S. Air Force Aqueous Film-Forming Foam Release Sites Other than Fire-Training Areas: Field-Validation of Critical Fate and Transport Properties. *Chemosphere* **2016**, *150*, 678–685. https://doi.org/10.1016/j.chemosphere.2016.01.014.

(12) Adamson, D. T.; Nickerson, A.; Kulkarni, P. R.; Higgins, C. P.; Popovic, J.; Field, J.; Rodowa, A.; Newell, C.; Deblanc, P.; Kornuc, J. J. Mass-Based, Field-Scale Demonstration of PFAS Retention within AFFF-Associated Source Areas. *Environ. Sci. Technol.* **2020**, *54* (24), 15768–15777. https://doi.org/10.1021/acs.est.0c04472.

(13) Houtz, E. F.; Sutton, R.; Park, J. S.; Sedlak, M. Poly- and Perfluoroalkyl Substances in Wastewater: Significance of Unknown Precursors, Manufacturing Shifts, and Likely AFFF Impacts. *Water Res.* **2016**, *95*, 142–149. https://doi.org/10.1016/j.watres.2016.02.055.

(14) Tang, C. Y.; Fu, Q. S.; Robertson, A. P.; Criddle, C. S.; Leckie, J. O. Use of Reverse Osmosis Membranes to Remove Perfluorooctane Sulfonate (PFOS) from Semiconductor Wastewater. *Environ. Sci. Technol.* **2006**, *40* (23), 7343–7349. https://doi.org/10.1021/es060831q.

(15) Jacob, P.; Barzen-Hanson, K. A.; Helbling, D. E. Target and Nontarget Analysis of Per- and Polyfluoralkyl Substances in Wastewater from Electronics Fabrication Facilities. *Environ. Sci. Technol.* **2021**, *55*, 2346–2356. https://doi.org/10.1021/acs.est.0c06690.

(16) Wang, Y.; Yu, N.; Zhu, X.; Guo, H.; Jiang, J.; Wang, X.; Shi, W.; Wu, J.; Yu, H.; Wei, S. Suspect and Nontarget Screening of Per- and Polyfluoroalkyl Substances in Wastewater from a Fluorochemical Manufacturing Park. *Environ. Sci. Technol.* **2018**, *52* (19), 11007–11016. https://doi.org/10.1021/acs.est.8b03030.

(17) Rankin, K.; Mabury, S. A.; Jenkins, T. M.; Washington, J. W. A North American and Global Survey of Perfluoroalkyl Substances in Surface Soils: Distribution Patterns and Mode of Occurrence. *Chemosphere* **2016**, *161*, 333–341.

https://doi.org/10.1016/j.chemosphere.2016.06.109.

(18) Xu, B.; Liu, S.; Zhou, J. L.; Zheng, C.; Weifeng, J.; Chen, B.; Zhang, T.; Qiu, W. PFAS and Their Substitutes in Groundwater: Occurrence, Transformation and Remediation. *J. Hazard. Mater.* **2021**, *412*, 125159. https://doi.org/10.1016/j.jhazmat.2021.125159.

(19) Gaballah, S.; Swank, A.; Sobus, J. R.; Howey, X. M.; Schmid, J.; Catron, T.; McCord, J.; Hines, E.; Strynar, M.; Tal, T. Evaluation of Developmental Toxicity, Developmental Neurotoxicity, and Tissue Dose in Zebrafish Exposed to GenX and Other PFAS. *Environ. Health Perspect.* **2020**, *128* (4), 047005. https://doi.org/10.1289/EHP5843.

(20) Hekster, F. M.; Laane, R. W. P. M.; De Voogt, P. Environmental and Toxicity Effects of Perfluoroalkylated Substances. *Rev. Environ. Contam. Toxicol.* **2003**, *179*, 99–121. https://doi.org/10.1007/0-387-21731-2_4.

(21) Wang, Z.; Cousins, I. T.; Scheringer, M.; Hungerbuehler, K. Hazard Assessment of Fluorinated Alternatives to Long-Chain Perfluoroalkyl Acids (PFAAs) and Their Precursors: Status Quo, Ongoing Challenges and Possible Solutions. *Environ. Int.* **2015**, *75*, 172–179. https://doi.org/10.1016/j.envint.2014.11.013.

(22) Grandjean, P.; Andersen, E. W.; Budtz-Jørgensen, E.; Nielsen, F.; Mølbak, K. R.; Weihe, P.; Heilmann, C. Serum Vaccine Antibody Concentrations in Children Exposed to Perfluorinated Compounds. *JAMA - J. Am. Med. Assoc.* **2012**, *307* (4), 391–397. https://doi.org/10.1001/jama.2011.2034.

(23) Braun, J. M.; Chen, A.; Romano, M. E.; Calafat, A. M.; Webster, G. M.; Yolton, K.; Lanphear, B. P. Prenatal Perfluoroalkyl Substance Exposure and Child Adiposity at 8 Years of Age: The HOME Study. *Obesity* **2016**, *24* (1), 231–237. https://doi.org/10.1002/oby.21258.

(24) Barry, V.; Winquist, A.; Steenland, K. Perfluorooctanoic Acid (PFOA) Exposures and Incident Cancers among Adults Living Near a Chemical Plant. *Environ. Health Perspect.* **2013**, *121* (11–12), 1313–1318. https://doi.org/10.1289/ehp.1306615.

(25) U.S. EPA. *Drinking Water Health Advisory for PerfluorooctanoicAcid (PFOA). Office of Water Document 822-R-16-005*; 2016.

(26) U.S. EPA. *Drinking Water Health Advisory for Perfluorooctane Sulfonate (PFOS). Office*

of Water Document 822-R-16-004; 2016.

(27) OECD. *Risk Reduction Approaches for PFASs – a Cross-Country Analysis*; 2015.

(28) ITRC. *PFAS Fact Sheet: 8 Basis of Regulations*; 2020.

(29) ECHA. *Submitted Restrictions under Consideration. European Chemicals Agency*; 2018.

(30) American Water Works Association. *Per- and Polyfluoroalkyl Substances (PFAS): Summary of State Regulation to Protect Drinking Water*.

(31) Cordner, A.; De La Rosa, V. Y.; Schaider, L. A.; Rudel, R. A.; Richter, L.; Brown, P. Guideline Levels for PFOA and PFOS in Drinking Water: The Role of Scientific Uncertainty, Risk Assessment Decisions, and Social Factors. *J. Expo. Sci. Environ. Epidemiol.* **2019**, *29* (2), 157–171. https://doi.org/10.1038/s41370-018-0099-9.

(32) U.S. EPA. *Monitoring Unregulated Drinking Water Contaminants Occurrence Data for the Unregulated Contaminant Monitoring Rule*; 2017.

(33) Linda S. Birnbaum. Hearing on the Federal Role in the Toxic PFAS Chemical Crisis, 2018. https://doi.org/10.1093/toxsci/12.3.442.

(34) Backe, W. J.; Day, T. C.; Field, J. A. Zwitterionic, Cationic, and Anionic Fluorinated Chemicals in Aqueous Film Forming Foam Formulations and Groundwater from U.S. Military Bases by Nonaqueous Large-Volume Injection HPLC-MS/MS. *Environ. Sci. Technol.* **2013**, *47* (10), 5226–5234. https://doi.org/10.1021/es3034999.

(35) Barzen-Hanson, K. A.; Roberts, S. C.; Choyke, S.; Oetjen, K.; McAlees, A.; Riddell, N.; McCrindle, R.; Ferguson, P. L.; Higgins, C. P.; Field, J. A. Discovery of 40 Classes of Per- and Polyfluoroalkyl Substances in Historical Aqueous Film-Forming Foams (AFFFs) and AFFF-Impacted Groundwater. *Environ. Sci. Technol.* **2017**, *51* (4), 2047–2057. https://doi.org/10.1021/acs.est.6b05843.

(36) Munoz, G.; Duy, S. V.; Labadie, P.; Botta, F.; Budzinski, H.; Lestremau, F.; Liu, J.; Sauvé, S. Analysis of Zwitterionic, Cationic, and Anionic Poly- And Perfluoroalkyl Surfactants in Sediments by Liquid Chromatography Polarity-Switching Electrospray Ionization Coupled to High Resolution Mass Spectrometry. *Talanta* **2016**, *152*, 447–456.

https://doi.org/10.1016/j.talanta.2016.02.021.

(37) D'Agostino, L. A.; Mabury, S. A. Identification of Novel Fluorinated Surfactants in Aqueous Film Forming Foams and Commercial Surfactant Concentrates. *Environ. Sci. Technol.* **2014**, *48* (1), 121–129. https://doi.org/10.1021/es403729e.

(38) Dauchy, X.; Boiteux, V.; Colin, A.; Hémard, J.; Bach, C.; Rosin, C.; Munoz, J. F. Deep Seepage of Per- and Polyfluoroalkyl Substances through the Soil of a Firefighter Training Site and Subsequent Groundwater Contamination. *Chemosphere* **2019**, *214*, 729–737. https://doi.org/10.1016/j.chemosphere.2018.10.003.

(39) Xiao, F.; Hanson, R. A.; Golovko, S. A.; Golovko, M. Y.; Arnold, W. A. PFOA and PFOS Are Generated from Zwitterionic and Cationic Precursor Compounds during Water Disinfection with Chlorine or Ozone. *Environ. Sci. Technol. Lett.* **2018**, *5* (6), 382–388. https://doi.org/10.1021/acs.estlett.8b00266.

(40) Mejia Avendaño, S.; Liu, J. Production of PFOS from Aerobic Soil Biotransformation of Two Perfluoroalkyl Sulfonamide Derivatives. *Chemosphere* **2015**, *119*, 1084–1090. https://doi.org/10.1016/j.chemosphere.2014.09.059.

(41) McGuire, M. E.; Schaefer, C.; Richards, T.; Backe, W. J.; Field, J. A.; Houtz, E.; Sedlak, D. L.; Guelfo, J. L.; Wunsch, A.; Higgins, C. P. Evidence of Remediation-Induced Alteration of Subsurface Poly- and Perfluoroalkyl Substance Distribution at a Former Firefighter Training Area. *Environ. Sci. Technol.* **2014**, *48* (12), 6644–6652. https://doi.org/10.1021/es5006187.

(42) Escher, B. I.; Stapleton, H. M.; Schymanski, E. L. Tracking Complex Mixtures of Chemicals in Our Changing Environment. *Science*. American Association for the Advancement of Science January 24, 2020, pp 388–392. https://doi.org/10.1126/science.aay6636.

(43) Krauss, M.; Singer, H.; Hollender, J. LC-High Resolution MS in Environmental Analysis: From Target Screening to the Identification of Unknowns. *Anal. Bioanal. Chem.* **2010**, *397* (3), 943–951. https://doi.org/10.1007/s00216-010-3608-9.

(44) Shoemaker, J. A.; Tettenhorst, D. R. *Method 537.1 Determination of Selected Per- and Polyflourinated Alkyl Substances in Drinking Water by Solid Phase Extraction and Liquid Chromatography/Tandem Mass Spectrometry (LC/MS/MS)*; U.S. Environmental Protection

Agency: Washington, DC, 2020.

(45) Laura Rosenblum. *Method 533: Determination of Per- and Polyfluoroalkyl Substances in Drinking Water by Isotope Dilution Anion Exchange Solid Phase Extraction and Liquid Chromatography/Tandem Mass Spectrometry*; U.S. Environmental Protection Agency, 2019.

(46) U.S. EPA. *Validated Test Method 8327: Per-and Polyfluoroalkyl Substances (PFAS) Using External Standard Calibration and Multiple Reaction Monitoring (MRM) Liquid Chromatography/Tandem Mass Spectrometry (LC/MS/MS)*; 2019.

(47) PFAS Analytical Methods Development and Sampling Research | Water Research | US EPA, https://www.epa.gov/water-research/pfas-analytical-methods-development-and-sampling-research (accessed Mar 30, 2021).

(48) Pochodylo, A. L.; Helbling, D. E. Emerging Investigators Series: Prioritization of Suspect Hits in a Sensitive Suspect Screening Workflow for Comprehensive Micropollutant Characterization in Environmental Samples. *Environ. Sci. Water Res. Technol.* **2017**, *3* (1), 54–65. https://doi.org/10.1039/c6ew00248j.

(49) Moschet, C.; Piazzoli, A.; Singer, H.; Hollender, J. Alleviating the Reference Standard Dilemma Using a Systematic Exact Mass Suspect Screening Approach with Liquid Chromatography-High Resolution Mass Spectrometry. *Anal. Chem.* **2013**, *85* (21), 10312–10320. https://doi.org/10.1021/ac4021598.

(50) Wang, A.; Abrahamsson, D. P.; Jiang, T.; Wang, M.; Morello-Frosch, R.; Park, J.-S.; Sirota, M.; Woodruff, T. J. Suspect Screening, Prioritization, and Confirmation of Environmental Chemicals in Maternal-Newborn Pairs from San Francisco. *Environ. Sci. Technol.* **2021**, acs.est.0c05984. https://doi.org/10.1021/acs.est.0c05984.

(51) Koelmel, J. P.; Paige, M. K.; Aristizabal-Henao, J. J.; Robey, N. M.; Nason, S. L.; Stelben, P. J.; Li, Y.; Kroeger, N. M.; Napolitano, M. P.; Savvaides, T.; Vasiliou, V.; Rostkowski, P.; Garrett, T. J.; Lin, E.; Deigl, C.; Jobst, K.; Townsend, T. G.; Godri Pollitt, K. J.; Bowden, J. A. Toward Comprehensive Per- A Nd Polyfluoroalkyl Substances Annotation Using FluoroMatch Software and Intelligent High-Resolution Tandem Mass Spectrometry Acquisition. *Anal. Chem.* **2020**, *92* (16), 11186–11194. https://doi.org/10.1021/acs.analchem.0c01591.

(52) Schymanski, E. L.; Singer, H. P.; Slobodnik, J.; Ipolyi, I. M.; Oswald, P.; Krauss, M.; Schulze, T.; Haglund, P.; Letzel, T.; Grosse, S.; Thomaidis, N. S.; Bletsou, A.; Zwiener, C.; Ibáñez, M.; Portolés, T.; De Boer, R.; Reid, M. J.; Onghena, M.; Kunkel, U.; Schulz, W.;

Guillon, A.; Noyon, N.; Leroy, G.; Bados, P.; Bogialli, S.; Stipaničev, D.; Rostkowski, P.; Hollender, J. Non-Target Screening with High-Resolution Mass Spectrometry: Critical Review Using a Collaborative Trial on Water Analysis. *Anal. Bioanal. Chem.* **2015**, *407* (21), 6237–6255. https://doi.org/10.1007/s00216-015-8681-7.

(53) Yu, N.; Guo, H.; Yang, J.; Jin, L.; Wang, X.; Shi, W.; Zhang, X.; Yu, H.; Wei, S. Non-Target and Suspect Screening of Per- and Polyfluoroalkyl Substances in Airborne Particulate Matter in China. *Environ. Sci. Technol.* **2018**, *52* (15), 8205–8214. https://doi.org/10.1021/acs.est.8b02492.

(54) Strynar, M.; Dagnino, S.; McMahen, R.; Liang, S.; Lindstrom, A.; Andersen, E.; McMillan, L.; Thurman, M.; Ferrer, I.; Ball, C. Identification of Novel Perfluoroalkyl Ether Carboxylic Acids (PFECAs) and Sulfonic Acids (PFESAs) in Natural Waters Using Accurate Mass Time-of-Flight Mass Spectrometry (TOFMS). *Environ. Sci. Technol.* **2015**, *49* (19), 11622–11630. https://doi.org/10.1021/acs.est.5b01215.

(55) Du, Z.; Deng, S.; Bei, Y.; Huang, Q.; Wang, B.; Huang, J.; Yu, G. Adsorption Behavior and Mechanism of Perfluorinated Compounds on Various Adsorbents-A Review. *Journal of Hazardous Materials*. Elsevier June 15, 2014, pp 443–454. https://doi.org/10.1016/j.jhazmat.2014.04.038.

(56) Merino, N.; Qu, Y.; Deeb, R. A.; Hawley, E. L.; Hoffmann, M. R.; Mahendra, S. Degradation and Removal Methods for Perfluoroalkyl and Polyfluoroalkyl Substances in Water. *Environ. Eng. Sci.* **2016**, *33* (9), 615–649. https://doi.org/10.1089/ees.2016.0233.

(57) Rahman, M. F.; Peldszus, S.; Anderson, W. B. Behaviour and Fate of Perfluoroalkyl and Polyfluoroalkyl Substances (PFASs) in Drinking Water Treatment: A Review. *Water Research*. Elsevier Ltd March 1, 2014, pp 318–340. https://doi.org/10.1016/j.watres.2013.10.045.

(58) Ross, I.; McDonough, J.; Miles, J.; Storch, P.; Thelakkat Kochunarayanan, P.; Kalve, E.; Hurst, J.; S. Dasgupta, S.; Burdick, J. A Review of Emerging Technologies for Remediation of PFASs. *Remediat. J.* **2018**, *28* (2), 101–126. https://doi.org/10.1002/rem.21553.

(59) Arvaniti, O. S.; Stasinakis, A. S. Review on the Occurrence, Fate and Removal of Perfluorinated Compounds during Wastewater Treatment. *Science of the Total Environment*. Elsevier August 5, 2015, pp 81–92. https://doi.org/10.1016/j.scitotenv.2015.04.023.

(60) Flores, C.; Ventura, F.; Martin-Alonso, J.; Caixach, J. Occurrence of Perfluorooctane Sulfonate (PFOS) and Perfluorooctanoate (PFOA) in N.E. Spanish Surface Waters and

Their Removal in a Drinking Water Treatment Plant That Combines Conventional and Advanced Treatments in Parallel Lines. *Sci. Total Environ.* **2013**, *461–462*, 618–626. https://doi.org/10.1016/j.scitotenv.2013.05.026.

(61) Thompson, J.; Eaglesham, G.; Reungoat, J.; Poussade, Y.; Bartkow, M.; Lawrence, M.; Mueller, J. F. Removal of PFOS, PFOA and Other Perfluoroalkyl Acids at Water Reclamation Plants in South East Queensland Australia. *Chemosphere* **2011**, *82* (1), 9–17. https://doi.org/10.1016/j.chemosphere.2010.10.040.

(62) Wang, Z.; Cousins, I. T.; Berger, U.; Hungerbühler, K.; Scheringer, M. Comparative Assessment of the Environmental Hazards of and Exposure to Perfluoroalkyl Phosphonic and Phosphinic Acids (PFPAs and PFPiAs): Current Knowledge, Gaps, Challenges and Research Needs. *Environment International*. Elsevier Ltd April 1, 2016, pp 235–247. https://doi.org/10.1016/j.envint.2016.01.023.

(63) Blum, A.; Balan, S. A.; Scheringer, M.; Trier, X.; Goldenman, G.; Cousins, I. T.; Diamond, M.; Fletcher, T.; Higgins, C.; Lindeman, A. E.; Peaslee, G.; Voogt, P. De; Wang, Z.; Weber, R. The Madrid Statement on Poly- and Perfluoroalkyl Substances (PFASs). *Environ. Health Perspect.* **2015**, *123* (5), A107–A111. https://doi.org/10.1289/ehp.1509934.

(64) Kucharzyk, K. H.; Darlington, R.; Benotti, M.; Deeb, R.; Hawley, E. Novel Treatment Technologies for PFAS Compounds: A Critical Review. *J. Environ. Manage.* **2017**, *204*, 757–764. https://doi.org/10.1016/j.jenvman.2017.08.016.

(65) Nzeribe, B. N.; Crimi, M.; Mededovic Thagard, S.; Holsen, T. M. Physico-Chemical Processes for the Treatment of Per- And Polyfluoroalkyl Substances (PFAS): A Review. *Crit. Rev. Environ. Sci. Technol.* **2019**, *49* (10), 866–915. https://doi.org/10.1080/10643389.2018.1542916.

(66) Wu, B.; Hao, S.; Choi, Y.; Higgins, C. P.; Deeb, R.; Strathmann, T. J. Rapid Destruction and Defluorination of Perfluorooctanesulfonate by Alkaline Hydrothermal Reaction. *Environ. Sci. Technol. Lett.* **2019**, *6* (10), 630–636. https://doi.org/10.1021/acs.estlett.9b00506.

(67) Zhang, K.; Huang, J.; Yu, G.; Zhang, Q.; Deng, S.; Wang, B. Destruction of Perfluorooctane Sulfonate (PFOS) and Perfluorooctanoic Acid (PFOA) by Ball Milling. *Environ. Sci. Technol.* **2013**, *47* (12), 6471–6477. https://doi.org/10.1021/es400346n.

(68) Tang, C. Y.; Fu, Q. S.; Criddle, C. S.; Leckie, J. O. Effect of Flux (Transmembrane Pressure) and Membrane Properties on Fouling and Rejection of Reverse Osmosis and Nanofiltration Membranes Treating Perfluorooctane Sulfonate Containing Wastewater. *Environ. Sci.*

Technol. **2007**, *41* (6), 2008–2014. https://doi.org/10.1021/es062052f.

(69) Appleman, T. D.; Higgins, C. P.; Quiñones, O.; Vanderford, B. J.; Kolstad, C.; Zeigler-Holady, J. C.; Dickenson, E. R. V. Treatment of Poly- and Perfluoroalkyl Substances in U.S. Full-Scale Water Treatment Systems. *Water Res.* **2014**, *51*, 246–255. https://doi.org/10.1016/j.watres.2013.10.067.

(70) Rizzo, L.; Malato, S.; Antakyali, D.; Beretsou, V. G.; Đolić, M. B.; Gernjak, W.; Heath, E.; Ivancev-Tumbas, I.; Karaolia, P.; Lado Ribeiro, A. R.; Mascolo, G.; McArdell, C. S.; Schaar, H.; Silva, A. M. T.; Fatta-Kassinos, D. Consolidated vs New Advanced Treatment Methods for the Removal of Contaminants of Emerging Concern from Urban Wastewater. *Science of the Total Environment*. Elsevier B.V. March 10, 2019, pp 986–1008. https://doi.org/10.1016/j.scitotenv.2018.11.265.

(71) Bertanza, G.; Capoferri, G. U.; Carmagnani, M.; Icarelli, F.; Sorlini, S.; Pedrazzani, R. Long-Term Investigation on the Removal of Perfluoroalkyl Substances in a Full-Scale Drinking Water Treatment Plant in the Veneto Region, Italy. *Sci. Total Environ.* **2020**, *734*, 139154. https://doi.org/10.1016/j.scitotenv.2020.139154.

(72) Zhang, D. Q.; Zhang, W. L.; Liang, Y. N. Adsorption of Perfluoroalkyl and Polyfluoroalkyl Substances (PFASs) from Aqueous Solution - A Review. *Science of the Total Environment*. Elsevier B.V. December 1, 2019, p 133606. https://doi.org/10.1016/j.scitotenv.2019.133606.

(73) Kennedy, A. M.; Reinert, A. M.; Knappe, D. R. U.; Ferrer, I.; Summers, R. S. Full- and Pilot-Scale GAC Adsorption of Organic Micropollutants. *Water Res.* **2015**, *68*, 238–248. https://doi.org/10.1016/j.watres.2014.10.010.

(74) Rossner, A.; Snyder, S. A.; Knappe, D. R. U. Removal of Emerging Contaminants of Concern by Alternative Adsorbents. *Water Res.* **2009**, *43* (15), 3787–3796. https://doi.org/10.1016/j.watres.2009.06.009.

(75) Ling, Y.; Klemes, M. J.; Xiao, L.; Alsbaiee, A.; Dichtel, W. R.; Helbling, D. E. Benchmarking Micropollutant Removal by Activated Carbon and Porous β-Cyclodextrin Polymers under Environmentally Relevant Scenarios. *Environ. Sci. Technol.* **2017**, *51* (13), 7590–7598. https://doi.org/10.1021/acs.est.7b00906.

(76) Woodard, S.; Berry, J.; Newman, B. Ion Exchange Resin for PFAS Removal and Pilot Test

Comparison to GAC. *Remediat. J.* **2017**, *27* (3), 19–27. https://doi.org/10.1002/rem.21515.

(77) Zaggia, A.; Conte, L.; Falletti, L.; Fant, M.; Chiorboli, A. Use of Strong Anion Exchange Resins for the Removal of Perfluoroalkylated Substances from Contaminated Drinking Water in Batch and Continuous Pilot Plants. *Water Res.* **2016**, *91*, 137–146. https://doi.org/10.1016/j.watres.2015.12.039.

(78) Haddad, M.; Oie, C.; Vo Duy, S.; Sauvé, S.; Barbeau, B. Adsorption of Micropollutants Present in Surface Waters onto Polymeric Resins: Impact of Resin Type and Water Matrix on Performance. *Sci. Total Environ.* **2019**, *660*, 1449–1458. https://doi.org/10.1016/j.scitotenv.2018.12.247.

(79) Deng, S.; Yu, Q.; Huang, J.; Yu, G. Removal of Perfluorooctane Sulfonate from Wastewater by Anion Exchange Resins: Effects of Resin Properties and Solution Chemistry. *Water Res.* **2010**, *44* (18), 5188–5195. https://doi.org/10.1016/j.watres.2010.06.038.

(80) Gao, Y.; Deng, S.; Du, Z.; Liu, K.; Yu, G. Adsorptive Removal of Emerging Polyfluoroalky Substances F-53B and PFOS by Anion-Exchange Resin: A Comparative Study. *J. Hazard. Mater.* **2017**, *323* (Pt A), 550–557. https://doi.org/10.1016/j.jhazmat.2016.04.069.

(81) Zhang, X.; Niu, H.; Pan, Y.; Shi, Y.; Cai, Y. Modifying the Surface of Fe3O4/SiO2 Magnetic Nanoparticles with C18/NH2 Mixed Group to Get an Efficient Sorbent for Anionic Organic Pollutants. *J. Colloid Interface Sci.* **2011**, *362* (1), 107–112. https://doi.org/10.1016/j.jcis.2011.06.032.

(82) Wang, W.; Xu, Z.; Zhang, X.; Wimmer, A.; Shi, E.; Qin, Y.; Zhao, X.; Zhou, B.; Li, L. Rapid and Efficient Removal of Organic Micropollutants from Environmental Water Using a Magnetic Nanoparticles-Attached Fluorographene-Based Sorbent. *Chem. Eng. J.* **2018**, *343*, 61–68. https://doi.org/10.1016/j.cej.2018.02.101.

(83) Liu, K.; Zhang, S.; Hu, X.; Zhang, K.; Roy, A.; Yu, G. Understanding the Adsorption of PFOA on MIL-101(Cr)-Based Anionic-Exchange Metal-Organic Frameworks: Comparing DFT Calculations with Aqueous Sorption Experiments. *Environ. Sci. Technol.* **2015**, *49* (14), 8657–8665. https://doi.org/10.1021/acs.est.5b00802.

(84) Klemes, M. J.; Skala, L. P.; Ateia, M.; Trang, B.; Helbling, D. E.; Dichtel, W. R. Polymerized Molecular Receptors as Adsorbents to Remove Micropollutants from Water. *Acc. Chem. Res.* **2020**, *53* (10), 2314–2324. https://doi.org/10.1021/acs.accounts.0c00426.

(85) Alsbaiee, A.; Smith, B. J.; Xiao, L.; Ling, Y.; Helbling, D. E.; Dichtel, W. R. Rapid

Removal of Organic Micropollutants from Water by a Porous β-Cyclodextrin Polymer. *Nature* **2016**, *529* (7585), 190–194. https://doi.org/10.1038/nature16185.

(86) Crini, G. Review: A History of Cyclodextrins. *Chemical Reviews*. American Chemical Society November 12, 2014, pp 10940–10975. https://doi.org/10.1021/cr500081p.

(87) Crini, G. Cyclodextrin–Epichlorohydrin Polymers Synthesis, Characterization and Applications to Wastewater Treatment: A Review. *Environmental Chemistry Letters*. Springer Science and Business Media Deutschland GmbH February 23, 2021, p 3. https://doi.org/10.1007/s10311-021-01204-z.

(88) Ling, Y.; Klemes, M. J.; Steinschneider, S.; Dichtel, W. R.; Helbling, D. E. QSARs to Predict Adsorption Affinity of Organic Micropollutants for Activated Carbon and B-Cyclodextrin Polymer Adsorbents. *Water Res.* **2019**, *154*, 217–226. https://doi.org/10.1016/j.watres.2019.02.012.

(89) Mocanu, G.; Vizitiu, D.; Carpov, A. Cyclodextrin Polymers. *J. Bioact. Compat. Polym.* **2001**, *16* (4), 315–342. https://doi.org/10.1106/JJUV-8F2K-JGYF-HNGF.

(90) Crini, G. Recent Developments in Polysaccharide-Based Materials Used as Adsorbents in Wastewater Treatment. *Progress in Polymer Science (Oxford)*. Pergamon January 1, 2005, pp 38–70. https://doi.org/10.1016/j.progpolymsci.2004.11.002.

(91) Xiao, L.; Ching, C.; Ling, Y.; Nasiri, M.; Klemes, M. J.; Reineke, T. M.; Helbling, D. E.; Dichtel, W. R. Cross-Linker Chemistry Determines the Uptake Potential of Perfluorinated Alkyl Substances by β-Cyclodextrin Polymers. *Macromolecules* **2019**. https://doi.org/10.1021/acs.macromol.9b00417.

(92) Ling, Y.; Alzate-Sánchez, D. M.; Klemes, M. J.; Dichtel, W. R.; Helbling, D. E. Evaluating the Effects of Water Matrix Constituents on Micropollutant Removal by Activated Carbon and β-Cyclodextrin Polymer Adsorbents. *Water Res.* **2020**, *173*, 115551. https://doi.org/10.1016/j.watres.2020.115551.

(93) Wu, C.; Klemes, M. J.; Trang, B.; Dichtel, W. R.; Helbling, D. E. Exploring the Factors That Influence the Adsorption of Anionic PFAS on Conventional and Emerging Adsorbents in Aquatic Matrices. *Water Res.* **2020**, *182*, 115950. https://doi.org/10.1016/j.watres.2020.115950.

(94) Ching, C.; Klemes, M. J.; Trang, B.; Dichtel, W. R.; Helbling, D. E. β-Cyclodextrin Polymers with Different Crosslinkers and Ion Exchange Resins Exhibit Variable

Adsorption of Anionic, Zwitterionic, and Non-Ionic PFASs. *Environ. Sci. Technol.* **2020**. https://doi.org/10.1021/acs.est.0c04028.

(95) Wang, R.; Ching, C.; Dichtel, W. R.; Helbling, D. E. Evaluating the Removal of Per- and Polyfluoroalkyl Substances from Contaminated Groundwater with Different Adsorbents Using a Suspect Screening Approach. *Environ. Sci. Technol. Lett.* **2020**, acs.estlett.0c00736. https://doi.org/10.1021/acs.estlett.0c00736.

(96) Hoffman, K.; Webster, T. F.; Bartell, S. M.; Weisskopf, M. G.; Fletcher, T.; Vieira, V. M. Private Drinking Water Wells as a Source of Exposure to Perfluorooctanoic Acid (PFOA) in Communities Surrounding a Fluoropolymer Production Facility. *Environ. Health Perspect.* **2011**, *119* (1), 92–97. https://doi.org/10.1289/ehp.1002503.

(97) Post, G. B.; Louis, J. B.; Lippincott, R. L.; Procopio, N. A. Occurrence of Perfluorinated Compounds in Raw Water from New Jersey Public Drinking Water Systems. *Environ. Sci. Technol.* **2013**, *47* (23), 13266–13275. https://doi.org/10.1021/es402884x.

(98) Moody, C. A.; Field, J. A. Determination of Perfluorocarboxylates in Groundwater Impacted by Fire- Fighting Activity. *Environ. Sci. Technol.* **1999**, *33* (16), 2800–2806. https://doi.org/10.1021/es981355+.

(99) Barzen-Hanson, K. A.; Field, J. A. Discovery and Implications of C2 and C3 Perfluoroalkyl Sulfonates in Aqueous Film-Forming Foams and Groundwater. *Environ. Sci. Technol. Lett.* **2015**, *2* (4), 95–99. https://doi.org/10.1021/acs.estlett.5b00049.

(100) Crone, B. C.; Speth, T. F.; Wahman, D. G.; Smith, S. J.; Abulikemu, G.; Kleiner, E. J.; Pressman, J. G. Occurrence of Per- and Polyfluoroalkyl Substances (PFAS) in Source Water and Their Treatment in Drinking Water. *Crit. Rev. Environ. Sci. Technol.* **2019**, *49* (24), 2359–2396. https://doi.org/10.1080/10643389.2019.1614848.

(101) Xiao, L.; Ling, Y.; Alsbaiee, A.; Li, C.; Helbling, D. E.; Dichtel, W. R. β-Cyclodextrin Polymer Network Sequesters Perfluorooctanoic Acid at Environmentally Relevant Concentrations. *J. Am. Chem. Soc.* **2017**, *139* (23), 7689–7692. https://doi.org/10.1021/jacs.7b02381.

(102) Klemes, M. J.; Ling, Y.; Ching, C.; Wu, C.; Xiao, L.; Helbling, D. E.; Dichtel, W. R. Reduction of a Tetrafluoroterephthalonitrile-β-Cyclodextrin Polymer to Remove Anionic Micropollutants and Perfluorinated Alkyl Substances from Water. *Angew. Chemie Int. Ed.*

2019, *58* (35), 12049–12053. https://doi.org/10.1002/anie.201905142.

(103) Du, Z.; Deng, S.; Zhang, S.; Wang, B.; Huang, J.; Wang, Y.; Yu, G.; Xing, B. Selective and High Sorption of Perfluorooctanesulfonate and Perfluorooctanoate by Fluorinated Alkyl Chain Modified Montmorillonite. *J. Phys. Chem. C* **2016**, *120* (30), 16782–16790. https://doi.org/10.1021/acs.jpcc.6b04757.

(104) Du, Z.; Deng, S.; Chen, Y.; Wang, B.; Huang, J.; Wang, Y.; Yu, G. Removal of Perfluorinated Carboxylates from Washing Wastewater of Perfluorooctanesulfonyl Fluoride Using Activated Carbons and Resins. *J. Hazard. Mater.* **2015**, *286*, 136–143. https://doi.org/10.1016/j.jhazmat.2014.12.037.

(105) Liu, Y.; Pereira, A. D. S.; Martin, J. W. Discovery of C5-C17 Poly- and Perfluoroalkyl Substances in Water by in-Line Spe-HPLC-Orbitrap with in-Source Fragmentation Flagging. *Anal. Chem.* **2015**, *87* (8), 4260–4268. https://doi.org/10.1021/acs.analchem.5b00039.

(106) Xiao, X.; Ulrich, B. A.; Chen, B.; Higgins, C. P. Sorption of Poly- and Perfluoroalkyl Substances (PFASs) Relevant to Aqueous Film-Forming Foam (AFFF)-Impacted Groundwater by Biochars and Activated Carbon. *Environ. Sci. Technol.* **2017**, *51* (11), 6342–6351. https://doi.org/10.1021/acs.est.7b00970.

(107) Murray, C. C.; Vatankhah, H.; McDonough, C. A.; Nickerson, A.; Hedtke, T. T.; Cath, T. Y.; Higgins, C. P.; Bellona, C. L. Removal of Per- and Polyfluoroalkyl Substances Using Super-Fine Powder Activated Carbon and Ceramic Membrane Filtration. *J. Hazard. Mater.* **2019**, *366*, 160–168. https://doi.org/10.1016/j.jhazmat.2018.11.050.

(108) McCleaf, P.; Englund, S.; Östlund, A.; Lindegren, K.; Wiberg, K.; Ahrens, L. Removal Efficiency of Multiple Poly- and Perfluoroalkyl Substances (PFASs) in Drinking Water Using Granular Activated Carbon (GAC) and Anion Exchange (AE) Column Tests. *Water Res.* **2017**, *120*, 77–87. https://doi.org/10.1016/j.watres.2017.04.057.

(109) Xiao, F.; Zhang, X.; Penn, L.; Gulliver, J. S.; Simcik, M. F. Effects of Monovalent Cations on the Competitive Adsorption of Perfluoroalkyl Acids by Kaolinite: Experimental Studies and Modeling. *Environ. Sci. Technol.* **2011**, *45* (23), 10028–10035. https://doi.org/10.1021/es202524y.

(110) Li, C.; Klemes, M. J.; Dichtel, W. R.; Helbling, D. E. Tetrafluoroterephthalonitrile-Crosslinked β-Cyclodextrin Polymers for Efficient Extraction and Recovery of Organic Micropollutants from Water. *J. Chromatogr. A* **2018**, *1541*, 52–56.

https://doi.org/10.1016/j.chroma.2018.02.012.

(111) Place, B. J.; Field, J. A. Identification of Novel Fluorochemicals in Aqueous Film-Forming Foams Used by the US Military. *Environ. Sci. Technol.* **2012**, *46* (13), 7120–7127. https://doi.org/10.1021/es301465n.

(112) Patterson, C.; Burkhardt, J.; Schupp, D.; Krishnan, E. R.; Dyment, S.; Merritt, S.; Zintek, L.; Kleinmaier, D. Effectiveness of Point-of-use/Point-of-entry Systems to Remove Per- and Polyfluoroalkyl Substances from Drinking Water. *AWWA Water Sci.* **2019**, *1* (2), e1131. https://doi.org/10.1002/aws2.1131.

(113) Schaefer, C. E.; Nguyen, D.; Ho, P.; Im, J.; Leblanc, A. Assessing Rapid Small-Scale Column Tests for Treatment of Perfluoroalkyl Acids by Anion Exchange Resin. *Ind. Eng. Chem. Res.* **2019**, *58* (22), 9701–9706. https://doi.org/10.1021/acs.iecr.9b00858.

(114) Park, M.; Daniels, K. D.; Wu, S.; Ziska, A. D.; Snyder, S. A. Magnetic Ion-Exchange (MIEX) Resin for Perfluorinated Alkylsubstance (PFAS) Removal in Groundwater: Roles of Atomic Charges for Adsorption. *Water Res.* **2020**, *181*, 115897. https://doi.org/10.1016/j.watres.2020.115897.

(115) Krafft, M. P.; Riess, J. G. Chemistry, Physical Chemistry, and Uses of Molecular Fluorocarbon- Hydrocarbon Diblocks, Triblocks, and Related Compounds-Unique "Apolar" Components for Self-Assembled Colloid and Interface Engineering. *Chem. Rev.* **2009**, *109* (5), 1714–1792. https://doi.org/10.1021/cr800260k.

(116) Ellis, D. A.; Denkenberger, K. A.; Burrow, T. E.; Mabury, S. A. The Use of 19 F NMR to Interpret the Structural Properties of Perfluorocarboxylate Acids: A Possible Correlation with Their Environmental Disposition. **2004**. https://doi.org/10.1021/jp049372a.

(117) Knochenhauer, G.; Reiche, J.; Brehmer, L.; Barberka, T.; Woolley, M.; Tredgold, R.; Hodge, P. Do Perfluorinated Chains Always Have to Be Twisted? *J. Chem. Soc. Chem. Commun.* **1995**, No. 16, 1619–1620. https://doi.org/10.1039/C39950001619.

(118) Yang, A.; Ching, C.; Easler, M.; Helbling, D. E.; Dichtel, W. R. Cyclodextrin Polymers with Nitrogen-Containing Tripodal Crosslinkers for Efficient PFAS Adsorption. *ACS Mater. Lett.* **2020**, *2* (9), 1240–1245. https://doi.org/10.1021/acsmaterialslett.0c00240.

(119) Sun, M.; Arevalo, E.; Strynar, M.; Lindstrom, A.; Richardson, M.; Kearns, B.; Pickett, A.; Smith, C.; Knappe, D. R. U. Legacy and Emerging Perfluoroalkyl Substances Are Important Drinking Water Contaminants in the Cape Fear River Watershed of North Carolina.

Environ. Sci. Technol. Lett. **2016**, *3* (12), 415–419. https://doi.org/10.1021/acs.estlett.6b00398.

(120) Yu, Q.; Zhang, R.; Deng, S.; Huang, J.; Yu, G. Sorption of Perfluorooctane Sulfonate and Perfluorooctanoate on Activated Carbons and Resin: Kinetic and Isotherm Study. *Water Res.* **2009**, *43* (4), 1150–1158. https://doi.org/10.1016/j.watres.2008.12.001.

(121) Carter, K. E.; Farrell, J. Removal of Perfluorooctane and Perfluorobutane Sulfonate from Water via Carbon Adsorption and Ion Exchange. *Sep. Sci. Technol.* **2010**, *45* (6), 762–767. https://doi.org/10.1080/01496391003608421.

(122) Wang, F.; Shih, K. Adsorption of Perfluorooctanesulfonate (PFOS) and Perfluorooctanoate (PFOA) on Alumina: Influence of Solution PH and Cations. *Water Res.* **2011**, *45* (9), 2925–2930. https://doi.org/10.1016/j.watres.2011.03.007.

(123) Punyapalakul, P.; Suksomboon, K.; Prarat, P.; Khaodhiar, S. Effects of Surface Functional Groups and Porous Structures on Adsorption and Recovery of Perfluorinated Compounds by Inorganic Porous Silicas. *Sep. Sci. Technol.* **2013**, *48* (5), 775–788. https://doi.org/10.1080/01496395.2012.710888.

(124) Ochoa-Herrera, V.; Sierra-Alvarez, R. Removal of Perfluorinated Surfactants by Sorption onto Granular Activated Carbon, Zeolite and Sludge. *Chemosphere* **2008**, *72* (10), 1588–1593. https://doi.org/10.1016/j.chemosphere.2008.04.029.

(125) Zhou, Q.; Pan, G.; Shen, W. Enhanced Sorption of Perfluorooctane Sulfonate and Cr(VI) on Organo Montmorillonite: Influence of Solution PH and Uptake Mechanism. In *Adsorption*; Kluwer Academic Publishers, 2013; Vol. 19, pp 709–715. https://doi.org/10.1007/s10450-013-9496-5.

(126) Zhang, Q.; Deng, S.; Yu, G.; Huang, J. Removal of Perfluorooctane Sulfonate from Aqueous Solution by Crosslinked Chitosan Beads: Sorption Kinetics and Uptake Mechanism. **2010**. https://doi.org/10.1016/j.biortech.2010.10.040.

(127) Kawano, S.; Kida, T.; Takemine, S.; Matsumura, C.; Nakano, T.; Kuramitsu, M.; Adachi, K.; Akashi, M. Efficient Removal and Recovery of Perfluorinated Compounds from Water by Surface-Tethered β-Cyclodextrins on Polystyrene Particles. *Chem. Lett.* **2013**, *42* (4), 392–394. https://doi.org/10.1246/cl.121239.

(128) Wang, F.; Liu, C.; Shih, K. Adsorption Behavior of Perfluorooctanesulfonate (PFOS) and Perfluorooctanoate (PFOA) on Boehmite. *Chemosphere* **2012**, *89* (8), 1009–1014.

https://doi.org/10.1016/j.chemosphere.2012.06.071.

(129) Yu, Q.; Deng, S.; Yu, G. Selective Removal of Perfluorooctane Sulfonate from Aqueous Solution Using Chitosan-Based Molecularly Imprinted Polymer Adsorbents. *Water Res.* **2008**, *42* (12), 3089–3097. https://doi.org/10.1016/j.watres.2008.02.024.

(130) You, C.; Jia, C.; Pan, G. Effect of Salinity and Sediment Characteristics on the Sorption and Desorption of Perfluorooctane Sulfonate at Sediment-Water Interface. *Environ. Pollut.* **2010**, *158* (5), 1343–1347. https://doi.org/10.1016/j.envpol.2010.01.009.

(131) Lath, S.; Navarro, D. A.; Losic, D.; Kumar, A.; McLaughlin, M. J. Sorptive Remediation of Perfluorooctanoic Acid (PFOA) Using Mixed Mineral and Graphene/Carbon-Based Materials. *Environ. Chem.* **2018**, *15* (8), 472. https://doi.org/10.1071/EN18156.

(132) Campos-Pereira, H.; Kleja, D. B.; Sjöstedt, C.; Ahrens, L.; Klysubun, W.; Gustafsson, J. P. The Adsorption of Per- And Polyfluoroalkyl Substances (PFASs) onto Ferrihydrite Is Governed by Surface Charge. *Environ. Sci. Technol.* **2020**, *54* (24), 15722–15730. https://doi.org/10.1021/acs.est.0c01646.

(133) Tang, C. Y.; Shiang Fu, Q.; Gao, D.; Criddle, C. S.; Leckie, J. O. Effect of Solution Chemistry on the Adsorption of Perfluorooctane Sulfonate onto Mineral Surfaces. *Water Res.* **2010**, *44* (8), 2654–2662. https://doi.org/10.1016/j.watres.2010.01.038.

(134) Kwon, Y.-N.; Shih, K.; Tang, C.; Leckie, J. O. Adsorption of Perfluorinated Compounds on Thin-Film Composite Polyamide Membranes. *J. Appl. Polym. Sci.* **2012**, *124* (2), 1042–1049. https://doi.org/10.1002/app.35182.

(135) Chen, H.; Zhang, C.; Yu, Y.; Han, J. Sorption of Perfluorooctane Sulfonate (PFOS) on Marine Sediments. *Mar. Pollut. Bull.* **2012**, *64* (5), 902–906. https://doi.org/10.1016/j.marpolbul.2012.03.012.

(136) Haghani, A.; Eaton, A.; Eaton, E.; Jack, R.; Bromirski, M.; Thermo Fisher Scientific. *Secondary Validation Study for EPA Method 537.1 Using Automated SPE Followed by LC-Q Exactive Orbitrap MS*; 2019.

(137) Parida, S. K.; Dash, S.; Patel, S.; Mishra, B. K. Adsorption of Organic Molecules on Silica Surface. *Advances in Colloid and Interface Science*. Elsevier September 13, 2006, pp 77–

110. https://doi.org/10.1016/j.cis.2006.05.028.

(138) Xie, W. H.; Shiu, W. Y.; Mackay, D. A Review of the Effect of Salts on the Solubility of Organic Compounds in Seawater. *Marine Environmental Research*. Elsevier Ltd December 1, 1997, pp 429–444. https://doi.org/10.1016/S0141-1136(97)00017-2.

(139) Bauer, C.; Cramer, R.; Schuchhardt, J. Evaluation of Peak-Picking Algorithms for Protein Mass Spectrometry. In *Data Mining in Proteomics: From Standards to Applications*; Hamacher, M., Eisenacher, M., Stephan, C., Eds.; Humana Press: Totowa, NJ, 2011; pp 341–352. https://doi.org/10.1007/978-1-60761-987-1_22.

(140) González-Gaya, B.; Lopez-Herguedas, N.; Santamaria, A.; Mijangos, F.; Etxebarria, N.; Olivares, M.; Prieto, A.; Zuloaga, O. Suspect Screening Workflow Comparison for the Analysis of Organic Xenobiotics in Environmental Water Samples. *Chemosphere* **2021**, *274*, 129964. https://doi.org/10.1016/j.chemosphere.2021.129964.

(141) Celma, A.; Sancho, J. V.; Schymanski, E. L.; Fabregat-Safont, D.; Ibáñez, M.; Goshawk, J.; Barknowitz, G.; Hernández, F.; Bijlsma, L. Improving Target and Suspect Screening High-Resolution Mass Spectrometry Workflows in Environmental Analysis by Ion Mobility Separation. *Environ. Sci. Technol.* **2020**, *54* (23), 15120–15131. https://doi.org/10.1021/acs.est.0c05713.

(142) Nason, S. L.; Koelmel, J.; Zuverza-Mena, N.; Stanley, C.; Tamez, C.; Bowden, J. A.; Godri Pollitt, K. J. Software Comparison for Nontargeted Analysis of PFAS in AFFF-Contaminated Soil. *J. Am. Soc. Mass Spectrom.* **2020**. https://doi.org/10.1021/jasms.0c00261.

(143) Hollender, J.; Schymanski, E. L.; Singer, H. P.; Ferguson, P. L. Nontarget Screening with High Resolution Mass Spectrometry in the Environment: Ready to Go? *Environ. Sci. Technol.* **2017**, *51* (20), 11505–11512. https://doi.org/10.1021/acs.est.7b02184.

(144) Gago-Ferrero, P.; Schymanski, E. L.; Bletsou, A. A.; Aalizadeh, R.; Hollender, J.; Thomaidis, N. S. Extended Suspect and Non-Target Strategies to Characterize Emerging Polar Organic Contaminants in Raw Wastewater with LC-HRMS/MS. *Environ. Sci. Technol.* **2015**, *49* (20), 12333–12341. https://doi.org/10.1021/acs.est.5b03454.

(145) Wang, Q.; Ruan, Y.; Jin, L.; Zhang, X.; Li, J.; He, Y.; Wei, S.; Lam, J. C. W.; Lam, P. K. S. Target, Nontarget, and Suspect Screening and Temporal Trends of Per- And Polyfluoroalkyl Substances in Marine Mammals from the South China Sea. *Environ. Sci.*

Technol. **2021**, *55* (2), 1045–1056. https://doi.org/10.1021/acs.est.0c06685.

(146) Kutarna, S.; Tang, S.; Hu, X.; Peng, H. Enhanced Nontarget Screening Algorithm Reveals Highly Abundant Chlorinated Azo Dye Compounds in House Dust. *Environ. Sci. Technol.* **2021**, acs.est.0c06382. https://doi.org/10.1021/acs.est.0c06382.

(147) Baygi, S. F.; Fernando, S.; Hopke, P. K.; Holsen, T. M.; Crimmins, B. S. Nontargeted Discovery of Novel Contaminants in the Great Lakes Region: A Comparison of Fish Fillets and Fish Consumers. *Environ. Sci. Technol.* **2021**, *55* (6), 3765–3774. https://doi.org/10.1021/acs.est.0c08507.

(148) Zhang, C.; Hopkins, Z. R.; McCord, J.; Strynar, M. J.; Knappe, D. R. U. Fate of Per- And Polyfluoroalkyl Ether Acids in the Total Oxidizable Precursor Assay and Implications for the Analysis of Impacted Water. *Environ. Sci. Technol. Lett.* **2019**, *6* (11), 662–668. https://doi.org/10.1021/acs.estlett.9b00525.

(149) Schaider, L. A.; Balan, S. A.; Blum, A.; Andrews, D. Q.; Strynar, M. J.; Dickinson, M. E.; Lunderberg, D. M.; Lang, J. R.; Peaslee, G. F. Fluorinated Compounds in U.S. Fast Food Packaging. *Environ. Sci. Technol. Lett.* **2017**, *4* (3), 105–111. https://doi.org/10.1021/acs.estlett.6b00435.

(150) Ritter, E. E.; Dickinson, M. E.; Harron, J. P.; Lunderberg, D. M.; DeYoung, P. A.; Robel, A. E.; Field, J. A.; Peaslee, G. F. PIGE as a Screening Tool for Per- and Polyfluorinated Substances in Papers and Textiles. *Nucl. Instruments Methods Phys. Res. Sect. B Beam Interact. with Mater. Atoms* **2017**, *407*, 47–54. https://doi.org/10.1016/j.nimb.2017.05.052.

(151) Koch, A.; Aro, R.; Wang, T.; Yeung, L. W. Y. Towards a Comprehensive Analytical Workflow for the Chemical Characterisation of Organofluorine in Consumer Products and Environmental Samples. *TrAC - Trends in Analytical Chemistry*. Elsevier B.V. February 1, 2020, p 115423. https://doi.org/10.1016/j.trac.2019.02.024.

(152) Karoyo, A. H.; Sidhu, P.; Wilson, L. D.; Hazendonk, P. Characterization and Dynamic Properties for the Solid Inclusion Complexes of β-Cyclodextrin and Perfluorooctanoic Acid. *J. Phys. Chem. B* **2013**, *117* (27), 8269–8282. https://doi.org/10.1021/jp402559n.

(153) Karoyo, A. H.; Wilson, L. D. Investigation of the Adsorption Processes of Fluorocarbon and Hydrocarbon Anions at the Solid-Solution Interface of Macromolecular Imprinted Polymer Materials. *J. Phys. Chem. C* **2016**, *120* (12), 6553–6568.

https://doi.org/10.1021/acs.jpcc.5b12246.

(154) Blanch, G. P.; Ruiz del Castillo, M. L.; del Mar Caja, M.; Pérez-Méndez, M.; Sánchez-Cortés, S. Stabilization of All-Trans-Lycopene from Tomato by Encapsulation Using Cyclodextrins. *Food Chem.* **2007**, *105* (4), 1335–1341. https://doi.org/10.1016/j.foodchem.2007.04.060.

(155) Schymanski, E. L.; Jeon, J.; Gulde, R.; Fenner, K.; Ruff, M.; Singer, H. P.; Hollender, J. Identifying Small Molecules via High Resolution Mass Spectrometry: Communicating Confidence. *Environmental Science and Technology*. American Chemical Society February 18, 2014, pp 2097–2098. https://doi.org/10.1021/es5002105.

(156) Klemes, M. J.; Ling, Y.; Chiapasco, M.; Alsbaiee, A.; Helbling, D. E.; Dichtel, W. R. Phenolation of Cyclodextrin Polymers Controls Their Lead and Organic Micropollutant Adsorption. *Chem. Sci.* **2018**, *9* (47), 8883–8889. https://doi.org/10.1039/c8sc03267j.

(157) Alzate-Sánchez, D. M.; Ling, Y.; Li, C.; Frank, B. P.; Bleher, R.; Fairbrother, D. H.; Helbling, D. E.; Dichtel, W. R. β-Cyclodextrin Polymers on Microcrystalline Cellulose as a Granular Media for Organic Micropollutant Removal from Water. *ACS Appl. Mater. Interfaces* **2019**, *11* (8), 8089–8096. https://doi.org/10.1021/acsami.8b22100.

APPENDICES

APPENDICES LIST OF FIGURES

APPENDICES LIST OF TABLES

APPENDIX A – Evaluating the Removal of Per- and Polyfluoroalkyl Substances from Contaminated Groundwater with Different Adsorbents Using a Suspect Screening Approach

A.1 Adsorbents

Table A-1. Characterization information of adsorbents.

Type	Adsorbent	Functional group/charge	Particle diameter (µm)	Surface area[b] (m^2 g^{-1})	Micropore volume[c] (cm^3 g^{-1})	Zeta potential at pH 7[d] (mV)
Cyclodextrin polymer	DEXSORB	Weakly acidic	<150	30	0 (mesoporous)	-20 ± 4
	DEXSORB+	Permanently cationic	<63	20	0 (mesoporous)	+20 ± 1
	M+	Permanently cationic	<150	80	0 (mesoporous)	+20
Anion exchange resin	Purolite (Purofine® PFA694E)[a]	Complex amino acids	675 ± 75	n.a.	n.a.	n.a.
AC	CalgonCarbon (Filtrasorb® 400-M)	n.a.	75 - 125	900	0.3	-8 ± 1

[a] Data from Purolite product sheets;

[b] Brunauer-Emmet-Teller surface area. Data from Klemes et al. (2019)[102] for DEXSORB, from Wu et al. (2020)[93] for DEXSORB+ and AC, and from measurements made with previous batches of CDPs synthesized with the same crosslinker for M+;

[c] Micropore volume values were estimated using the default software settings of a N_2-cylindrical pore-oxide surface DFT model and a regularization of 0.01000. Data from Wu et al. (2020)[93].

[d] The zeta potential measurements were performed on a Nano Zetasizer (Malvern Instruments Ltd.) with a He-Ne laser (633 nm, Max 5mW). Data for DEXSORB and DEXSORB+ from Ching et al. (2020)[94], for AC from Wu et al. (2020)[93], and for M+ from measurements made with previous batches of CDPs synthesized with the same co-monomers;

n.a. indicates not applicable data for a particular adsorbent.

A.2 Water samples

Table A-2. Characterization information of groundwater sample.

	Parameter	Value
Water quality parameters (**mg/L**)	pH[a]	6.7
	Sulfate[b]	23.44 ± 0.07
	Chloride[b]	15.92 ± 0.06
	Total dissolved solids (TDS)[a]	200
	Dissolved organic carbon (DOC)[a]	0.83
	Total suspended solids (TSS)[a]	2.8
Target PFAS concentrations[c] (**ng/L**)	PFBS[d]	280 ± 27
	PFPeS[d]	629 ± 20
	PFHxS[d]	2256 ± 52
	PFHpS[d]	584 ± 26
	PFOS[d]	14746 ± 353
	PFNS[d]	7 ± 1
	PFHxA[d]	489 ± 13
	PFHpA[d]	210 ± 9
	PFOA[d]	593 ± 20
	PFNA[d]	15 ± 2
	PFDA[d]	9 ± 1

[a] pH, TDS, DOC and TSS were provided by the operator of the facility that provided the groundwater sample;

[b] Sulfate and chloride ion were measured by means of ion chromatography (ThermoFisher Scientific) according to EPA Method 300.1;

[c] All target PFAS concentrations are for the linear PFASs; the standard deviation of triplicate concentration values, calculated using the "= STDEV( )" function in MS Excel;

[d] PFAS concentrations were measured by means of high-performance liquid chromatography coupled to high-resolution mass spectrometry using the analytical method described in Wu et al. (2020)[93].

A.3 HRMS analysis and suspect screening

The mobile phase consisted of (A) LC-MS grade water amended with 20 mM ammonium acetate and (B) LC-MS grade methanol. Samples were injected at 5 mL volumes onto a Hypersil Gold dC18 12 µm 2.1 x 20 mm trap column (ThermoFisher Scientific) at room temperature (21-22°C) using an isocratic mobile phase of 99% A pumped at 1 $mL \cdot min^{-1}$ via a low-pressure loading pump. Elution from the trap column and subsequent separation of analytes on an Atlantis® dC18 5 µm 2.1 x 150 mm analytical column (Waters) at 25°C was achieved using an initial mobile phase of 60% A pumped at 0.3 $mL \cdot min^{-1}$ via a high pressure elution pump. The isocratic mobile phase delivered from the loading pump changed to 2% A at 37.3 minutes to rinse the trap column and returned to 99% A at 41.3 minutes to prepare for the next sample injection. The mobile phase gradient delivered from the loading pump remained at 60% A until 6.1 minutes and then increased linearly to 10% A at 30.1 minutes. The mobile phase was held at 10% A until 37.1 minutes before it returned to 60% A to prepare for the next sample. The chromatography program had a total duration of 42.1 minutes.

Full-scan mass spectral acquisitions were acquired in the m/z range of 100 – 1200 and data-dependent MS2 scans (to collect fragments) were triggered using an inclusion list containing the exact masses of each suspect PFAS. The suspect screening resulted in a list of 98 PFASs that were putatively present in the groundwater samples; 68 suspect hits were identified in negative polarity mode and 30 suspect hits were identified in positive polarity mode. These suspect hits were identified based on the matching of a theoretical exact mass of a suspect PFAS with the accurate mass of a picked peak in our full-scan mass spectral acquisition within a mass (*m/z*) tolerance of

10 ppm. The *blind* filter excluded suspect hits that were measured in at least one of the triplicate groundwater samples with a peak area less than 100 times the maximum peak area among the blank samples. The *replicate* filter excluded suspect hits that were not present in each of the triplicate groups within a mass (*m/z*) tolerance of 12 ppm and a retention time window of 30 seconds. Each of the 98 PFASs were then manually checked to ensure that we were confident in the final list of identified PFASs.

Twelve suspect PFASs were identified as duplicate hits during positive mode acquisition (*e.g.*, as the [M+H]+ and [M+] adducts) and were removed from the list (86 suspect PFAS remaining). There were also six suspect PFASs that were measured in both negative polarity mode and positive polarity mode; we examined the extracted ion chromatograms for each of these PFASs in each polarity mode and selected the polarity mode that generated the greater peak area for further consideration (80 suspect PFASs remaining). We then inspected the chromatographic peak shape of each of the remaining PFASs using the XCalibur software (ThermoFisher Scientific); peaks that did not have at least five scans across the peak width and MS spectra that matched the molecular formula of the suspect hit were excluded from the list. We also examined the data-dependent MS2 spectra for each of the remaining suspect PFASs and excluded suspect hits that did not contain an MS2 fragment that was characteristic of PFASs; we note that database MS2 spectra are not available for most PFASs on our suspect list so the presence of at least one MS2 fragment that is characteristic of PFAS was the only diagnostic criterion used here. Twelve suspect hits were removed from our list based on insufficient MS or MS2 data (68 suspect PFASs remaining). We then organized the list of 68 remaining PFASs into groups of putative homologous series; we

reasoned that suspect PFASs that are present as members of a homologous series are likely to be true positive suspect hits. We further vetted this idea by examining the retention times (RTs) of each member of the homologous series. The RT had to increase with increasing chain-length for the PFAS to continue to be considered a suspect hit. We also cross-referenced the list of suspect hits with possible isomers in the original suspect database and modified some of the suspect annotations to align better with the homologous series that were identified. This analysis led us to remove three more suspect PFASs from our list (65 suspect PFASs remaining). Finally, we examined each of the identified homologous series by manually searching for additional homologues of the identified homologous series. We found sufficient analytical data to support the addition of three more PFASs to our list, resulting in a final list of 68 PFASs examined in our study. We provide the component name, component acronym, class acronym and SMILES notation for each of the 68 PFASs in **Table A-3**; the class name and class acronym are provided in **Table A-4**, and the analytical details, PFAS chain length, putative charge state in **Table A-5.** Confidence levels provided in **Table A-5** were adapted from elsewhere and are defined as: level 1 = structure confirmed with an authentic standard; level 2 = only plausible structure from our suspect list; level 3 = likely isomer, but other structures from our suspect list are plausible.[107,155]

Table A-3. List of 68 PFASs identified in groundwater sample.

No.	Component Name	Component Acronym	Class Acronym	SMILES
1	N-dimethylammoniocarboxypropyl-perfluorobutane sulfonamide	Am-CPr-FBSA	Am-CPr-FASA	C[NH+](C)CCC(NS(=O)(=O)C(F)(F)C(F)(F)C(F)(F)C(F)(F)C(F)(F)C([O-])=O
2	N-dimethylammoniocarboxypropyl-perfluorooctane sulfonamide	Am-CPr-FOSA	Am-CPr-FASA	C[NH+](C)CCC(NS(=O)(=O)C(F)(F)C(F)(F)C(F)(F)C(F)(F)C(F)(F)C(F)(F)C(F)(F)C(F)(F)C(F)(F)C([O-])=O
3	perfluoro ethyl cyclohexane sulfonate	PFEtCHxS	CHxS	OS(=O)(=O)C1(F)C(F)(F)C(F)(F)C(F)(C(F)(F)C(F)(F)F)C(F)(F)C1(F)F
4	perfluoro propyl cyclohexane sulfonate	PFPrCHxS	CHxS	OS(=O)(=O)C1(F)C(F)(F)C(F)(F)C(F)(C(F)(F)C(F)(F)C(F)(F)F)C(F)(F)C1(F)F
5	Chloro-perfluorooctane sulfonate	Cl-PFOS	Cl-PFSA	OS(=O)(=O)C(F)(Cl)C(F)(F)C(F)(F)C(F)(F)C(F)(F)C(F)(F)C(F)(F)C(F)(F)F
6	N-Carboxymethyldimethylammoniopropyl-perfluorohexanesulfonamide	CMeAmPr-FHxSA	CMeAmPr-FASA	C[N+](C)(CCCNS(=O)(=O)C(F)(F)C(F)(F)C(F)(F)C(F)(F)C(F)(F)C(F)(F)F)CC([O-])=O
7	N-ethylperfluoro-1-methane sulfonamide	EtFMeSA	EtFASA	CCNS(=O)(=O)C(F)(F)F
8	N-ethylperfluoro-1-butane sulfonamide	EtFBSA	EtFASA	CCNS(=O)(=O)C(F)(F)C(F)(F)C(F)(F)C(F)(F)F
9	PentaFluoroSulfide perfluorooctane sulfonate	F5S-PFOS	F5S-PFSA	OS(=O)(=O)C(F)(F)C(F)(F)C(F)(F)C(F)(F)C(F)(F)C(F)(F)C(F)(F)C(F)(F)S(F)(F)(F)(F)F
10	perfluoropropane sulfonamide	FPrSA	FASA	NS(=O)(=O)C(F)(F)C(F)(F)C(F)(F)F
11	perfluorobutane sulfonamide	FBSA	FASA	NS(=O)(=O)C(F)(F)C(F)(F)C(F)(F)C(F)(F)F
12	perfluoropentane sulfonamide	FPeSA	FASA	NS(=O)(=O)C(F)(F)C(F)(F)C(F)(F)C(F)(F)C(F)(F)F
13	perfluorohexane sulfonamide	FHxSA	FASA	NS(=O)(=O)C(F)(F)C(F)(F)C(F)(F)C(F)(F)C(F)(F)C(F)(F)C(F)(F)F

14	perfluoroheptane sulfonamide	FHpSA	FASA	NS(=O)(=O)C(F)(F)C(F)(F)C(F)(F)C(F)(F)C(F)(F)C(F)(F)C(F)(F)F
15	perfluorooctane sulfonamide	FOSA	FASA	NS(=O)(=O)C(F)(F)C(F)(F)C(F)(F)C(F)(F)C(F)(F)C(F)(F)C(F)(F)C(F)(F)F
16	Perfluorobutane sulfonamido acetic acid	FBSAA	FASAA	OC(=O)CNS(=O)(=O)C(F)(F)C(F)(F)C(F)(F)C(F)(F)F
17	Perfluoropentane sulfonamido acetic acid	FPeSAA	FASAA	OC(=O)CNS(=O)(=O)C(F)(F)C(F)(F)C(F)(F)C(F)(F)C(F)(F)F
18	Perfluorohexane sulfonamido acetic acid	FHxSAA	FASAA	OC(=O)CNS(=O)(=O)C(F)(F)C(F)(F)C(F)(F)C(F)(F)C(F)(F)C(F)(F)F
19	Hydrido-perfluorooctanoic acid	H-PFOA	H-PFCA	OC(=O)C(F)C(F)(F)C(F)(F)C(F)(F)C(F)(F)C(F)(F)C(F)(F)C(F)(F)F
20	Hydrido-perfluorononanoic acid	H-PFNA	H-PFCA	OC(=O)C(F)C(F)(F)C(F)(F)C(F)(F)C(F)(F)C(F)(F)C(F)(F)C(F)(F)F
21	Hydrido-perfluorodecananoic acid	H-PFDA	H-PFCA	OC(=O)C(F)C(F)(F)C(F)(F)C(F)(F)C(F)(F)C(F)(F)C(F)(F)C(F)(F)F
22	Hydrido-PerFluoroHexane Sulfonate	H-PFHxS	H-PFSA	OS(=O)(=O)C(F)C(F)(F)C(F)(F)C(F)(F)C(F)(F)C(F)(F)F
23	Hydrido-PerFluoroHeptane Sulfonate	H-PFHpS	H-PFSA	OS(=O)(=O)C(F)(F)C(F)(F)C(F)(F)C(F)(F)C(F)(F)C(F)(F)C(F)C(F)(F)F
24	Hydrido-PerFluoroOctane Sulfonate	H-PFOS	H-PFSA	OS(=O)(=O)C(F)(F)C(F)(F)C(F)(F)C(F)(F)C(F)(F)C(F)(F)C(F)(F)C(F)(F)F
25	Hydrido-PerFluoroDecane Sulfonate	H-PFDS	H-PFSA	OS(=O)(=O)C(F)(F)C(F)(F)C(F)(F)C(F)(F)C(F)(F)C(F)(F)C(F)(F)C(F)(F)C(F)(F)C(F)C(F)(F)F
26	perfluoropropane unsaturated ether/alcohol (-1F, +1H)	H-UPFPr-O/OH	H-UPFA-O/OH	FCOC(F)=C(F)F
27	Hydrido-Unsaturated PerFluoroOctane Sulfonate	H-UPFOS	H-UPFSA	OS(=O)(=O)C(F)(F)C(F)(F)C(F)(F)C(F)(F)C(F)(F)C(F)C(\F)=C(/F)C(F)(F)F

28	Keto-perfluorooctane sulfonate	K-PFOS	K-PFSA	OS(=O)(=O)C(F)(F)C(F)(F)C(F)(F)C(F)(F)C(F)(F)C(F)(F)C(=O)C(F)(F)F
29	N-methylethyl-carboxymethyl dimethyl ammonio propyl perfluoropentane amide	MeEtCMeAmPr-FPeAd	MeEtCMeAmPr-FAAd	CC(C)OC(=O)C[N+](C)(C)CCC[N-]C(=O)C(F)(F)C(F)(F)C(F)(F)C(F)(F)F
30	N-methyl perfluoro-1-butane sulfonamide	MeFBSA	MeFASA	CNS(=O)(=O)C(F)(F)C(F)(F)C(F)(F)C(F)(F)F
31	N-methyl perfluoro-1-pentane sulfonamide	MeFPeSA	MeFASA	CNS(=O)(=O)C(F)(F)C(F)(F)C(F)(F)C(F)(F)C(F)(F)F
32	N-methyl perfluoro-1-hexane sulfonamide	MeFHxSA	MeFASA	CNS(=O)(=O)C(F)(F)C(F)(F)C(F)(F)C(F)(F)C(F)(F)C(F)(F)F
33	N-methylperfluorobutane sulfonamido acetic acid	MeFBSAA	MeFASAA	CN(CC(O)=O)S(=O)(=O)C(F)(F)C(F)(F)C(F)(F)C(F)(F)F
34	N-methylperfluoropentane sulfonamido acetic acid	MeFPeSAA	MeFASAA	CN(CC(O)=O)S(=O)(=O)C(F)(F)C(F)(F)C(F)(F)C(F)(F)C(F)(F)F
35	N-methylperfluorohexane sulfonamido acetic acid	MeFHxSAA	MeFASAA	CN(CC(O)=O)S(=O)(=O)C(F)(F)C(F)(F)C(F)(F)C(F)(F)C(F)(F)C(F)(F)F
36	perfluoropentane sulfinate	PFPeSi	PFSAi	OS(=O)C(F)(F)C(F)(F)C(F)(F)C(F)(F)C(F)(F)F
37	perfluorohexane sulfinate	PFHxSi	PFSAi	OS(=O)C(F)(F)C(F)(F)C(F)(F)C(F)(F)C(F)(F)C(F)(F)F
38	perfluoro-n-pentanoic acid	PFPeA	PFCA	OC(=O)C(F)(F)C(F)(F)C(F)(F)C(F)(F)F
39	perfluoro-n-hexanoic acid	PFHxA	PFCA	OC(=O)C(F)(F)C(F)(F)C(F)(F)C(F)(F)C(F)(F)F
40	perfluoro-n-heptanoic acid	PFHpA	PFCA	OC(=O)C(F)(F)C(F)(F)C(F)(F)C(F)(F)C(F)(F)C(F)(F)F
41	perfluoro-n-octanoic acid	PFOA	PFCA	OC(=O)C(F)(F)C(F)(F)C(F)(F)C(F)(F)C(F)(F)C(F)(F)C(F)(F)F

42	perfluoro-n-nonanoic acid	PFNA	PFCA	OC(=O)C(F)(F)C(F)(F)C(F)(F)C(F)(F)C(F)(F)C(F)(F)C(F)(F)C(F)(F)C(F)(F)F
43	perfluoro-n-decanoic acid	PFDA	PFCA	OC(=O)C(F)(F)C(F)(F)C(F)(F)C(F)(F)C(F)(F)C(F)(F)C(F)(F)C(F)(F)C(F)(F)C(F)(F)F
44	perfluoro methyl cyclohexane carboxylic acid	PFMeCHxCA	PFCHxCA	OC(=O)C1(F)C(F)(F)C(F)(F)C(F)(C(F)(F)F)C(F)(F)C1(F)F
45	perfluoro propyl cyclohexane carboxylic acid	PFPrCHxCA	PFCHxCA	OC(=O)C1(F)C(F)(F)C(F)(F)C(F)(C(F)(F)C(F)(F)C(F)(F)F)C(F)(F)C1(F)F
46	perfluoropropane sulfonate	PFPrS	PFSA	OS(=O)(=O)C(F)(F)C(F)(F)C(F)(F)F
47	perfluorobutane sulfonate	PFBS	PFSA	OS(=O)(=O)C(F)(F)C(F)(F)C(F)(F)C(F)(F)F
48	perfluoropentane sulfonate	PFPeS	PFSA	OS(=O)(=O)C(F)(F)C(F)(F)C(F)(F)C(F)(F)C(F)(F)F
49	perfluorohexane sulfonate	PFHxS	PFSA	OS(=O)(=O)C(F)(F)C(F)(F)C(F)(F)C(F)(F)C(F)(F)C(F)(F)F
50	perfluoroheptane sulfonate	PFHpS	PFSA	OS(=O)(=O)C(F)(F)C(F)(F)C(F)(F)C(F)(F)C(F)(F)C(F)(F)C(F)(F)F
51	perfluorooctane sulfonate	PFOS	PFSA	OS(=O)(=O)C(F)(F)C(F)(F)C(F)(F)C(F)(F)C(F)(F)C(F)(F)C(F)(F)C(F)(F)F
52	perfluorononane sulfonate	PFNS	PFSA	OS(=O)(=O)C(F)(F)C(F)(F)C(F)(F)C(F)(F)C(F)(F)C(F)(F)C(F)(F)C(F)(F)C(F)(F)F
53	N-sulfo propyl dimethyl ammonio propyl perfluoropentane sulfonamide	SPrAmPr-FPeSA	SPrAmPr-FASA	C[N+](C)(CCCNS(=O)(=O)C(F)(F)C(F)(F)C(F)(F)C(F)(F)C(F)(F)F)CCCS([O-])(=O)=O
54	N-sulfo propyl dimethyl ammonio propyl perfluorohexane sulfonamide	SPrAmPr-FHxSA	SPrAmPr-FASA	C[N+](C)(CCCNS(=O)(=O)C(F)(F)C(F)(F)C(F)(F)C(F)(F)C(F)(F)C(F)(F)C(F)(F)F)CCCS([O-])(=O)=O
55	N-sulfopropyldimethylammoniopropyl-perfluorobutane sulfonamido acetic acid	SPrAmPr-FBSAA	SPrAmPr-FASAA	C[N+](C)(CCCN(CC(O)=O)S(=O)(=O)C(F)(F)C(F)(F)C(F)(F)C(F)(F)F)CCCS([O-])(=O)=O

56	N-sulfopropyldimethylammoniopropyl-perfluoropentane sulfonamido acetic acid	SPrAmPr-FPeSAA	SPrAmPr-FASAA	C[N+](C)(CCCN(CC(O)=O)S(=O)(=O)C(F)(F)C(F)(F)C(F)(F)C(F)(F)C(F)(F)C(F)(F)F)CCCS([O-])(=O)=O
57	N-sulfopropyldimethylammoniopropyl-perfluorohexane sulfonamido acetic acid	SPrAmPr-FHxSAA	SPrAmPr-FASAA	C[N+](C)(CCCN(CC(O)=O)S(=O)(=O)C(F)(F)C(F)(F)C(F)(F)C(F)(F)C(F)(F)C(F)(F)C(F)(F)F)CCCS([O-])(=O)=O
58	N-sulfopropyl dimethylammoniopropyl perfluorobutane sulfonamido propyl sulfonate	SPrAmPr-FBSAPrS	SPrAmPr-FASAPrS	C[N+](C)(CCCN(CCCS(O)(=O)=O)S(=O)(=O)C(F)(F)C(F)(F)C(F)(F)C(F)(F)C(F)(F)F)CCCS([O-])(=O)=O
59	N-sulfopropyl dimethylammoniopropyl perfluoropentane sulfonamido propyl sulfonate	SPrAmPr-FPeSAPrS	SPrAmPr-FASAPrS	C[N+](C)(CCCN(CCCS(O)(=O)=O)S(=O)(=O)C(F)(F)C(F)(F)C(F)(F)C(F)(F)C(F)(F)C(F)(F)C(F)(F)F)CCCS([O-])(=O)=O
60	N-sulfopropyl dimethylammoniopropyl perfluorohexane sulfonamido propyl sulfonate	SPrAmPr-FHxSAPrS	SPrAmPr-FASAPrS	C[N+](C)(CCCN(CCCS(O)(=O)=O)S(=O)(=O)C(F)(F)C(F)(F)C(F)(F)C(F)(F)C(F)(F)C(F)(F)C(F)(F)C(F)(F)F)CCCS([O-])(=O)=O
61	N-sulfo propyl perfluorobutane sulfonamide	SPr-FBSA	SPr-FASA	OS(=O)(=O)CCCNS(=O)(=O)C(F)(F)C(F)(F)C(F)(F)C(F)(F)C(F)(F)F
62	N-sulfo propyl perfluoropentane sulfonamide	SPr-FPeSA	SPr-FASA	OS(=O)(=O)CCCNS(=O)(=O)C(F)(F)C(F)(F)C(F)(F)C(F)(F)C(F)(F)C(F)(F)F
63	N-sulfo propyl perfluorohexane sulfonamide	SPr-FHxSA	SPr-FASA	OS(=O)(=O)CCCNS(=O)(=O)C(F)(F)C(F)(F)C(F)(F)C(F)(F)C(F)(F)C(F)(F)C(F)(F)F
64	7:1 perfluorooctane sulfonate	7:1 PFOS	X:1 PFSA	OS(=O)(=O)CC(F)(C(F)(F)F)C(F)(F)C(F)(F)C(F)(F)C(F)(F)C(F)(F)C(F)(F)F
65	6:2 fluorotelomer sulfonate	6:2 FTS	X:2 FTS	OS(=O)(=O)CCC(F)(F)C(F)(F)C(F)(F)C(F)(F)C(F)(F)C(F)(F)C(F)(F)F
66	6:2 fluorotelomer sulfonamide	6:2 FTSA	X:2 FTSA	OS(=N)(=O)CCC(F)(F)C(F)(F)C(F)(F)C(F)(F)C(F)(F)C(F)(F)C(F)(F)F
67	6:2 fluorotelomer sulfonamido propyl betaine	6:2 FTSA-PrB	X:2 FTSA-PrB	C[N+](C)(CCCNS(=O)(=O)CCC(F)(F)C(F)(F)C(F)(F)C(F)(F)C(F)(F)C(F)(F)C(F)(F)F)CC([O-])=O
68	1:3 fluorotelomer carboxylic acid	1:3 FTCA	X:3 FTCA	OC(=O)CCC(F)(F)F

Table A-4. List of 29 PFAS classes identified in groundwater sample.

No.	Class Acronym	Class Name
1	X:3 FTCA	X:3 fluorotelomer carboxylic acid
2	X:2 FTSA	X:2 fluorotelomer sulfonamide
3	X:2 FTSA-PrB	X:2 fluorotelomer sulfonamido propyl betaine
4	X:2 FTS	X:2 FluoroTelomer Sulfonate
5	X:1 PFAS	X:1 PerFluoroAlkaneSulfonate
6	Am-CPr-FASA	N-dimethylammoniocarboxypropyl-perfluoroalkane sulfonamide
7	Cl-PFAS	Chloro-PerFluoroAlkaneSulfonate
8	CMeAmPr-FASA	N-CarboxyMethyldimethylAmmonioPropyl- perFluoroAlkaneSulfonamide
9	EtFASA	N-ethylperfluoro-1-alkanesulfonamide
10	F5S-PFAS	PentaFluoroSulfide-PerFluoroAlkane Sulfonate
11	FASA	perFluoroAlkane SulfonAmide
12	FASAA	perfluoroAlkaneSulfonamidoAcetic Acid
13	H-PFAA	Hydrido-PerFluoroAlkanoic Acid
14	H-PFAS	Hydrido-PerFluoroAlkane Sulfonate
15	H-UPFAS	Hydrido-Unsaturated PerFluoroAlkane Sulfonate
16	H-UPFA-O/OH	unsaturated perfluoroalkane ether/alcohol (-1F, +1H)
17	K-PFAS	Keto-PerFluoroAlkaneSulfonate
18	MeEtCMeAmPr-FAAd	N-methylethyl-carboxymethyl dimethyl ammonio propyl perfluoroalkane amide
19	MeFASA	N-methyl perfluoroalkane sulfonamide
20	MeFASAA	N-MethylperFluoroAlkaneSulfonamidoAcetic Acid
21	PFSA	Perfluoroalkane sulfonate
22	PFCA	perfluoro-n-alkanoic acid
23	CHxS	cyclohexane sulfonate
24	PFASi	PerFluoroAlkaneSulfinate
25	PFCHxCA	perfluoro cyclohexane carboxylic acid
26	SPr-FASA	N-Sulfo Propyl perFluoroAlkaneSulfonAmide
27	SPrAmPr-FASAA	N-SulfoPropyldimethylAmmonioPropyl-perFluoroAlkaneSulfonamido Acetic Acid
28	SPrAmPr-FASAPrS	N-SulfoPropyldimethylAmmonioPropyl perFluoroAlkane SulfonAmidoPropylSulfonate
29	SPrAmPr-FASA	N-Sulfo Propyl dimethyl Ammonio Propyl perFluoroAlkaneSulfonamide

Table A-5. Analytical details for the 68 detected PFASs.

No.	Component Acronym	Molecular Formula	Neutral Mass (Da)	Adduct	Exact Mass (Da)	Accurate Mass (Da)	Mass Error[a] (ppm)	RT[b] (min)	MS2 Fragment	#CF_2[d]	Charge State[e]	Confidence Level[107,155]
1	Am-CPr-FBSA	C10H13O4SN2F9	428.0458	[M-H]-	427.0379	427.0379	-0.128	6.66	59.01, 63.96	4	zw	2
2	Am-CPr-FOSA	C14H13O4SN2F17	628.0330	[M+H]+	629.0397	629.0417	3.126	20.68	59.06, 70.07	8	zw	2
3	PFEtCHxS	C8HO3SF15	461.9412	[M-H]-	460.9334	460.9339	1.061	21.93	79.96, 98.95	8 [c]	an	3
4	PFPrCHxS	C9HO3SF17	511.9380	[M-H]-	510.9302	510.9301	-0.230	23.80	79.96, 98.95	9 [c]	an	3
5	Cl-PFOS	C8HO3SClF16	515.9085	[M-H]-	514.9007	514.9005	-0.324	24.50	79.96, 98.95	7	an	2
6	CMeAmPr-FHxSA	C13H15O4SN2F13	542.0550	[M+H]+	543.0618	543.0618	0.054	21.48	58.06, 68.99	6	zw	2
7	EtFMeSA	C3H6O2SNF3	177.0077	[M+]	177.0065	177.0069	1.778	6.77	71.95, 98.97	1	non	2
8	EtFBSA	C6H6O2SNF9	326.9981	[M-H]-	325.9903	325.9904	0.380	18.87	63.96, 77.96	4	non	3
9	F5S-PFOS	C8HO3S2F21	607.9037	[M-H]-	606.8959	606.8966	1.152	27.03	79.96	8	an	2
10	FPrSA	C3H2O2SNF7	248.9700	[M-H]-	247.9622	247.9623	0.525	12.61	63.96, 77.96	3	non	2
11	FBSA	C4H2O2SNF9	298.9668	[M-H]-	297.9590	297.9591	0.416	16.71	77.96	4	non	2
12	FPeSA	C5H2O2SNF11	348.9636	[M-H]-	347.9558	347.9557	-0.237	20.05	77.96, 118.99	5	non	2
13	FHxSA	C6H2O2SNF13	398.9604	[M-H]-	397.9525	397.9528	0.530	22.66	77.96, 118.99	6	non	2
14	FHpSA	C7H2O2SNF15	448.9572	[M-H]-	447.9494	447.9498	0.903	24.85	61.99, 77.96	7	non	2
15	FOSA	C8H2O2SNF17	498.9540	[M-H]-	497.9470	497.9467	1.001	26.67	63.96, 77.96	8	non	2
16	FBSAA	C6H4O4SNF9	356.9723	[M-H]-	355.9644	355.9648	0.968	16.21	63.96, 77.96	4	an	2
17	FPeSAA	C7H4O4SNF11	406.9691	[M-H]-	405.9613	405.9615	0.587	19.24	63.96, 77.96	5	an	2
18	FHxSAA	C8H4O4SNF13	456.9659	[M-H]-	455.9581	455.9583	0.508	21.73	63.96, 77.96	6	an	2
19	H-PFOA	C8H2O2F14	395.9837	[M-H]-	394.9758	394.9758	-0.120	16.87	59.01	6	an	2
20	H-PFNA	C9H2O2F16	445.9799	[M-H]-	444.9726	444.9731	1.003	19.86	59.01, 79.96	7	an	2
21	H-PFDA	C10H2O2F18	495.9773	[M-H]-	494.9695	494.9697	0.484	22.12	59.01	8	an	2
22	H-PFHxS	C6H2O3SF12	381.9539	[M-H]-	380.946	380.9463	0.718	15.53	79.96, 98.95	5	an	2
23	H-PFHpS	C7H2O3SF14	431.9501	[M-H]-	430.9428	430.9431	0.620	18.23	79.96, 98.95	6	an	2
24	H-PFOS	C8H2O3SF16	481.9475	[M-H]-	480.9396	480.9401	0.958	21.04	79.96, 98.95	7	an	2
25	H-PFDS	C10H2O3SF20	581.9411	[M-H]-	580.9333	580.9337	0.771	24.10	79.96, 98.95	9	an	2
26	H-UPFPr-O/OH	C3H2OF4	130.0047	[M+H]+	131.0114	131.0103	-8.809	12.10	98.98	3	non	2
27	H-UPFOS	C8H2O3SF14	443.9507	[M-H]-	442.9428	442.9430	0.378	22.18	79.96	4	an	2
28	K-PFOS	C8HO4SF15	477.9362	[M-H]-	476.9283	476.9284	0.156	22.67	79.96, 98.95	6	an	2
29	MeEtCMeAmPr-FPeAd	C15H21O3N2F9	448.1414	[M-H]-	447.1336	447.1346	2.304	22.22	61.99, 77.96	4	zw	2
30	MeFBSA	C5H4O2SNF9	312.9825	[M-H]-	311.9746	311.9748	0.557	21.55	63.96, 68.99	4	non	2
31	MeFPeSA	C6H4O2SNF11	362.9793	[M-H]-	361.9714	367.9717	0.739	24.05	63.96, 68.99	5	non	2
32	MeFHxSA	C7H4O2SNF13	412.9761	[M-H]-	411.9682	411.9686	0.876	26.11	63.96, 68.99	6	non	2
33	MeFBSAA	C7H6O4SNF9	370.9879	[M-H]-	369.9801	369.9803	0.526	17.10	63.96, 77.96	4	an	2

34	MeFPeSAA	C8H6O4SNF11	420.9847	[M-H]-	419.9769	419.9774	1.162	19.97	63.96, 77.96	5	an	2
35	MeFHxSAA	C9H6O4SNF13	470.9815	[M-H]-	469.9737	469.9739	0.387	22.35	77.96, 118.99	6	an	2
36	PFPeSi	C5HO2SF11	333.9527	[M-H]-	332.9449	332.9452	0.951	18.12	68.99, 82.96	5	an	2
37	PFHxSi	C6HO2SF13	383.9495	[M-H]-	382.9417	382.9421	1.071	20.79	68.99, 82.96	6	an	2
38	PFPeA	C5HO2F9	263.9838	[M-H]-	262.9760	262.9762	0.736	13.31	68.99, 79.96	4	an	2
39	PFHxA	C6HO2F11	313.9806	[M-H]-	312.9728	312.9729	0.279	16.87	68.99, 118.99	5	an	1
40	PFHpA	C7HO2F13	363.9774	[M-H]-	362.9696	362.9698	0.498	19.73	68.99, 118.99	6	an	1
41	PFOA	C8HO2F15	413.9743	[M-H]-	412.9664	412.9665	0.180	22.12	68.99, 118.99	7	an	1
42	PFNA	C9HO2F17	463.9711	[M-H]-	462.9632	462.9632	1.011	24.15	68.99	8	an	1
43	PFDA	C10HO2F19	513.9673	[M-H]-	512.9459	512.9457	-0.326	25.85	59.01	9	an	1
44	PFMeCHxCA	C8HO2F13	375.9774	[M-H]-	374.9754	374.9732	-5.959	16.88	63.96, 79.96	7 [c]	an	3
45	PFPrCHxCA	C10HO2F17	475.9711	[M-H]-	474.9632	474.9671	8.144	22.12	59.01	9 [c]	an	2
46	PFPrS	C3HO3SF7	249.9540	[M-H]-	248.9462	248.946	-0.744	10.50	79.96, 98.95	3	an	2
47	PFBS	C4HO3SF9	299.9508	[M-H]-	298.9430	298.9431	0.362	13.98	79.96, 98.95	4	an	1
48	PFPeS	C5HO3SF11	349.9476	[M-H]-	348.9398	348.9399	0.292	17.19	79.96, 98.95	5	an	1
49	PFHxS	C6HO3SF13	399.9444	[M-H]-	398.9366	398.9366	-0.011	19.89	79.96, 98.95	6	an	1
50	PFHpS	C7HO3SF15	449.9412	[M-H]-	448.9334	448.9336	0.421	22.17	79.96, 98.95	7	an	1
51	PFOS	C8HO3SF17	499.9380	[M-H]-	498.9302	498.9308	1.168	24.11	79.96, 98.95	8	an	1
52	PFNS	C9HO3SF19	549.9348	[M-H]-	548.9270	548.9276	1.050	25.05	79.96, 98.95	9	an	1
53	SPrAmPr-FPeSA	C13H19O5S2N2F11	556.0565	[M+H]+	557.0632	557.0630	-0.448	17.94	58.06, 68.99	5	zw	2
54	SPrAmPr-FHxSA	C14H19O5S2N2F13	606.0533	[M+H]+	607.0600	607.0595	-0.916	20.68	58.07, 68.05	6	zw	2
55	SPrAmPr-FBSAA	C14H21O7S2N2F9	564.0652	[M-H]-	563.0574	563.0579	0.942	14.05	79.96, 166.05	4	zw	2
56	SPrAmPr-FPeSAA	C15H21O7S2N2F11	614.0615	[M+H]+	615.0687	615.0686	-0.21	17.20	58.06, 70.06	5	zw	2
57	SPrAmPr-FHxSAA	C16H21O7S2N2F13	664.0588	[M+H]+	665.0655	665.0652	-0.504	19.93	58.06, 70.06	6	zw	2
58	SPrAmPr-FBSAPrS	C15H25O8S3N2F9	628.0635	[M-H]-	627.0556	627.0570	2.145	14.76	64.97, 79.96	4	zw	3
59	SPrAmPr-FPeSAPrS	C16H25O8S3N2F11	678.0603	[M-H]-	677.0525	677.0535	1.534	17.78	63.96, 79.96	5	zw	3
60	SPrAmPr-FHxSAPrS	C17H25O8S3N2F13	728.0571	[M-H]-	727.0493	727.0502	1.282	20.38	63.96, 79.96	6	zw	3
61	SPr-FBSA	C7H8O5S2NF9	420.9706	[M-H]-	419.9627	419.9633	1.332	17.10	77.96	4	an	2
62	SPr-FPeSA	C8H8O5S2NF11	470.9674	[M-H]-	469.9595	469.9598	0.538	19.90	77.96	5	an	2
63	SPr-FHxSA	C9H8O5S2NF13	520.9642	[M-H]-	519.9564	519.9564	0.089	22.25	63.96, 77.96	6	an	2
64	7:1 PFOS	C8H3O3SF15	463.9569	[M-H]-	462.9491	462.9494	0.732	22.67	79.96, 98.95	7	an	2
65	6:2 FTS	C8H5O3SF13	427.9757	[M-H]-	426.9679	426.9681	0.458	21.97	79.96, 80.96	6	an	1
66	6:2 FTSA	C8H6O2SNF13	426.9917	[M-H]-	425.9839	425.9843	0.965	24.20	63.96, 168.99	6	an	3
67	6:2 FTSA-PrB	C15H19O4SN2F13	570.0863	[M+H]+	571.0931	571.0930	-0.124	22.98	58.06, 68.99	6	zw	3
68	1:3 FTCA	C4H5O2F3	142.0247	[M-H]-	141.0169	141.0158	-7.711	6.63	59.01	1	an	2

[a] Deviations in mass error across triplicate samples were negligible; [b] Deviations in retention time across triplicate samples were negligible;

[c] Component contains a cyclohexane group; [d] The column **#CF_2** represents number of perfluorinated carbon atoms or the perfluorinated chain length for each PFAS;

[e] For the column **Charge state**, "zw" means zwitterionic PFAS, "an" means anionic PFAS and "non" means nonionic PFAS at circumneutral pH.

A.4 Removal of PFASs in groundwater

Table A-6. Removal efficiency of 68 PFASs in the groundwater on DEXSORB at three timepoints.

DEXSORB[a,b]		0.5 hr		9 hr		48 hr	
Component	**Charge State[c]**	**Removal (%)**	**stdev (%)**	**Removal (%)**	**stdev (%)**	**Removal (%)**	**stdev (%)**
6:2 FTSA-PrB	zw	29.14	7.10	60.92	1.66	68.72	5.64
Am-CPr-FOSA	zw	6.30	3.50	7.74	5.96	14.40	2.03
CMeAmPr-FHxSA	zw	0.00	6.17	13.92	1.14	13.45	7.93
EtFMeSA	non	1.57	2.07	0.00	1.14	0.90	3.93
H-UPFPr-O/OH	non	0.00	2.57	4.72	4.08	0.00	3.19
SPrAmPr-FHxSA	zw	3.97	0.71	10.97	0.48	14.10	6.40
SPrAmPr-FHxSAA	zw	7.01	5.18	6.63	7.24	7.64	5.32
SPrAmPr-FPeSA	zw	4.81	1.97	7.50	5.32	3.06	3.21
SPrAmPr-FPeSAA	zw	3.86	10.81	0.05	2.92	2.64	5.20
1:3_FTCA	an	0.00	2.11	5.90	2.85	2.90	2.76
6:2 FTSA	an	30.47	11.14	54.73	9.18	51.28	9.16
6:2_FTS	an	5.50	3.24	1.05	3.36	3.72	3.16
7:1_PFOS	an	15.60	4.39	24.07	16.74	26.60	17.37
Am-CPr-FBSA	zw	8.73	16.49	0.00	20.10	4.26	8.23
Cl-PFOS	an	16.75	3.86	43.39	3.89	54.73	0.48
EtFBSA	non	14.87	4.51	8.82	2.34	5.92	3.98
F5S-PFOS	an	25.20	17.45	58.34	17.03	67.68	35.30
FBSA	non	0.00	1.76	1.06	2.01	0.33	2.64
FBSAA	an	0.00	1.22	3.63	1.52	2.93	12.46
FHpSA	non	7.73	1.99	16.24	2.08	18.08	3.13
FHxSA	non	3.90	0.86	5.81	2.67	4.90	1.72
FHxSAA	an	2.16	3.75	4.07	3.62	5.68	4.26
FOSA	non	11.60	2.09	30.59	5.49	32.66	6.27
FPeSA	non	1.59	0.61	3.21	1.05	1.07	10.21
FPeSAA	an	2.28	2.04	0.75	1.91	0.79	5.08
FPrSA	non	0.00	3.50	1.18	3.96	0.90	0.98
H-PFDA	an	0.00	16.37	0.00	7.76	7.13	22.63
H-PFDS	an	10.10	6.71	32.52	6.95	45.64	5.37
H-PFHpS	an	0.00	18.57	18.06	15.91	48.10	2.11
H-PFHxS	an	0.00	3.90	14.72	6.28	21.00	4.21
H-PFNA	an	11.81	17.99	18.92	5.40	15.83	18.94
H-PFOA	an	0.00	8.82	1.81	4.40	5.08	5.55
H-PFOS	an	17.69	2.67	36.58	3.68	49.40	1.80
H-UPFOS	an	1.04	1.47	5.90	4.87	3.92	3.56
K-PFOS	an	4.33	1.83	23.95	1.53	31.94	3.01

MeEtCMeAmPr-FPeAd	zw	0.00	4.00	6.98	1.98	5.92	3.67
MeFBSA	non	12.66	8.95	9.58	4.04	6.19	2.95
MeFBSAA	an	0.00	2.77	0.00	2.21	1.08	11.55
MeFHxSA	non	28.17	2.94	53.13	3.59	50.32	7.90
MeFHxSAA	an	0.00	6.20	13.12	11.00	7.78	5.54
MeFPeSA	non	13.97	1.86	33.99	4.02	31.12	5.66
MeFPeSAA	an	3.66	5.15	1.59	6.22	0.00	0.25
PFBS	an	0.00	1.04	4.04	1.19	4.84	2.31
PFDA	an	0.00	1.26	17.92	13.41	23.37	3.80
PFEtCHxS	an	6.80	1.87	27.37	1.56	26.61	2.44
PFHpA	an	2.76	0.89	5.46	2.08	2.60	1.71
PFHpS	an	9.77	1.63	23.30	1.80	31.48	3.28
PFHxA	an	0.65	2.21	2.17	2.09	2.32	0.95
PFHxS	an	6.67	1.36	9.59	1.75	13.19	0.66
PFHxSi	an	6.38	1.25	6.20	1.49	13.93	7.41
PFMeCHxCA	an	1.83	11.45	10.36	5.83	4.14	4.51
PFNA	an	0.00	6.29	1.14	2.39	0.00	7.71
PFNS	an	14.94	8.21	37.41	14.40	50.81	14.25
PFOA	an	4.13	4.16	4.13	0.94	7.53	2.30
PFOS	an	8.75	2.41	27.87	2.62	34.83	3.94
PFPeA	an	0.00	90.56	0.00	2.69	3.13	2.13
PFPeS	an	4.56	3.68	7.40	1.32	9.24	1.87
PFPeSi	an	2.57	2.34	2.97	2.03	5.76	3.57
PFPrCHxCA	an	7.76	13.40	13.57	3.82	16.60	5.52
PFPrCHxS	an	3.75	8.32	33.09	3.28	42.68	5.47
PFPrS	an	0.00	1.81	1.85	3.18	2.35	1.42
SPrAmPr-FBSAA	zw	6.14	2.51	2.19	3.47	3.95	2.26
SPrAmPr-FBSAPrS	zw	2.62	4.18	0.48	1.56	2.15	4.26
SPrAmPr-FHxSAPrS	zw	3.98	2.47	13.05	3.36	15.57	4.07
SPrAmPr-FPeSAPrS	zw	6.80	3.26	6.14	1.62	7.74	4.26
SPr-FBSA	an	0.00	6.25	0.79	6.49	0.36	7.79
SPr-FHxSA	an	13.33	4.46	0.00	3.07	0.00	12.73
SPr-FPeSA	an	3.42	4.83	0.00	2.46	0.00	3.59

Table A-7. Removal efficiency of 68 PFASs in the groundwater on DEXSORB+ at three timepoints.

DEXSORB+[a,b]		0.5 hr		9 hr		48 hr	
Component	**Charge State[c]**	**Removal (%)**	**stdev (%)**	**Removal (%)**	**stdev (%)**	**Removal (%)**	**stdev (%)**
6:2 FTSA-PrB	zw	10.74	8.48	15.45	4.79	3.33	4.80
Am-CPr-FOSA	zw	51.73	7.48	43.81	8.24	46.99	5.34
CMeAmPr-FHxSA	zw	45.22	1.64	50.10	3.22	46.32	3.49
EtFMeSA	non	0.00	4.31	1.30	2.62	0.60	4.57
H-UPFPr-O/OH	non	0.00	4.49	1.77	5.02	0.00	4.64
SPrAmPr-FHxSA	zw	50.85	2.41	57.16	1.02	54.71	1.13
SPrAmPr-FHxSAA	zw	53.11	3.48	58.15	3.86	55.69	2.28
SPrAmPr-FPeSA	zw	31.25	1.88	39.99	2.22	31.66	3.32
SPrAmPr-FPeSAA	zw	37.66	2.66	37.83	2.07	35.70	7.79
1:3_FTCA	an	0.00	1.07	6.13	3.25	0.00	8.14
6:2 FTSA	an	0.00	1.20	0.00	1.89	0.00	5.36
6:2_FTS	an	49.14	1.86	54.74	1.13	52.35	1.92
7:1_PFOS	an	100.00	0.00	95.62	4.63	96.86	5.45
Am-CPr-FBSA	zw	0.00	13.50	0.00	9.40	8.43	3.05
Cl-PFOS	an	97.91	1.15	99.53	0.81	99.42	1.00
EtFBSA	non	1.20	4.17	3.86	6.86	1.41	4.94
F5S-PFOS	an	100.00	0.00	100.00	0.00	100.00	0.00
FBSA	non	16.70	2.38	27.26	2.06	20.42	4.19
FBSAA	an	44.82	2.81	61.78	3.77	57.40	8.62
FHpSA	non	77.04	0.40	83.01	0.86	83.56	1.37
FHxSA	non	47.08	0.77	55.67	0.76	56.56	0.84
FHxSAA	an	85.52	0.82	89.28	0.96	91.45	0.53
FOSA	non	87.98	0.36	90.78	0.67	91.14	1.29
FPeSA	non	28.09	6.10	36.23	4.48	41.97	0.62
FPeSAA	an	69.79	0.90	78.19	0.88	80.93	1.51
FPrSA	non	7.59	3.55	11.19	2.60	4.59	5.65
H-PFDA	an	57.39	6.89	67.63	7.32	66.89	3.92
H-PFDS	an	93.36	0.48	95.13	0.74	96.18	1.54
H-PFHpS	an	100.00	0.00	100.00	0.00	100.00	0.00
H-PFHxS	an	88.49	2.42	91.39	0.49	93.29	0.89
H-PFNA	an	43.58	29.01	43.35	12.22	58.04	7.96
H-PFOA	an	23.87	4.23	25.73	5.57	32.29	3.94
H-PFOS	an	96.69	0.77	98.34	0.43	99.02	0.29
H-UPFOS	an	77.93	4.65	78.14	4.15	83.04	1.06
K-PFOS	an	97.56	1.04	98.78	1.29	99.30	0.70
MeEtCMeAmPr-FPeAd	zw	7.68	2.65	25.32	6.71	14.23	0.74
MeFBSA	non	22.53	1.48	25.43	3.46	21.21	4.75
MeFBSAA	an	45.47	6.90	59.39	2.21	57.27	6.64
MeFHxSA	non	58.46	2.17	68.70	1.09	63.29	1.88

MeFHxSAA	an	87.12	0.52	87.66	4.18	90.10	3.41
MeFPeSA	non	29.22	2.66	44.88	0.67	37.71	5.67
MeFPeSAA	an	58.43	1.56	72.13	1.64	71.77	1.01
PFBS	an	52.47	1.18	64.05	1.56	62.72	1.43
PFDA	an	87.11	0.11	89.48	1.00	90.04	3.22
PFEtCHxS	an	93.20	0.56	95.97	0.18	96.27	0.76
PFHpA	an	36.83	1.12	46.52	1.37	46.65	3.11
PFHpS	an	91.82	0.77	93.95	0.53	94.58	0.38
PFHxA	an	21.07	2.59	28.77	2.03	24.91	2.98
PFHxS	an	79.86	0.38	83.99	0.57	85.87	0.66
PFHxSi	an	57.33	0.72	65.88	1.30	61.26	2.17
PFMeCHxCA	an	25.94	1.64	28.39	1.12	31.92	1.90
PFNA	an	51.07	1.96	61.85	3.31	66.44	0.40
PFNS	an	98.90	0.02	99.56	0.09	99.57	0.56
PFOA	an	56.77	0.71	63.98	1.36	67.18	0.29
PFOS	an	91.66	0.45	94.49	0.62	94.47	0.46
PFPeA	an	16.57	3.14	19.93	1.44	19.49	4.35
PFPeS	an	70.51	1.92	77.34	0.73	77.97	0.42
PFPeSi	an	41.08	0.45	49.97	0.40	43.30	2.96
PFPrCHxCA	an	74.92	1.34	79.49	3.05	82.18	1.51
PFPrCHxS	an	98.19	1.65	100.00	0.00	100.00	0.00
PFPrS	an	30.42	1.98	42.81	1.08	38.12	2.17
SPrAmPr-FBSAA	zw	15.35	4.48	17.74	3.11	13.91	2.00
SPrAmPr-FBSAPrS	zw	29.52	2.33	35.34	1.79	30.06	1.32
SPrAmPr-FHxSAPrS	zw	69.85	0.39	72.49	0.98	71.65	1.66
SPrAmPr-FPeSAPrS	zw	54.73	2.00	61.43	3.35	58.73	1.29
SPr-FBSA	an	77.79	1.67	84.87	1.11	84.33	0.83
SPr-FHxSA	an	93.91	0.41	95.37	0.45	96.03	0.42
SPr-FPeSA	an	81.09	0.52	86.10	0.14	88.25	0.19

Table A-8. Removal efficiency of 68 PFASs in the groundwater on M+ at three timepoints.

M+[a,b]		0.5 hr		9 hr		48 hr	
Component	**Charge State[c]**	**Removal (%)**	**stdev (%)**	**Removal (%)**	**stdev (%)**	**Removal (%)**	**stdev (%)**
6:2 FTSA-PrB	zw	0.00	9.59	0.00	3.91	0.00	11.61
Am-CPr-FOSA	zw	0.00	89.25	13.07	7.18	11.50	22.32
CMeAmPr-FHxSA	zw	1.74	15.61	22.29	1.91	13.28	3.87
EtFMeSA	non	4.88	2.73	0.00	4.16	1.84	5.68
H-UPFPr-O/OH	non	4.74	3.45	11.03	15.66	3.26	5.92
SPrAmPr-FHxSA	zw	11.67	10.37	19.92	0.56	18.51	6.96
SPrAmPr-FHxSAA	zw	21.05	7.18	27.75	5.88	35.09	3.14
SPrAmPr-FPeSA	zw	2.92	2.91	8.48	3.30	1.35	1.97
SPrAmPr-FPeSAA	zw	11.19	5.75	18.56	4.99	13.66	3.61
1:3_FTCA	an	0.00	6.73	0.55	5.93	2.19	2.98
6:2 FTSA	an	0.00	11.31	0.00	13.88	0.00	22.13
6:2_FTS	an	17.58	27.96	18.23	2.54	15.60	1.11
7:1_PFOS	an	34.47	2.82	52.63	6.42	52.27	6.30
Am-CPr-FBSA	zw	8.52	1.58	0.00	7.11	6.74	0.62
Cl-PFOS	an	56.78	0.97	76.21	0.75	79.06	3.93
EtFBSA	non	1.12	3.86	0.83	3.75	0.00	5.32
F5S-PFOS	an	76.73	3.57	83.73	16.02	100.00	0.00
FBSA	non	0.00	4.61	2.58	2.83	0.00	13.64
FBSAA	an	34.21	7.09	38.95	10.37	39.84	21.07
FHpSA	non	27.56	3.51	39.05	1.39	41.50	1.82
FHxSA	non	11.53	2.70	16.54	4.20	17.71	1.35
FHxSAA	an	62.69	6.98	82.02	1.99	85.89	1.34
FOSA	non	37.94	3.98	52.90	3.54	55.43	4.22
FPeSA	non	0.00	7.62	8.55	2.67	10.07	1.68
FPeSAA	an	50.80	6.53	66.33	3.12	69.59	3.06
FPrSA	non	0.00	2.80	0.00	1.91	0.00	6.95
H-PFDA	an	0.00	14.12	15.49	3.50	21.51	17.91
H-PFDS	an	20.91	17.68	59.37	8.46	59.60	9.90
H-PFHpS	an	34.53	6.98	58.41	4.73	83.12	4.47
H-PFHxS	an	32.03	0.12	46.66	0.07	51.90	0.67
H-PFNA	an	6.93	16.05	1.44	12.01	20.11	4.70
H-PFOA	an	0.00	7.10	13.80	5.68	19.46	9.58
H-PFOS	an	43.91	2.51	65.11	2.22	71.11	1.29
H-UPFOS	an	21.08	3.36	43.97	11.13	24.46	4.58
K-PFOS	an	27.59	6.20	49.52	3.41	55.32	3.97
MeEtCMeAmPr-FPeAd	zw	0.00	8.34	10.75	16.88	5.11	5.09
MeFBSA	non	0.00	8.30	1.44	4.91	5.72	5.68

MeFBSAA	an	33.77	3.53	37.14	7.33	44.37	8.73
MeFHxSA	non	19.77	2.95	26.17	1.96	18.33	2.86
MeFHxSAA	an	50.12	13.69	82.92	1.76	85.27	1.68
MeFPeSA	non	0.00	13.10	5.38	4.28	8.21	5.64
MeFPeSAA	an	43.33	9.59	60.62	8.01	59.97	2.84
PFBS	an	5.69	5.62	7.28	2.84	4.77	12.92
PFDA	an	45.53	6.41	56.76	4.45	64.29	1.52
PFEtCHxS	an	24.50	3.28	47.86	1.47	46.77	1.59
PFHpA	an	11.18	5.20	13.10	4.25	16.15	3.60
PFHpS	an	32.09	1.13	53.92	2.43	56.52	1.15
PFHxA	an	2.01	5.31	6.83	3.32	10.23	4.73
PFHxS	an	25.28	1.56	30.41	2.14	31.80	1.72
PFHxSi	an	8.81	5.02	19.02	1.99	3.82	1.04
PFMeCHxCA	an	0.00	112.93	4.03	7.32	4.15	13.63
PFNA	an	8.87	9.29	15.29	5.63	13.56	6.89
PFNS	an	55.81	5.04	74.42	2.49	75.30	14.58
PFOA	an	13.40	2.21	24.20	3.53	28.50	3.25
PFOS	an	37.48	5.68	54.64	2.41	56.54	7.64
PFPeA	an	0.00	8.58	0.00	12.11	3.59	10.59
PFPeS	an	15.33	1.37	21.31	3.47	17.97	1.82
PFPeSi	an	12.34	2.84	10.10	3.01	6.19	1.48
PFPrCHxCA	an	34.06	119.16	38.98	6.18	46.59	2.76
PFPrCHxS	an	20.71	34.83	79.35	7.68	78.09	1.55
PFPrS	an	2.90	4.68	0.04	1.77	3.02	5.82
SPrAmPr-FBSAA	zw	8.13	3.06	6.34	4.21	7.51	1.04
SPrAmPr-FBSAPrS	zw	8.24	1.71	12.20	6.31	11.26	1.22
SPrAmPr-FHxSAPrS	zw	24.85	1.79	41.42	1.07	44.39	2.01
SPrAmPr-FPeSAPrS	zw	18.87	3.32	24.66	1.29	20.56	3.63
SPr-FBSA	an	60.46	23.68	62.43	2.93	63.98	2.09
SPr-FHxSA	an	77.96	13.56	86.76	0.72	90.51	0.23
SPr-FPeSA	an	70.26	22.78	70.74	1.58	75.72	2.89

Table A-9. Removal efficiency of 68 PFASs in the groundwater on AC at three timepoints.

AC[a,b]		0.5 hr		9 hr		48 hr	
Component	**Charge State[c]**	**Removal (%)**	**stdev (%)**	**Removal (%)**	**stdev (%)**	**Removal (%)**	**stdev (%)**
6:2 FTSA-PrB	zw	42.93	7.20	93.07	2.52	99.43	0.55
Am-CPr-FOSA	zw	27.40	14.68	53.37	10.16	88.30	9.27
CMeAmPr-FHxSA	zw	30.16	0.83	70.06	2.96	88.01	0.68
EtFMeSA	non	0.73	3.01	0.86	4.06	4.49	0.89
H-UPFPr-O/OH	non	0.00	9.93	3.25	4.49	0.00	5.60
SPrAmPr-FHxSA	zw	32.65	2.08	69.82	1.13	89.14	1.04
SPrAmPr-FHxSAA	zw	28.55	4.92	53.17	4.39	81.37	1.14
SPrAmPr-FPeSA	zw	26.36	2.22	63.50	1.74	83.58	2.10
SPrAmPr-FPeSAA	zw	22.93	0.70	46.36	5.40	72.38	1.31
1:3_FTCA	an	0.00	3.62	6.63	3.07	1.52	2.25
6:2 FTSA	an	50.49	7.41	93.57	0.25	96.82	0.40
6:2_FTS	an	27.64	1.55	61.36	3.27	79.12	2.35
7:1_PFOS	an	37.48	2.40	79.17	5.97	96.33	4.09
Am-CPr-FBSA	zw	0.00	11.32	0.00	9.58	2.97	11.22
Cl-PFOS	an	40.00	2.98	83.36	0.47	96.68	0.65
EtFBSA	non	46.49	1.81	76.72	4.25	81.07	1.76
F5S-PFOS	an	32.08	3.31	82.32	17.06	97.53	4.27
FBSA	non	12.27	3.35	25.19	2.64	19.44	1.35
FBSAA	an	12.86	1.43	32.49	0.16	41.93	3.34
FHpSA	non	33.12	0.80	74.55	1.37	91.05	0.91
FHxSA	non	21.61	1.22	49.72	2.71	67.92	0.35
FHxSAA	an	23.97	2.10	56.73	2.18	79.23	1.36
FOSA	non	36.82	1.60	80.86	1.10	95.02	0.67
FPeSA	non	18.43	1.88	35.13	4.76	48.62	1.49
FPeSAA	an	20.97	1.04	45.35	1.03	62.17	2.43
FPrSA	non	6.02	0.63	14.22	5.12	1.82	3.17
H-PFDA	an	5.33	14.35	52.65	6.54	71.88	7.09
H-PFDS	an	25.54	8.74	69.75	2.31	92.32	0.81
H-PFHpS	an	40.58	23.57	78.52	4.42	97.98	3.51
H-PFHxS	an	25.66	1.58	60.74	2.05	76.09	2.05
H-PFNA	an	37.56	7.36	33.82	11.03	51.84	9.82
H-PFOA	an	10.08	2.56	23.30	3.55	24.03	12.11
H-PFOS	an	39.55	3.83	81.19	1.89	94.33	0.52
H-UPFOS	an	34.12	4.02	68.78	7.21	89.07	1.42
K-PFOS	an	28.26	2.45	67.50	3.79	89.98	0.57
MeEtCMeAmPr-FPeAd	zw	0.00	2.39	37.46	2.15	29.66	6.92
MeFBSA	non	33.90	3.99	64.40	0.40	75.40	1.09
MeFBSAA	an	18.40	5.65	29.91	1.81	42.59	4.46
MeFHxSA	non	47.85	3.24	91.84	0.77	97.19	0.44

MeFHxSAA	an	23.10	7.18	54.82	2.06	81.09	1.59
MeFPeSA	non	38.11	4.23	82.51	0.77	90.64	1.01
MeFPeSAA	an	14.50	4.56	33.50	1.44	48.67	2.47
PFBS	an	15.94	0.87	32.56	1.10	27.07	1.05
PFDA	an	26.28	4.91	73.59	1.53	90.83	0.05
PFEtCHxS	an	28.63	2.10	65.01	3.11	80.88	1.23
PFHpA	an	21.46	2.83	38.75	2.19	48.54	1.49
PFHpS	an	31.75	3.97	72.76	2.66	89.49	0.58
PFHxA	an	15.32	2.53	25.06	2.23	25.08	1.65
PFHxS	an	24.57	2.67	55.62	1.90	70.59	0.63
PFHxSi	an	27.44	1.33	63.00	5.02	84.58	2.56
PFMeCHxCA	an	17.00	11.35	22.50	14.17	27.56	7.48
PFNA	an	11.57	6.36	42.60	1.77	70.65	3.29
PFNS	an	25.81	5.74	73.53	0.76	95.82	1.43
PFOA	an	21.05	2.02	48.58	2.29	69.82	0.52
PFOS	an	23.87	1.87	68.51	1.61	91.03	0.86
PFPeA	an	10.30	1.46	11.35	2.39	4.95	2.99
PFPeS	an	24.17	1.30	46.07	2.18	53.44	1.49
PFPeSi	an	22.24	1.58	46.39	4.77	59.61	4.33
PFPrCHxCA	an	33.98	6.37	65.08	5.37	82.88	0.45
PFPrCHxS	an	27.38	2.38	77.75	5.67	98.29	2.96
PFPrS	an	12.29	4.06	19.78	3.44	4.27	3.74
SPrAmPr-FBSAA	zw	21.11	2.10	44.20	2.18	59.31	1.92
SPrAmPr-FBSAPrS	zw	21.57	1.14	51.08	3.04	71.73	1.12
SPrAmPr-FHxSAPrS	zw	25.65	1.91	63.17	1.53	85.21	1.86
SPrAmPr-FPeSAPrS	zw	28.75	1.96	58.77	3.25	80.66	1.32
SPr-FBSA	an	21.51	7.74	50.23	3.53	55.80	3.08
SPr-FHxSA	an	26.12	3.04	58.72	3.83	81.82	2.50
SPr-FPeSA	an	11.92	3.31	32.47	3.65	53.28	5.76

Table A-10. Removal efficiency of 68 PFASs in the groundwater on AE resin at three timepoints.

AE resin[a,b]		0.5 hr		9 hr		48 hr	
Component	Charge State[c]	Removal (%)	stdev (%)	Removal (%)	stdev (%)	Removal (%)	stdev (%)
6:2 FTSA-PrB	zw	0.00	9.60	3.31	4.11	0.45	3.46
Am-CPr-FOSA	zw	5.32	13.41	0.00	15.95	0.00	30.60
CMeAmPr-FHxSA	zw	0.00	3.49	7.22	7.69	16.78	1.07
EtFMeSA	non	0.00	2.13	0.00	3.46	0.00	2.91
H-UPFPr-O/OH	non	0.00	2.13	0.00	3.19	0.00	6.33
SPrAmPr-FHxSA	zw	0.63	0.89	9.41	4.31	15.89	2.48
SPrAmPr-FHxSAA	zw	0.00	5.59	2.47	9.23	3.04	3.57
SPrAmPr-FPeSA	zw	0.00	3.07	5.48	4.56	7.81	4.35
SPrAmPr-FPeSAA	zw	0.00	5.50	0.00	3.80	0.00	1.14
1:3_FTCA	an	0.00	2.53	4.92	6.00	0.47	2.85
6:2 FTSA	an	0.00	11.35	0.00	15.62	0.00	21.78
6:2_FTS	an	0.00	5.29	7.09	5.15	38.82	3.64
7:1_PFOS	an	0.00	6.27	14.32	10.79	55.57	2.79
Am-CPr-FBSA	zw	0.00	10.41	0.00	7.35	1.37	12.81
Cl-PFOS	an	0.00	1.58	11.97	1.77	54.24	3.83
EtFBSA	non	0.00	4.04	0.00	3.12	0.00	7.13
F5S-PFOS	an	0.00	11.08	0.00	16.49	44.10	39.36
FBSA	non	0.00	1.08	11.42	5.55	39.17	1.81
FBSAA	an	0.00	5.49	14.08	9.91	60.11	2.44
FHpSA	non	0.00	1.49	16.83	6.53	53.94	3.97
FHxSA	non	0.00	2.71	8.23	6.66	42.06	3.70
FHxSAA	an	0.00	3.71	12.79	6.53	51.91	4.90
FOSA	non	0.00	2.84	11.81	3.45	53.64	3.05
FPeSA	non	0.00	8.18	5.36	13.63	43.54	5.20
FPeSAA	an	0.00	4.93	11.12	8.60	55.88	5.07
FPrSA	non	0.00	1.23	11.75	4.29	29.26	3.52
H-PFDA	an	0.00	3.29	11.64	16.71	44.49	5.35
H-PFDS	an	0.00	6.29	3.33	11.57	46.59	4.29
H-PFHpS	an	0.00	14.99	7.55	7.82	68.48	3.54
H-PFHxS	an	0.00	7.92	18.50	2.87	64.23	4.21
H-PFNA	an	26.78	7.17	11.01	22.75	48.28	10.38
H-PFOA	an	0.00	7.02	15.58	3.97	40.50	3.40
H-PFOS	an	0.00	3.15	11.29	7.58	59.92	4.39
H-UPFOS	an	12.76	20.15	19.81	25.63	70.58	2.01
K-PFOS	an	0.00	7.34	11.76	2.57	66.16	6.45
MeEtCMeAmPr-FPeAd	zw	0.00	4.14	10.56	4.47	0.00	10.46
MeFBSA	non	0.00	10.36	13.18	7.34	43.54	3.10
MeFBSAA	an	1.39	8.45	9.01	3.84	55.63	2.47
MeFHxSA	non	0.00	3.67	14.55	7.02	49.45	1.55

MeFHxSAA	an	1.16	7.28	19.60	9.29	43.12	3.46
MeFPeSA	non	0.00	8.83	13.35	12.64	44.50	4.62
MeFPeSAA	an	4.66	11.27	9.96	4.59	40.46	3.24
PFBS	an	0.00	2.99	15.94	7.11	62.91	3.39
PFDA	an	0.00	4.10	6.12	1.64	51.95	2.54
PFEtCHxS	an	0.00	3.92	22.73	4.47	59.43	3.48
PFHpA	an	1.85	1.41	15.19	5.65	48.02	3.75
PFHpS	an	0.00	2.73	15.21	6.54	60.44	1.97
PFHxA	an	0.00	4.67	11.27	8.63	40.76	3.78
PFHxS	an	0.14	3.43	13.72	2.74	54.86	2.89
PFHxSi	an	0.02	1.29	14.52	7.62	49.21	6.39
PFMeCHxCA	an	6.14	11.51	16.32	20.55	51.71	8.54
PFNA	an	0.00	14.20	9.80	8.22	38.38	3.58
PFNS	an	0.00	9.31	3.81	7.33	54.94	9.87
PFOA	an	0.00	4.46	11.84	7.23	50.37	2.22
PFOS	an	0.00	2.85	7.49	4.09	44.63	5.36
PFPeA	an	0.00	1.12	8.44	4.63	33.68	4.43
PFPeS	an	0.00	0.52	15.69	8.96	60.50	3.58
PFPeSi	an	0.00	4.82	13.29	7.89	49.00	3.72
PFPrCHxCA	an	4.50	12.05	22.77	11.70	66.63	3.58
PFPrCHxS	an	0.00	44.62	22.17	7.62	60.41	7.72
PFPrS	an	0.00	2.97	14.67	5.61	65.13	3.25
SPrAmPr-FBSAA	zw	3.79	0.77	0.00	1.00	4.31	1.70
SPrAmPr-FBSAPrS	zw	0.00	4.89	0.00	4.27	1.39	4.83
SPrAmPr-FHxSAPrS	zw	0.00	3.57	3.39	1.61	13.22	0.97
SPrAmPr-FPeSAPrS	zw	0.77	5.05	5.42	7.99	6.84	5.20
SPr-FBSA	an	0.00	6.61	12.23	3.63	56.00	0.58
SPr-FHxSA	an	2.53	4.54	1.78	2.87	44.86	1.58
SPr-FPeSA	an	0.00	4.38	7.67	3.99	36.55	3.32

[a] **Removal (%)**: is the average removal percentage of each PFAS, calculated as (1 – average peak area in experimental group/average peak area in control group) x 100%; Note that for all samples with higher average peak area than the control average peak area (*i.e.*, with removal percentages lower than 0%), the avg removal were indicated as 0% in this table;

[b] **stdev (%)**: is the standard deviation of triplicate removal values, calculated using the "= STDEV( )" function in MS Excel;

[c] "zw" means zwitterionic PFAS, "an" means anionic PFAS and "non" means nonionic PFAS at circumneutral pH.

It is important to note that there is no abundance-dependency in the removal of the 68 PFASs from groundwater by any of the adsorbents. We plotted the peak area of each of the 68 PFASs in the control samples (untreated groundwater) against the removal percentage for each of the five adsorbents at each of the three time points. The data are presented in **Figure A-1**, and no trend was identified.

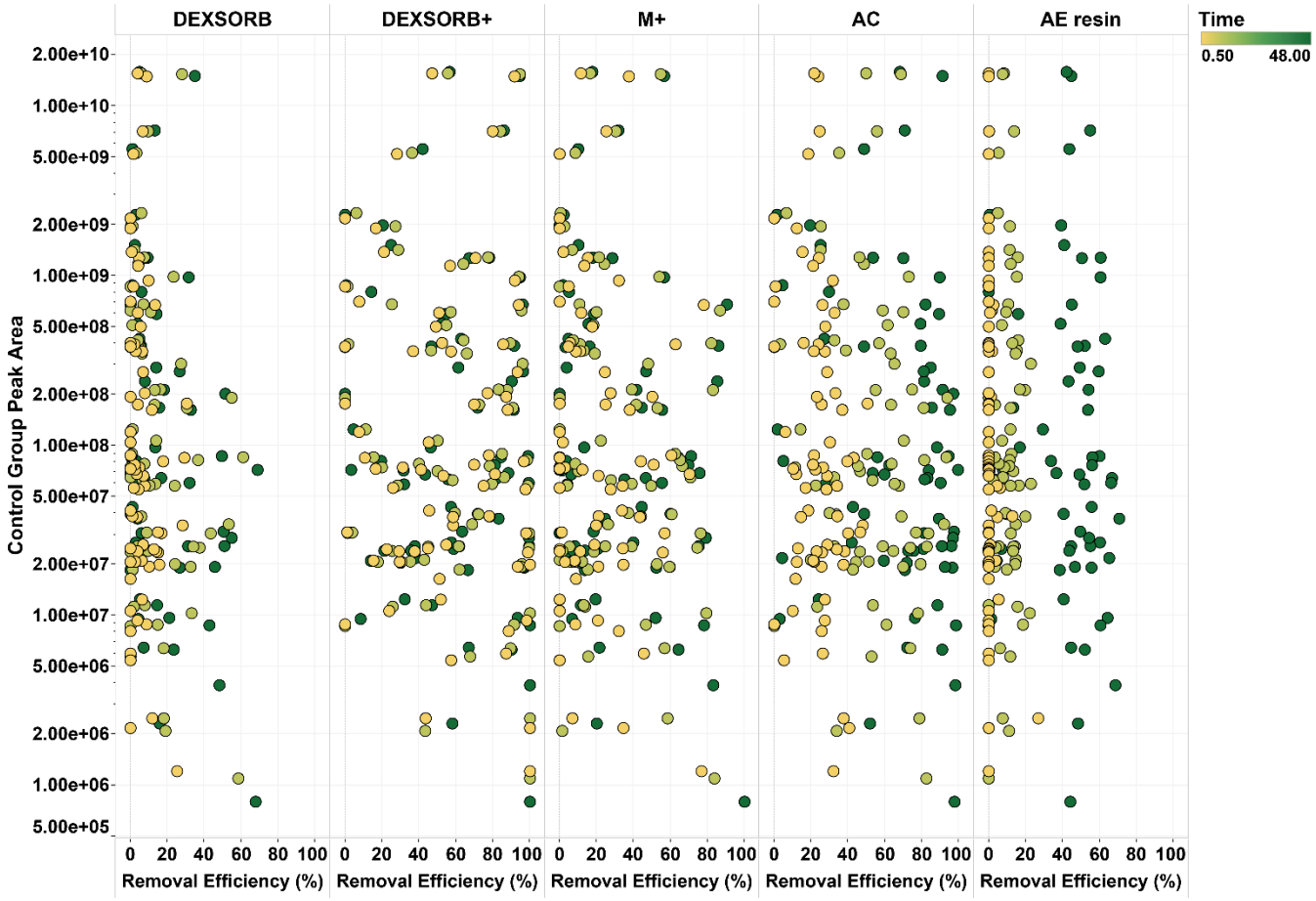

Figure A-1. 68 PFASs control group component peak area versus removal efficiency in groundwater.

A.5 Effects of PFAS properties on removal from groundwater

Table A-11. Class acronym, class name, and structure for the eleven PFAS classes that contain at least three unique homologues with varying CF_2 chain length.

Class Acronym	Class Name	Structure[a] (#CF_2 = 6[b], ionized form)
PFCA	Perfluoro-n-alkanoic acid	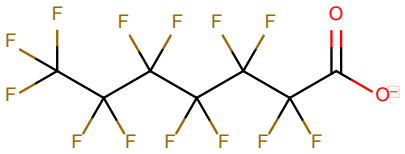
PFSA	Perfluoroalkane sulfonate	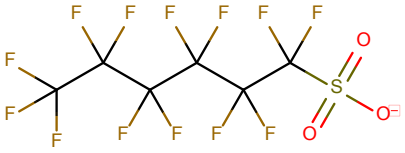
H-PFCA	Hydrido-PerFluoroAlkanoic Acid	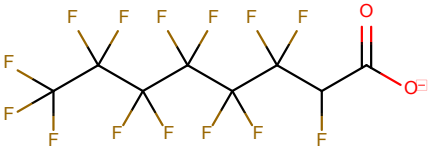
H-PFSA	Hydrido-PerFluoroAlkane Sulfonate	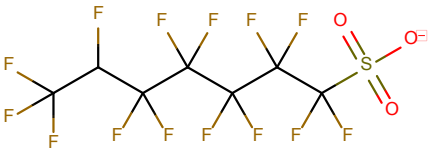
FASA	PerFluoroAlkane SulfonAmide	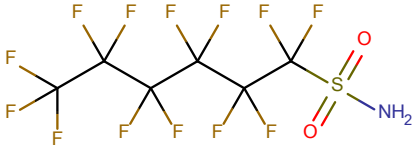
FASAA	PerfluoroAlkaneSulfonamido Acetic Acid	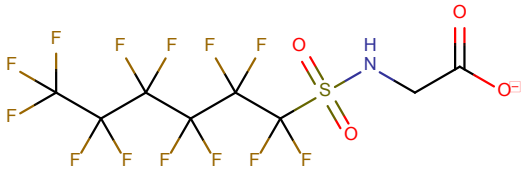
MeFASA	N-methyl perfluoroalkane sulfonamide	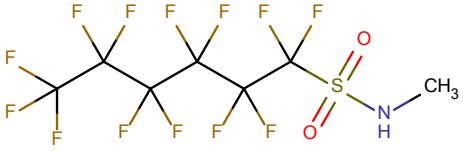
MeFASAA	N-MethylperFluoroAlkaneSulfonamidoAcetic Acid	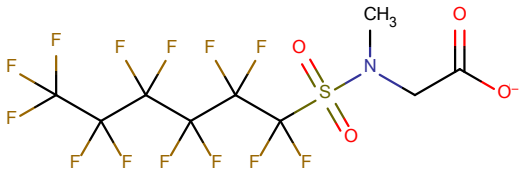

SPr-FASA	N-Sulfo Propyl perFluoroAlkaneSulfonAmide	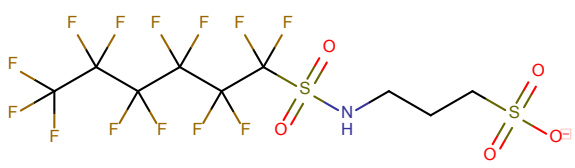
SPrAmPr-FASAA	N-SulfoPropyldimethylAmmonio Propyl-perFluoroAlkaneSulfonamido Acetic Acid	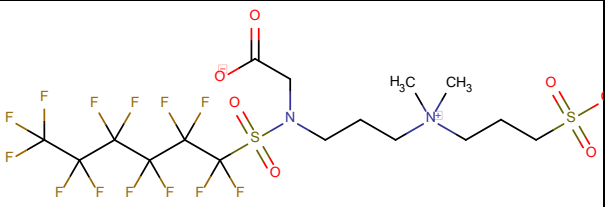
SPrAmPr-FASAPrS	N-SulfoPropyldimethylAmmonio Propyl perFluoroAlkane SulfonAmidoPropylSulfonate	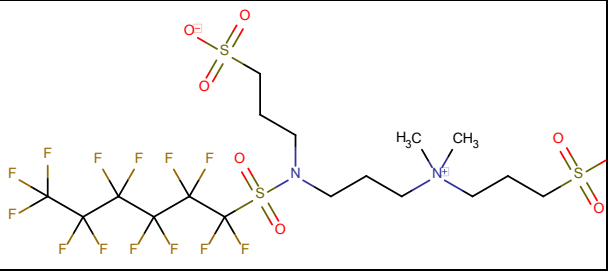

[a] There might be other alternative isomers existing; One isomer was drawn to represent the class structure;
[b] #CF_2 = 6 represents that the perfluorinated chain length in PFAS component is 6, which is counted as the total number of perfluorinated carbon atoms.

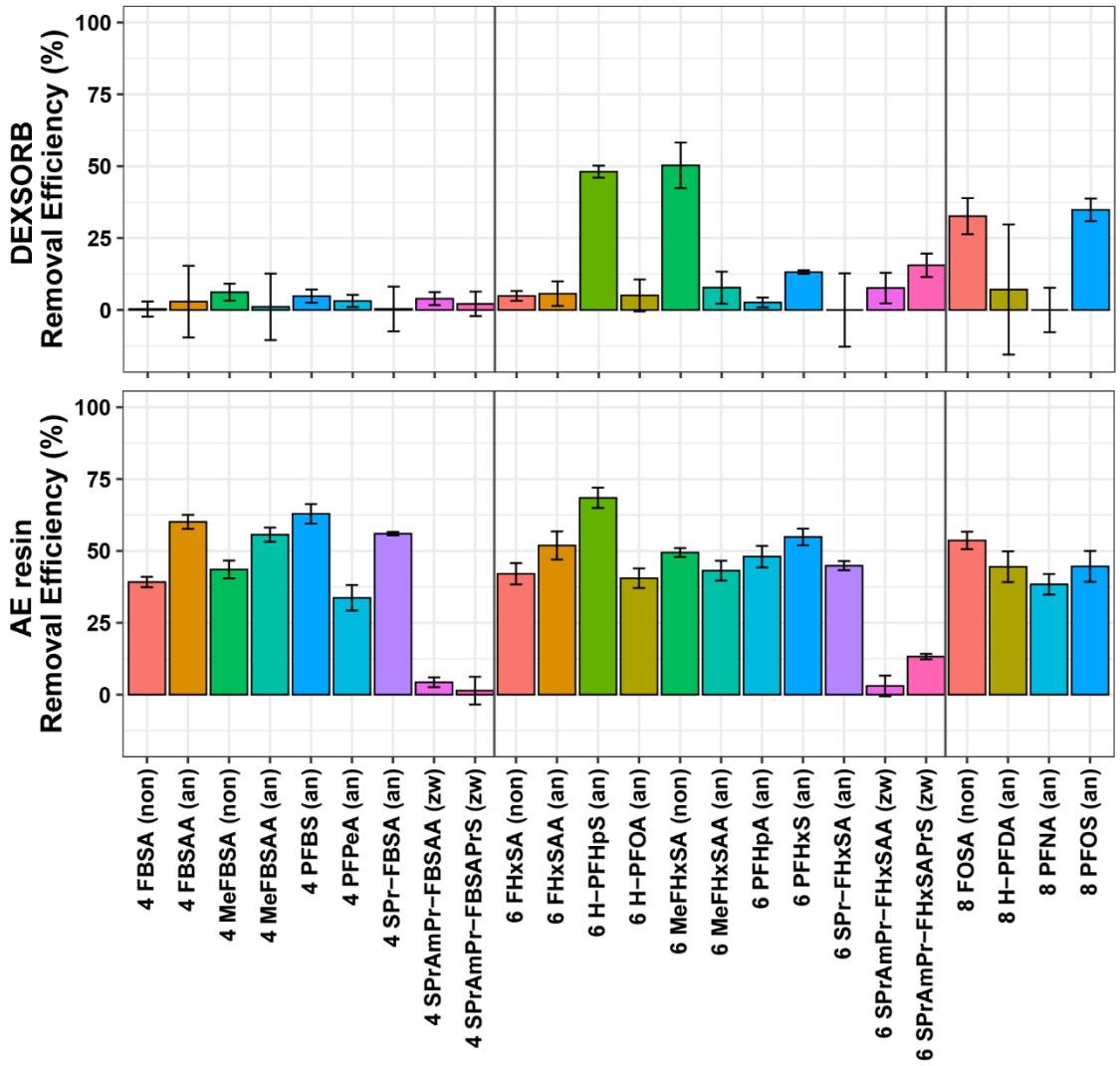

Figure A-2. Bar plots showing the removal efficiencies for PFASs in 11 different homologue series grouped by 4, 6 and 8 CF_2 chain length on DEXSORB and AE resin after 48 hr contact time. On the horizontal axis, the number in front of PFAS acronym represents the CF_2 chain length counted as the total number of perfluorinated carbon atoms. The notations in the parentheses represent anionic (an) PFASs, nonionic (non) PFASs, and zwitterionic (zw) PFASs.

APPENDIX B – Identifying the Relative Contributions of Hydrophobic and Electrostatic Interactions on Adsorption of Perfluoroalkyl Acids on Cyclodextrin Polymers

B.1 Adsorbents

Table B-1. Characterization information of adsorbent materials.

Adsorbent	Functional group/charge	Average particle diameter (µm)[c]	BET surface Area (m^2 g^{-1})[a]	Yield (%)[a]	Zeta potential (mV)[b]
Stydex/+	Permanently cationic	162	237	96	+ 23.8 ± 1.6
Stydex/MA	Weakly anionic	149	402	94	- 8.2 ± 0.6
Stydex/Styrene	Weakly anionic	118	392	93	- 9.9 ± 0.9

[a] The data is from Dr. Max Klemes's Ph.D. dissertation;
[b] Zeta potentials were measured in 1 mM $CaCl_2$ solution with a concentration of polymer at 100 mg L^{-1};
[c] Actual particle diameter ranges rather uniformly between 300 microns and 75 microns, the reported value here is the mass-weighted average of the particle size.

B.2 Chemicals and reagents

Table B-2. PFAS target compounds and their isotopically labeled internal standards (ILISs).

Mixture Name	Name	Acronym	Molecular Formula	Supplier	Concentration	Solvent
PFC-MXA	Perfluorobutanoic acid	PFBA	C4HF7O2	Wellington Laboratories	2 mg/L	MeOH:H_2O (H_2O<1%)
PFC-MXA	Perfluoropentanoic acid	PFPeA	C5HF9O2	Wellington Laboratories	2 mg/L	MeOH:H_2O (H_2O<1%)
PFC-MXA	Perfluorohexanoic acid	PFHxA	C6HF11O2	Wellington Laboratories	2 mg/L	MeOH:H_2O (H_2O<1%)
PFC-MXA	Perfluoroheptanoic acid	PFHpA	C7HF13O2	Wellington Laboratories	2 mg/L	MeOH:H_2O (H_2O<1%)
PFC-MXA	Perfluorooctanoic acid	PFOA	C8HF15O2	Wellington Laboratories	2 mg/L	MeOH:H_2O (H_2O<1%)
PFC-MXA	Perfluorononanoic acid	PFNA	C9HF17O2	Wellington Laboratories	2 mg/L	MeOH:H_2O (H_2O<1%)
PFC-MXA	Perfluorodecanoic acid	PFDA	C10HF19O2	Wellington Laboratories	2 mg/L	MeOH:H_2O (H_2O<1%)
PFC-MXA	Perfluoroundecanoic acid	PFUnA	C11HF21O2	Wellington Laboratories	2 mg/L	MeOH:H_2O (H_2O<1%)
PFC-MXA	Perfluorododecanoic acid	PFDoA	C12HF23O2	Wellington Laboratories	2 mg/L	MeOH:H_2O (H_2O<1%)
PFC-MXA	Perfluorotridecanoic acid	PFTrDA	C13HF25O2	Wellington Laboratories	2 mg/L	MeOH:H_2O (H_2O<1%)
PFC-MXA	Perfluorotetradecanoic acid	PFTeDA	C14HF27O2	Wellington Laboratories	2 mg/L	MeOH:H_2O (H_2O<1%)
PFS-MXA	Perfluorobutanesulfonic acid	PFBS	C4HF9O3S	Wellington Laboratories	2 mg/L	100% Methanol
PFS-MXA	Perfluorohexanesulfonic acid	PFHxS	C6HF13O3S	Wellington Laboratories	2 mg/L	100% Methanol
PFS-MXA	Perfluoroheptanesulfonic acid	PFHpS	C7HF15O3S	Wellington Laboratories	2 mg/L	100% Methanol
PFS-MXA	Perfluorooctanesulfonic acid	PFOS	C8HF17O3S	Wellington Laboratories	2 mg/L	100% Methanol
PFS-MXA	Perfluorodecanesulfonic acid	PFDS	C10HF21O3S	Wellington Laboratories	2 mg/L	100% Methanol

MPFAC-MXA	Perfluoro-n-[1,2,3,4-13C4]butanoic acid	13C4 - PFBA	[13]C4HF7O2	Wellington Laboratories	2 mg/L	MeOH:H_2O (H_2O<1%)
MPFAC-MXA	Perfluoro-n-[1,2-13C2]hexanoic acid	13C2 - PFHxA	[13]C2C4HF11O2	Wellington Laboratories	2 mg/L	MeOH:H_2O (H_2O<1%)
MPFAC-MXA	Perfluoro-n-[1,2,3,4-13C4]octanoic acid	13C4 - PFOA	[13]C4C4HF15O2	Wellington Laboratories	2 mg/L	MeOH:H_2O (H_2O<1%)
MPFAC-MXA	Perfluoro-n-[1,2,3,4,5-13C5]nonanoic acid	13C5 - PFNA	[13]C5C4HF17O2	Wellington Laboratories	2 mg/L	MeOH:H_2O (H_2O<1%)
MPFAC-MXA	Perfluoro-n-[1,2-13C2]decanoic acid	13C2 - PFDA	[13]C2C8HF19O2	Wellington Laboratories	2 mg/L	MeOH:H_2O (H_2O<1%)
MPFAC-MXA	Perfluoro-n-[1,2-13C2]undecanoic acid	13C2 - PFUnA	[13]C2C9HF21O2	Wellington Laboratories	2 mg/L	MeOH:H_2O (H_2O<1%)
MPFAC-MXA	Perfluoro-n-[1,2-13C2]dodecanoic acid	13C2 - PFDoA	[13]C2C10HF23O2	Wellington Laboratories	2 mg/L	MeOH:H_2O (H_2O<1%)
MPFAC-MXA	Sodium perfluoro-1-hexane[18O2]sulfonate	18O2 - PFHxS	C6HF13[18]O2OS	Wellington Laboratories	2 mg/L	MeOH:H_2O (H_2O<1%)
MPFAC-MXA	Sodium perfluoro-1-[1,2,3,4-13C4]octanesulfonate	13C4 - PFOS	[13]C4C4HF17O3S	Wellington Laboratories	2 mg/L	MeOH:H_2O (H_2O<1%)

B.3 Analytical methods

The mobile phase consisted of (A) LC-MS grade water amended with 20 mM ammonium acetate and (B) LC-MS grade methanol. Samples were injected at 5 mL volumes onto a Hypersil Gold dC18 12 µm 2.1 x 20 mm trap column (ThermoFisher Scientific) at room temperature (21-22°C) using an isocratic mobile phase of 99% A pumped at 1 $mL \cdot min^{-1}$ via a low-pressure loading pump. Elution from the trap column and subsequent separation of analytes on an Atlantis® dC18 5 µm 2.1 x 150 mm analytical column (Waters) at 25°C was achieved using an initial mobile phase of 60% A pumped at 0.3 $mL \cdot min^{-1}$ via a high pressure elution pump. The isocratic mobile phase delivered from the loading pump changed to 2% A at 37.3 minutes to rinse the trap column and returned to 99% A at 41.3 minutes to prepare for the next sample injection. The mobile phase gradient delivered from the loading pump remained at 60% A until 6.1 minutes and then increased linearly to 10% A at 30.1 minutes. The mobile phase was held at 10% A until 37.1 minutes before it returned to 60% A to prepare for the next sample. The chromatography program had a total duration of 42.1 minutes.

Table B-3. Analytical information of PFAS target compounds and their ILISs for PRM.

Acronym	Molecular Formula	Adduct	Precursor Ion Mass (Da)	Product Ion Mass (Da)	RT (min)	NCE	ILIS
PFBS	C4HF9O3S	[M-H]-	298.9430	79.9557	13.71	60	18O2 - PFHxS
PFHxS	C6HF13O3S	[M-H]-	398.9366	79.9557	19.80	60	18O2 - PFHxS
PFHpS	C7HF15O3S	[M-H]-	448.9334	79.9557	22.11	60	13C4 - PFOS
PFOS	C8HF17O3S	[M-H]-	498.9302	79.9558	24.04	60	13C4 - PFOS
PFBA	C4HF7O2	[M-H]-	212.9792	168.9897	9.70	20	13C4 - PFBA
PFPeA	C5HF9O2	[M-H]-	262.9760	218.9863	13.19	20	13C2 - PFHxA
PFHxA	C6HF11O2	[M-H]-	312.9728	268.9829	16.79	20	13C2 - PFHxA
PFHpA	C7HF13O2	[M-H]-	362.9696	318.9794	19.75	20	13C4 - PFOA
PFOA	C8HF15O2	[M-H]-	412.9664	368.9767	22.16	20	13C4 - PFOA
PFNA	C9HF17O2	[M-H]-	462.9632	418.9737	24.17	20	13C5 - PFNA
PFDA	C10HF19O2	[M-H]-	512.9600	468.9703	25.87	20	13C2 - PFDA